

Course of Geothermics

Dr. Magdala Tesauro

Course Outline:

1. Thermal conditions of the early Earth and present-day Earth's structure
2. **Thermal parameters of the rocks**
3. Thermal structure of the lithospheric continental areas (steady state)
4. Thermal structure of the lithospheric oceanic areas
5. Thermal structure of the lithosphere for transient conditions in various tectonic settings
6. Heat balance of the Earth
7. Thermal structure of the sedimentary basins
8. Thermal maturity of sediments
9. Mantle convection and hot spots
10. Magmatic processes and volcanoes
11. Heat transfer in hydrogeological settings
12. Geothermal Systems

Source of heat in the Earth

- **Two sources**
 - Earth's interior
 - Sun
- **Most of the heat from the Sun is radiated back into space**
 - surface water cycle
 - rainfall
 - erosion
- **Heat from the Earth's interior governed its geological and geodynamical evolution**
 - Plate tectonic
 - Igneous activity
 - Core evolution
 - Magnetic field of the Earth

Thermal state of the lithosphere (why do we want to know it?)

- Knowledge of the present thermal state of the Earth is crucial for models of crustal and mantle evolution, mantle dynamics, and processes of deep interior.
- Physical properties of crustal and mantle rocks are temperature dependant (density, seismic velocity, seismic attenuation, electrical conductivity, viscosity).

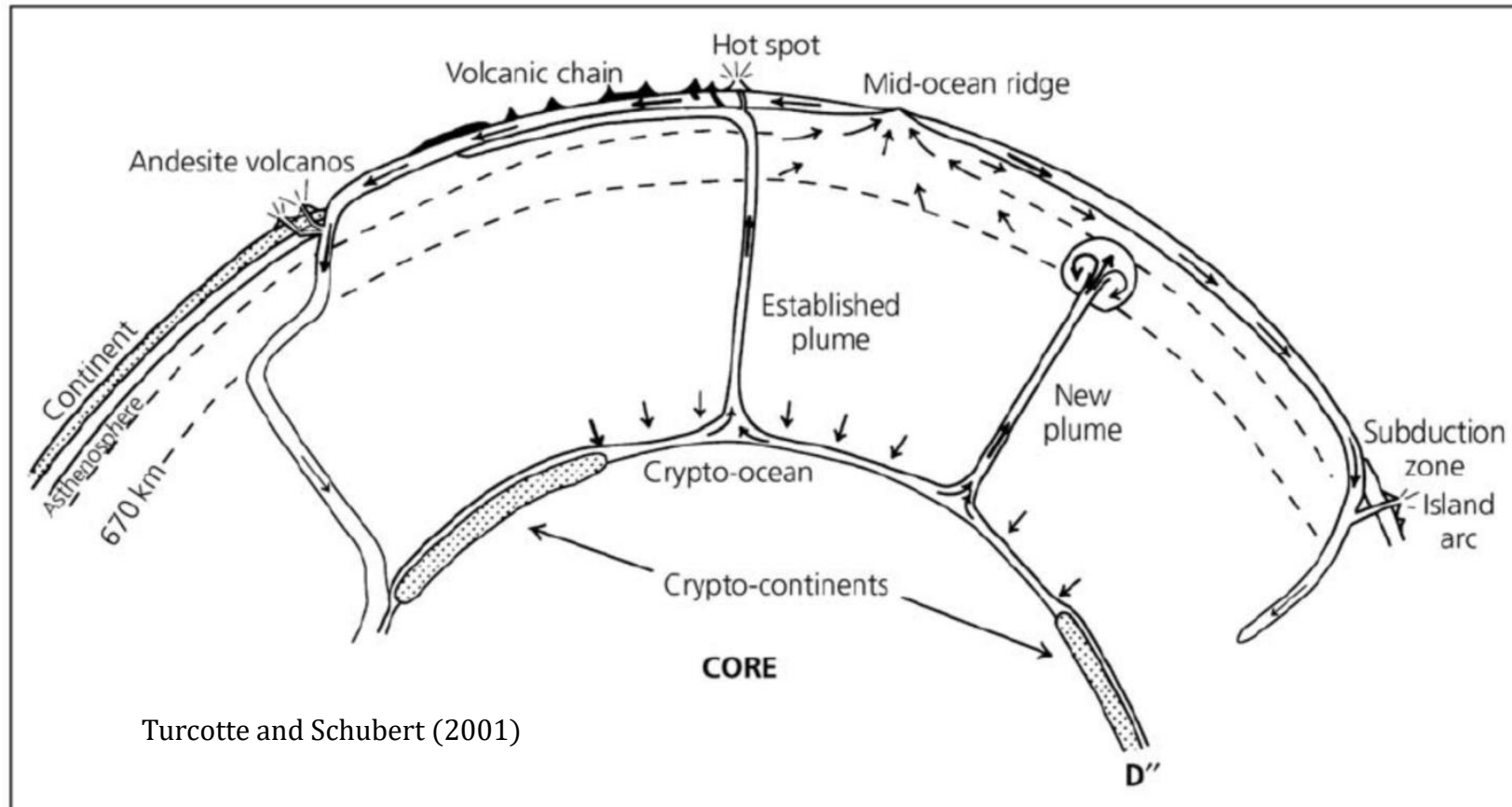
Temperature of the Earth is controlled by internal heat:

80% from the radiogenic heat production and 20 % comes from secular cooling of the Earth.

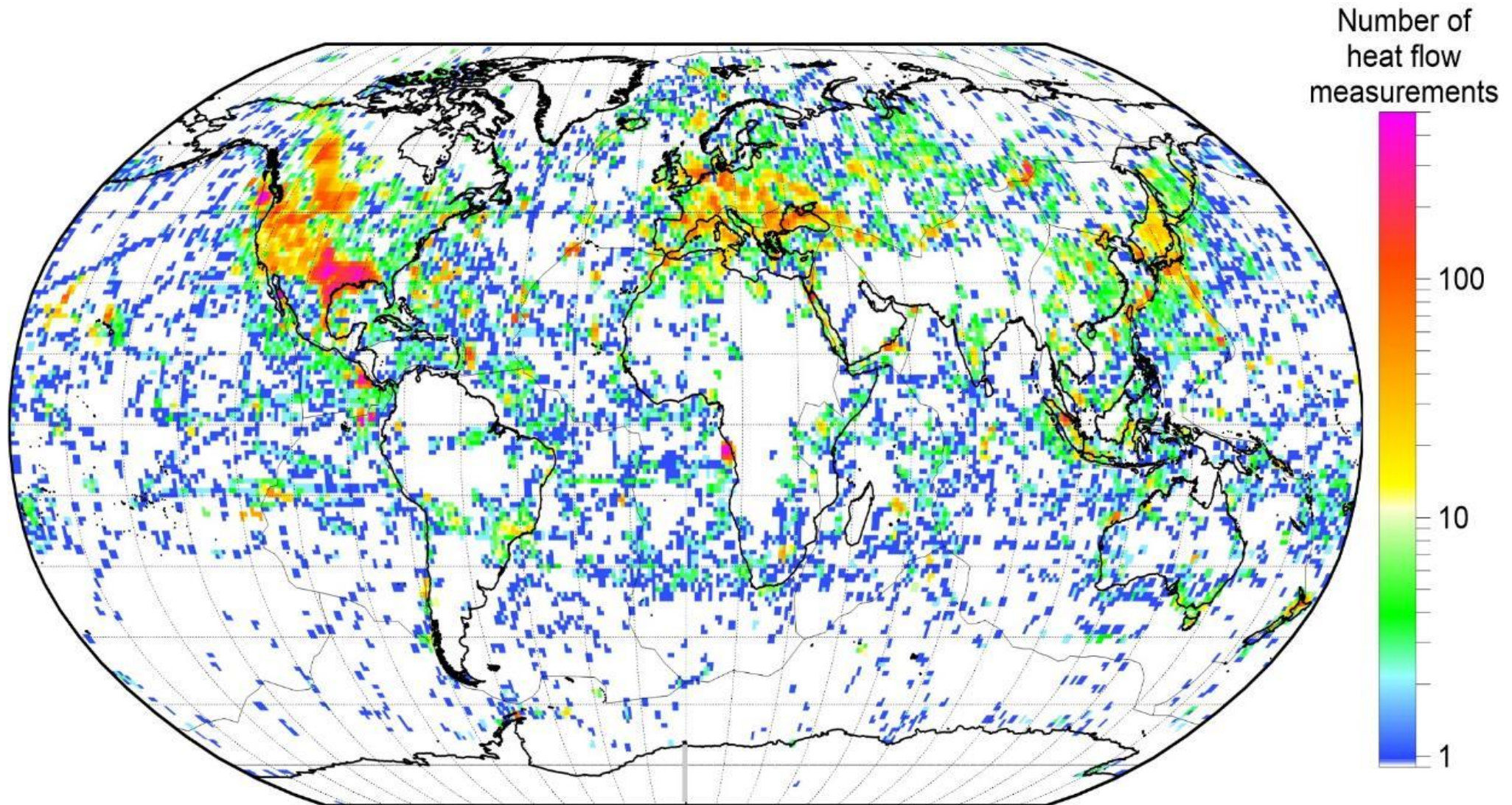
Heat is transferred to the surface of the Earth through three mechanisms: **conduction** (in the lithosphere), **convection** (below the lithosphere), and **advection** (hydrothermal circulation in sediments).

Knowledge of the thermal state of the lithosphere from more than 20000 heat flux measurements at the Earth's surface

Heat flow and tectonic setting



Global Heat Flow Data



Heat Flow

Heat flow density (HFD) determines the amount of heat per unit of area and per unit of time which is transmitted by heat conduction from the Earth's interior.

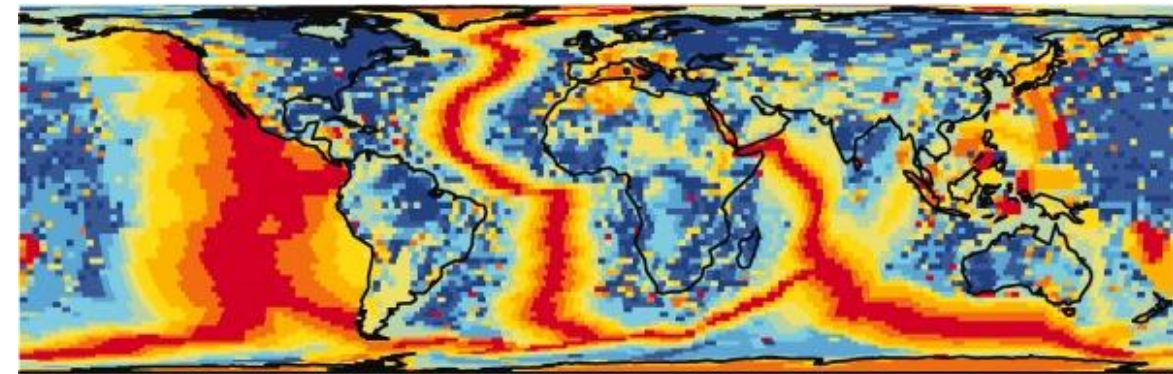
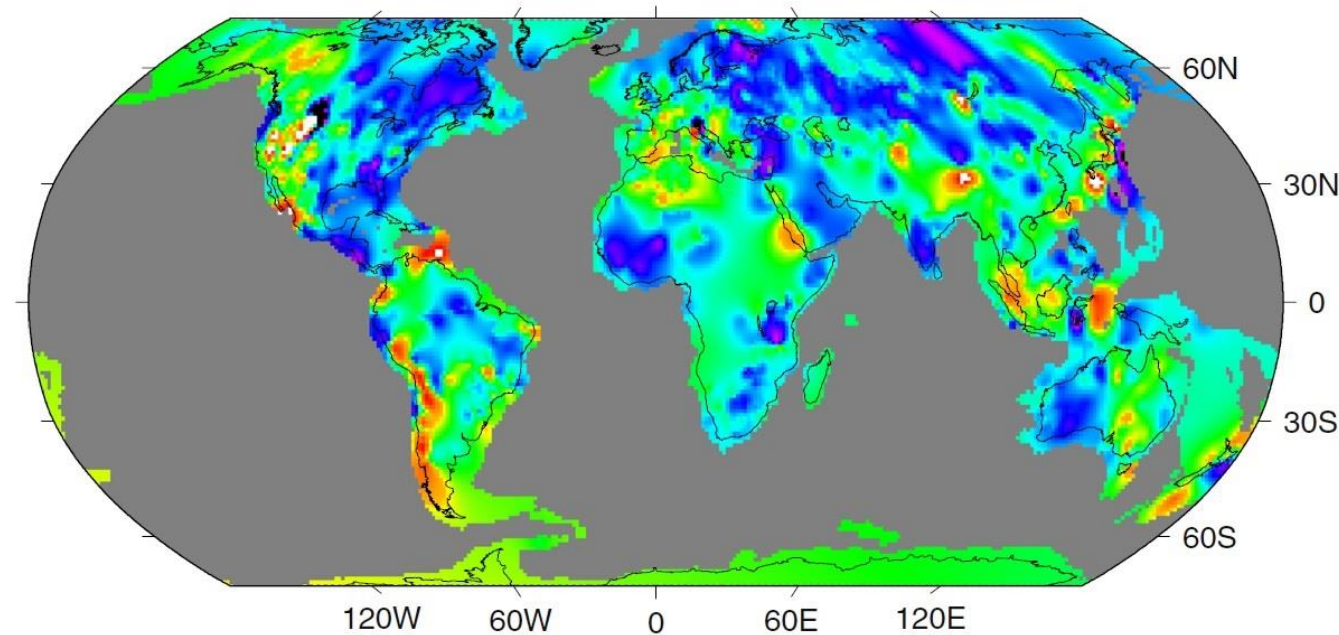
Fourier Law states that the rate of flow of heat is proportional to the temperature gradient:

$$\mathbf{q} = -\lambda \text{grad } T = -\lambda \nabla T.$$

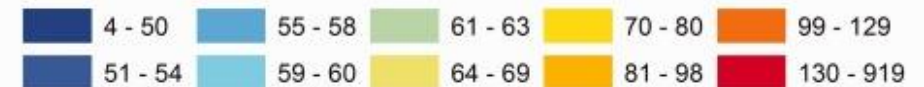
$$\text{For 1D: } q = -\lambda \frac{\partial T}{\partial x}$$

- minus sign shows that heat flows from points with high T to points with lower T
- λ or K = thermal conductivity (rocks dependent), for an isotropic and homogeneous layer has only one value

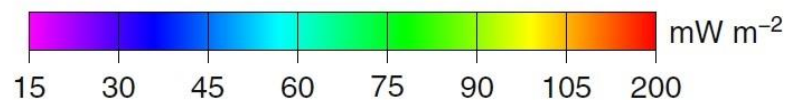
Continental heat flux



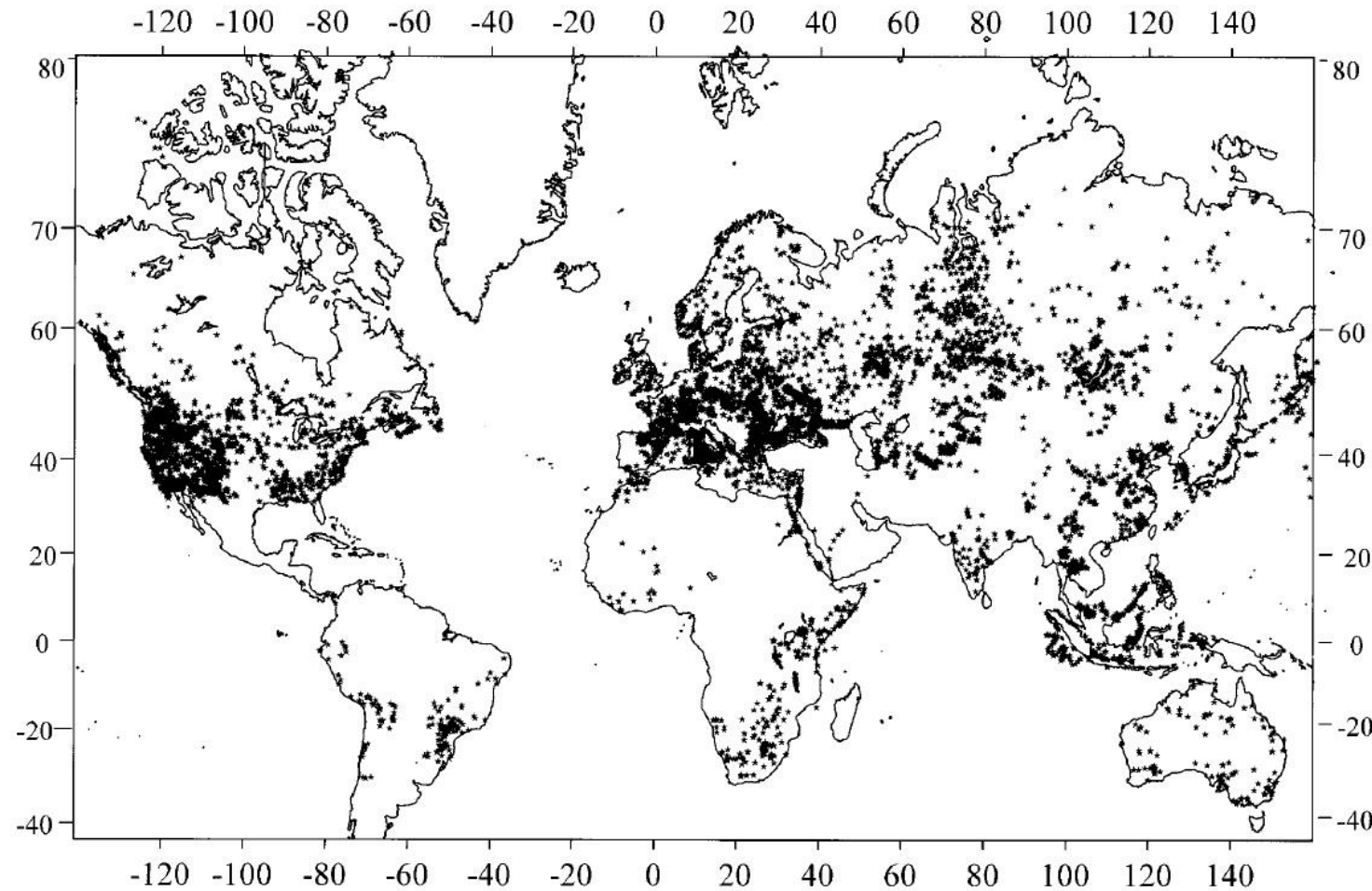
Final Estimate of Heat Flow (mW m^{-2}) (Area-weighted Median)



<http://www.heatflow.und.edu>



Heat Flow data



Country or region	HFD range (mW m^{-2})	References
Austria	43–127	Čermák (1984)
Bulgaria	8–132	Čermák (1984)
Cyprus	41–185	Čermák (1984)
France	45–176	Čermák (1984)
Eastern Germany	26–172	Čermák (1984)
Western Germany	21–168	Čermák (1984)
Greece	30–105	Čermák (1984)
Hungary	52–139	Čermák (1984)
Iceland	63–281	Čermák (1984)
Israel	7–93	Čermák (1984)
Italy	17–143	Čermák (1984)
Romania	19–118	Čermák (1984)
Spain	29–189	Čermák (1984)
USSR (European part)	19–142	Čermák (1984)
Greenland and Norwegian Seas	14–268	Čermák (1984)
Reykjanes range	2–343	Čermák (1984)
Ranges of the Atlantic	0–282	Čermák (1984)
Other regions of the Atlantic	11–90	Čermák (1984)
Mediterranean near Spain	55–155	Čermák (1984)
Mediterranean West of Sardinia	33–132	Čermák (1984)
Tyrrhenian Sea, Mediterranean	30–173	Čermák (1984)
Adriatic Sea, Mediterranean	36–104	Čermák (1984)
Aegean Sea, Mediterranean	47–114	Čermák (1984)
Ionic and Eastern Mediterranean Seas	10–74	Čermák (1984)
Black Sea	8–91	Čermák (1984)
Caspian Sea	40–99	Čermák (1984)
Alaskan interior	42–130	Williams et al. (2006)
Egypt	42–175	Morgan and Swanberg (1978)
Marmara Sea	35–115	Pfister et al. (1998)
Baltic Shield	25–70	Kukkonen et al. (1998)
Kura Depression, Azerbaijan	12–105	Pilchin (1983)
Cordillera, South America	25 to >160	Hamza and Muñoz (1996)
Brazilian platform	30 to >100	Hamza and Muñoz (1996)
Altiplano, Cordillera	50–180	Springer and Förster (1998)
Oregon Cascade Range, USA	40–100	Blackwell et al. (1980)
Pannonian basin	50–130	Lenkey et al. (2002)
Deccan basalt province, India	33–73	Kumar et al. (2007a)
Mesozoic Luangwa and Zambezi rifts	44–110	Nyblade et al. (1990)

Heat Flow data

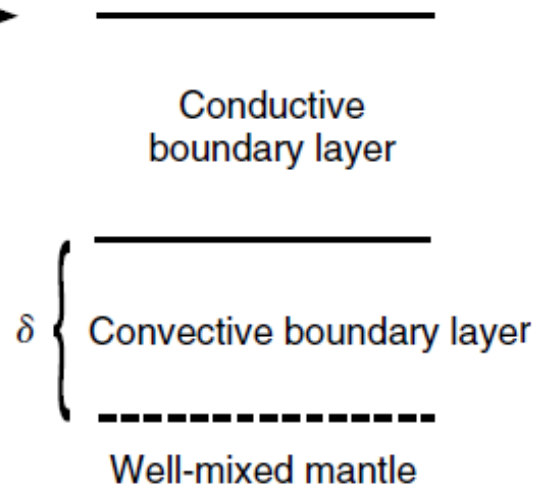
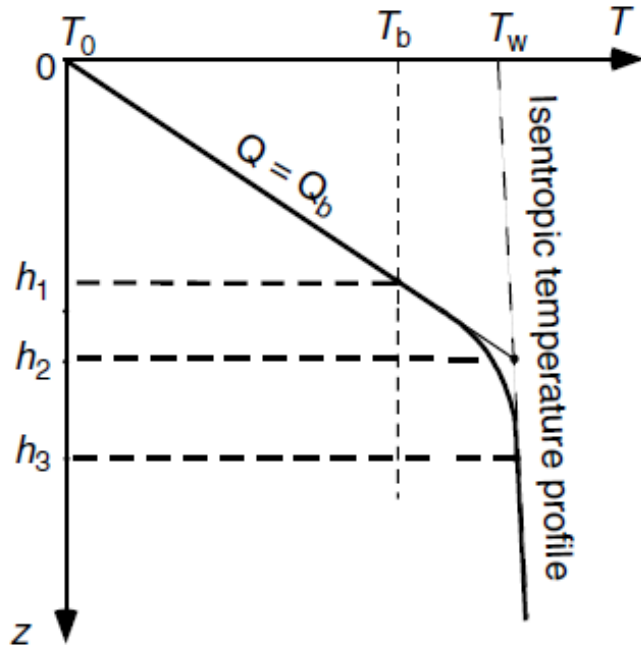
Abnormally low HFD values for some areas

Region	Values of HFD as low as (mW m^{-2})	References
Coastal Cordillera, South America	25	Hamza and Muñoz (1996)
Mesozoic Espirito Santos Basin, Brazil	26	Hamza and Muñoz (1996)
Continental part of Barents Sea region	20	Shwartsman (2001)
Drill holes, Kamennye Lakes, Eastern Karelia	2.4–11.6	Kukkonen et al. (1998)
Black Sea Basin	<20	Kutas et al. (1998)
Coastal Cordillera	20	Springer and Förster (1998)
Sierra Nevada Mountains, USA	<20	Blackwell et al. (1991)
Middle Rocky Mountains	30	Blackwell et al. (1991)
Canadian Shield	22	Mareschal et al. (2000b)
Mesozoic of Iberia abyssal plain, Galicia	47.5	Louden et al. (1997)
Pleistocene deposits, Gulf of Mexico	~20	Nagihara and Jones (2005)
The Urals	<20	Kukkonen et al. (1997)
East Ural Uplift	18	Kukkonen et al. (1997)
Transylvanian Depression	30	Şerban et al. (2001)
Outer Dinarides	<30	Lenkey et al. (2002)
Magadi, Late Archean Closepet Granite, India	25	Roy et al. (2008)
Ushachi, Belorussia	5	Zuy (2007)
Sudilovochi, Belorussia	4–10	Zuy (2007)
Kosari, Belorussia	3–7	Zuy (2007)
Kozlovka, Belorussia	3–6	Zuy (2007)
Senno, Belorussia	2–4	Zuy (2007)
Deccan basalt province, India	33	Kumar et al. (2007a)
Middle Kura Depression, Azerbaijan	11–12	Pilchin (1983)
Lower Kura Depression, Azerbaijan	12–16	Pilchin (1983)
Krivoy Rog, Ukrainian Shield	9.2–14.6	Lubimova et al. (1964)
Staraya Mazesta, Russia	15.9	Lubimova et al. (1964)
Sukhokumskaya, North Caucasus	8–12	Amirkhanov et al. (1975)
Dchevskaya, Saratov Province, Russia	1.3	Pilchin (1983)
Astrakhan Province	8.3	Suyetnov et al. (1980)

Abnormally high HFD values for some areas

Region	Values of HFD as high as ^a (mW m^{-2})	References
Central Valley, Cordillera	158	Hamza and Muñoz (1996)
Patagonian Cordillera	160	Hamza and Muñoz (1996)
Altiplano, Cordillera	180	Springer and Förster (1998)
Yellowstone, USA	>120	Blackwell et al. (1991)
Salton Trough, USA	>120	Blackwell et al. (1991)
Northeast German Basin	91	Norden et al. (2009)
North Caucasus, Russia	205	Suyetnov (1963)
Saratov province, Russia	267.5	Pilchin (1983)
Astrakhan Province, Russia	193	Suyetnov et al. (1980)
Baikal rift zone, Russia	≥200	Lysak and Sherman (2002)

Thermal Boundary layer at the top of the Earth's convective mantle



h_1 = lower boundary of the conductive part (bottom of the thermal lithosphere).
 h_2 = intersection between the downward extrapolation of the conductive geotherm and the temperature profile for the convective mantle.
 h_3 = lower limit of the thermal boundary layer (transition between lithospheric regime and fully convective mantle regime).
 T_0 = temperature at the surface
 T_b = temperature at the base of the lithosphere
 T_w = temperature of well-mixed convective interior

$$Q_0 = Q_{\text{crust}} + Q_{\text{lith}} + Q_b$$

Q_{crust} = heat flux due to the contribution of heat sources in the crust
 Q_{lith} = heat flux due to contribution of heat sources in the lithosphere
 Q_b = heat flux at the base of the lithosphere

In the absence of heat sources:

$$Q_0 = Q_b = \lambda \frac{T_b - T_0}{h_1}$$

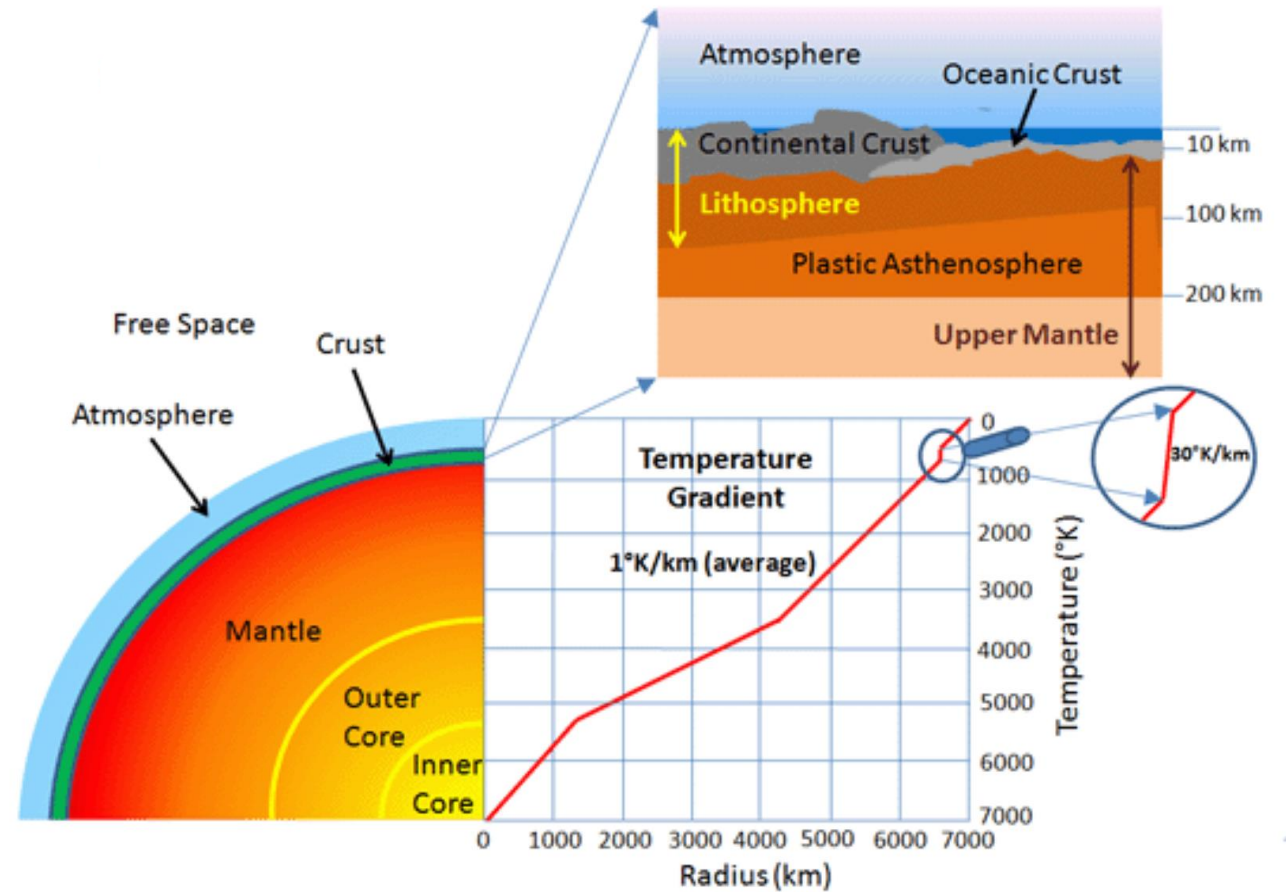
Similarly, across the convective boundary layer: $Q_b = B(T_w - T_b)$ B = heat transfer coefficient

For perfectly efficient heat transfer $B \rightarrow \infty$ then $T_b \rightarrow T_w$

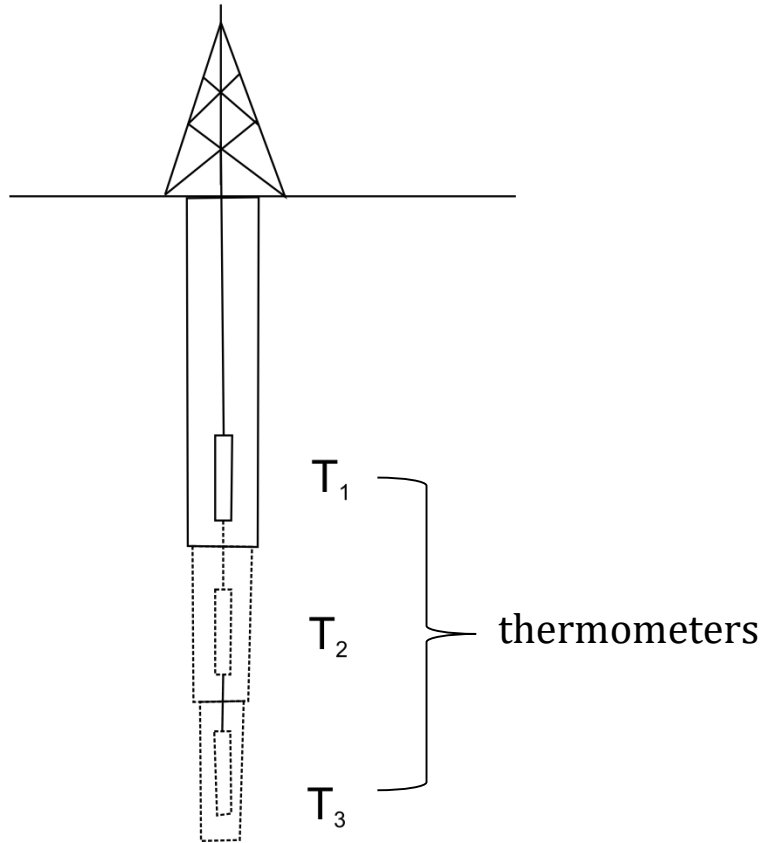
If convective mantle can maintain a fixed heat flux, Q_b is set to a constant

Geothermal gradient (∇T)

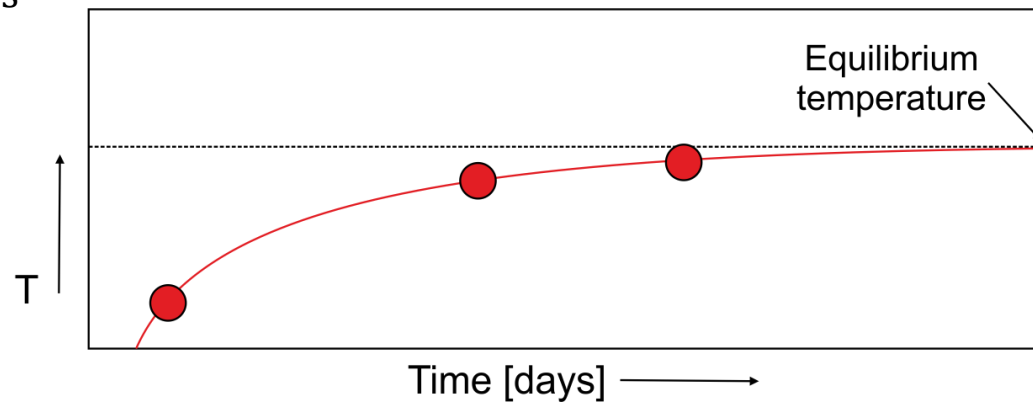
- Change of temperature with depth
- $\nabla T \propto [25 - 45] \text{ }^\circ\text{C}/\text{km}$
(continental average)
- Varies with tectonic setting



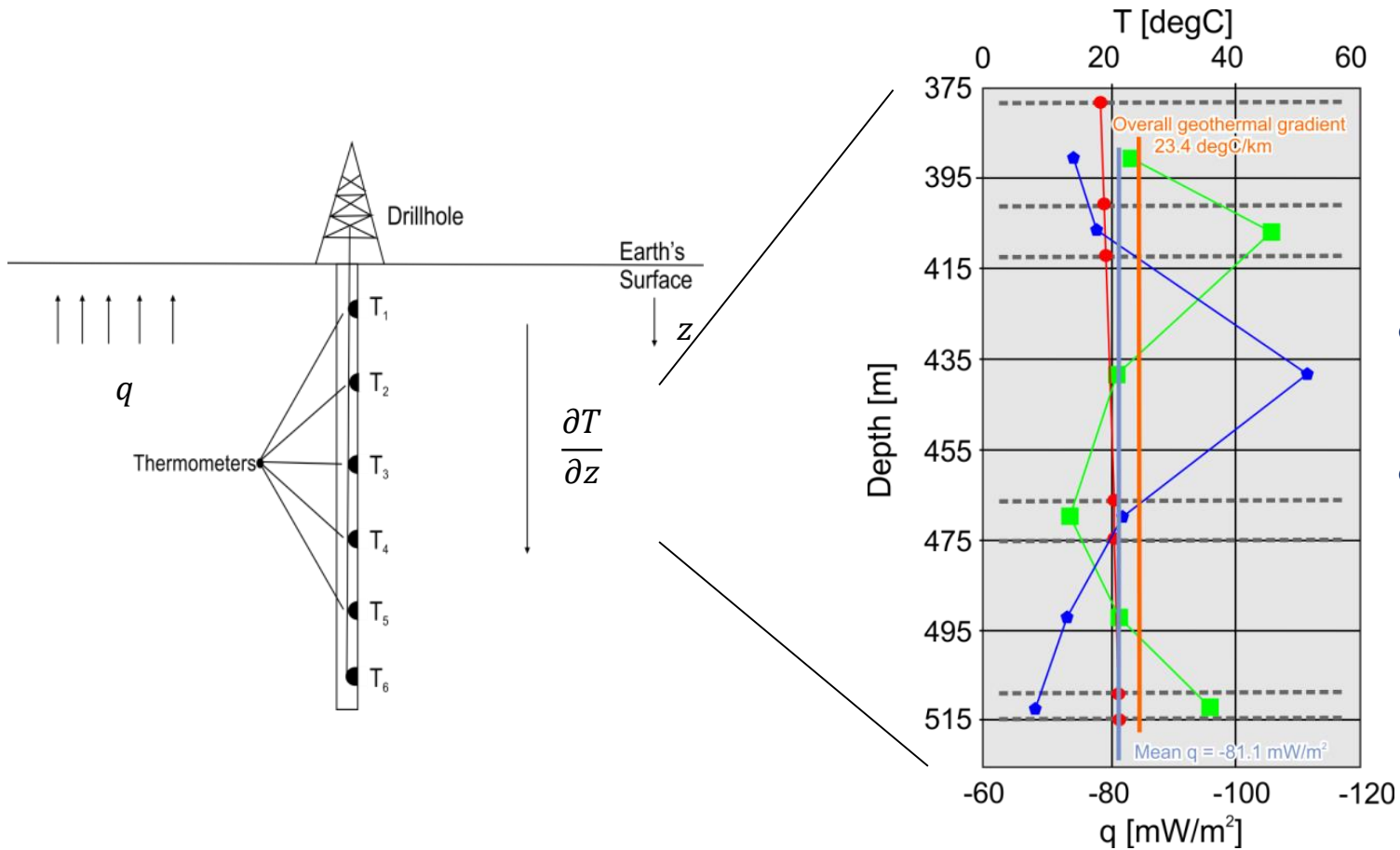
Measuring Temperature



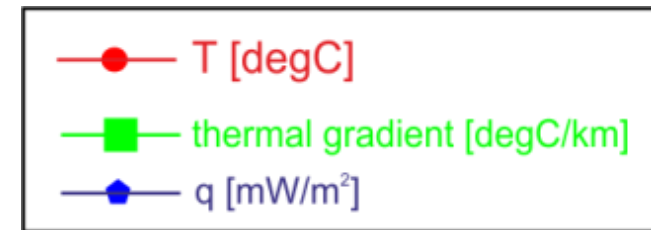
- Measure bottom hole T during each logging run
- Drilling mud is pumped down the well to control pressure
- Drilling fluid cools the wellbore



Measuring q



- Temperature readings are on the lithological boundaries
- Geothermal gradient and heat flow calculation values are placed at center-thickness of each unit



Measuring heat flow (q) is simply a matter of dropping a thermometer down a drill hole and logging the change in temperature with depth

Thermal Gradient

Thermal gradient is a vector quantity dependent on the distribution of temperature in 3D, magnitude and orientation of the max thermal gradient are given by:

$$\nabla T = \frac{\partial T}{\partial x} \mathbf{i} + \frac{\partial T}{\partial y} \mathbf{j} + \frac{\partial T}{\partial z} \mathbf{k}$$

$$\text{grad}(T(x, y, z)) = \left(\frac{\partial T(x, y, z)}{\partial x} \mathbf{i} + \frac{\partial T(x, y, z)}{\partial y} \mathbf{j} + \frac{\partial T(x, y, z)}{\partial z} \mathbf{k} \right)$$

T =temperature distribution function in 3D and i, j , and k are the unit vectors along the x, y , and z axes.

Thermal Gradient

If lateral temperature variation at depth are negligible in comparison with the vertical ones, all thermal gradient problems reduce to 1D and magnitude of the temperature gradient is the derivative of T with respect to depth:

$$\nabla T = (\partial T / \partial z) \times \mathbf{k} \quad \text{which can be written as: } G_z = \lim_{\Delta h \rightarrow 0} \frac{T(x, y, z + \Delta h) - T(x, y, z)}{\Delta h}$$

Since it is impossible to obtain two accurate measurements of T at zero distance ($\Delta h \rightarrow 0$), we can use finite difference methods:

We must find the value of the function in two different points:

$$\Delta_h(T(z)) = T(z + \Delta h) - T(z) \quad \text{Forward difference}$$

$$\Delta_h(T(z)) = T(z) - T(z - \Delta h) \quad \text{Backward difference}$$

$$\Delta_h(T(z)) = T(z + \Delta h) - T(z - \Delta h) \quad \text{Central difference}$$

Using the central difference form, the value of the vertical and horizontal geothermal gradient at an arbitrary depth h_i in a borehole is:

Vertical direction	Horizontal direction
$\left(\frac{dT(z)}{dz}\right)_{h_i} = \frac{T(h_i + \Delta h) - T(h_i - \Delta h)}{2 \cdot \Delta h}$	$\left(\frac{dT(x)}{dz}\right)_{l_i} = \frac{T(l_i + \Delta l) - T(l_i - \Delta l)}{2 \cdot \Delta l}$

Vertical Thermal Gradient

The value of the geothermal gradient declines with depth with the sharpest drop usually at depths less than 2 km, possibly because of water content and its circulation in the sedimentary cover.

Changes in the vertical geothermal gradient with depth for some regions (after Eppelbaum and Pilchin 2006)

Region	Depth interval (m)	Average geothermal gradient (K/km)	Percentage of geothermal gradient near the surface
Krasnodar region, Russia	0–2,000	30–40	70
	2,000–4,000	30–35	65
	4,000–6,000	25–32	57
Stavropol region, Russia	0–2,000	35–50	71
	2,000–4,000	35–45	67
	4,000–6,000	30–35	54
Middle-Kura Depression, Azerbaijan	0–2,000	25–43	76
	2,000–4,000	20–35	61
	4,000–6,000	20–30	42
Northern Israel	2,300	18–20	46–54
Dead Sea region, Israel	2,350–2,750	16–22	20–61
Utah, USA	440–619	48	83
Salton Sea, USA	762–884	178.9	73
Central Ventura Basin, USA	1,900–3,600	23–27	70–86
Williston Basin, Canada	2,000–3,000	20–Oct	30–80
Michigan Basin, USA	Phanerozoic	17.5	41

Horizontal and Vertical Thermal Gradient

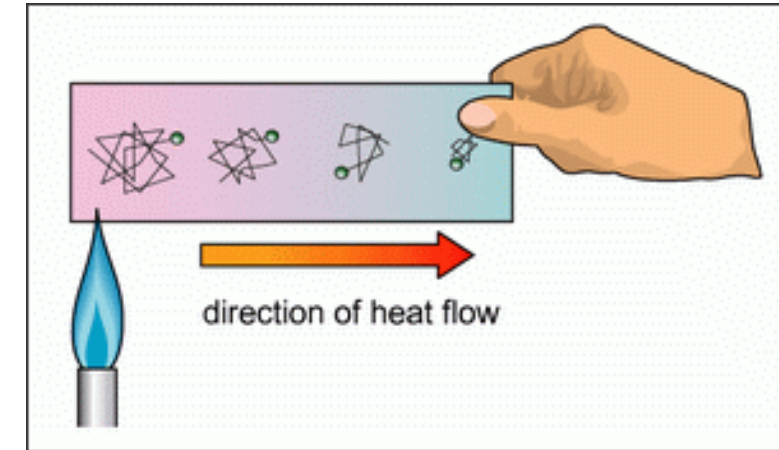
- Horizontal geothermal gradients are generally low (<10% of the vertical geothermal gradient) their values do not usually exceed 1 K/km.
- Horizontal geothermal gradients of one order less than vertical geothermal gradient are related to the presence of fractures and hydrothermal water activity.

Average values of vertical and horizontal geothermal gradients for some regions of the Caucasus

Region	At a depth of 4,000 m		At a depth of 6,000 m	
	Vertical geothermal gradient	Horizontal geothermal gradient	Vertical geothermal gradient	Horizontal geothermal gradient
Low Kura Depression	15–20	0.2–0.6	15–20	0.4–0.8
Middle Kura Depression	20–30	0.4–1.0	20–30	0.8–1.6
Kolkhida Depression	25–30	0.4–1.4	20–30	0.8–2.0
Dagestan	25–30	0.4–0.8	25	0.6–0.8
Stavropol province	35–40	0.4–0.8	25–30	0.2–1.0
Krasnodar province	30–35	0.2–0.8	30	0.2–1.0
Chechnya	30–35	0.4–0.8	25–30	0.4–0.8
South Caspian Depression	15	0.2–0.4	15	0.4–0.6

Conductive Heat Flow

Transfer of heat by microscopic (molecular and/or atomic) diffusion and collisions of particles within a body due to an existing temperature gradient



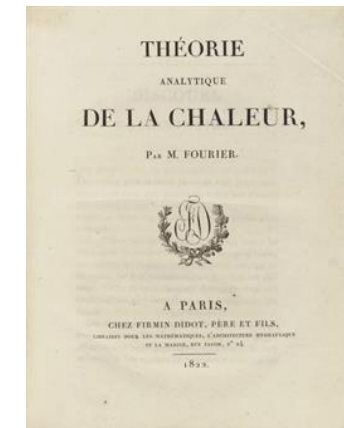
J. B. Fourier 1822 „*Theorie analytique de la chaleur*“

$$q = -\lambda \nabla T$$

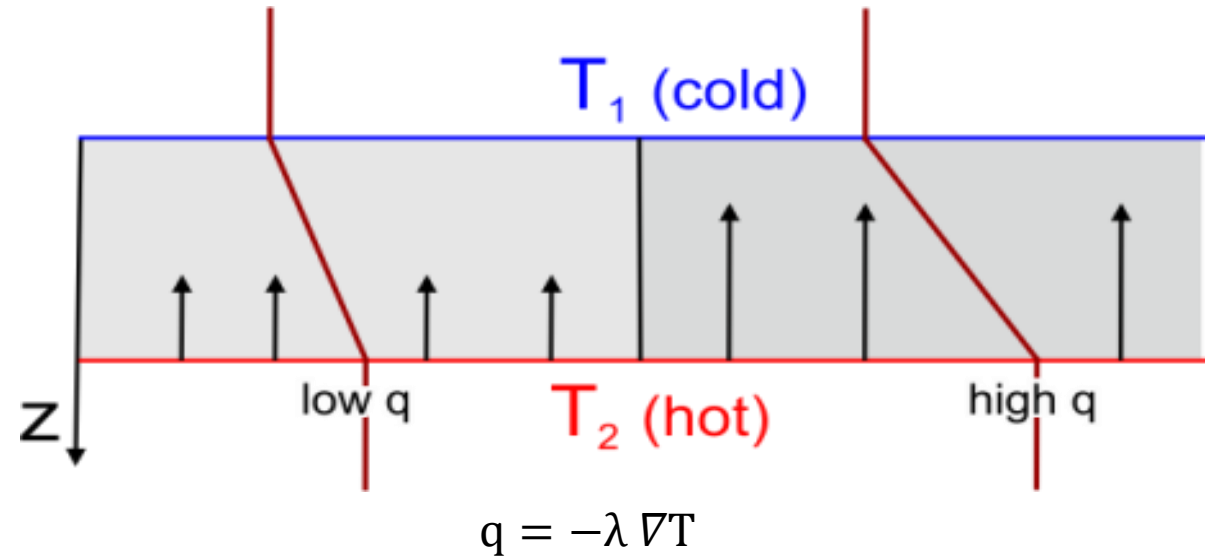
q = heat flux [$W \cdot m^{-2}$]

λ = heat conductivity [$W \cdot m^{-1} \cdot K^{-1}$]

∇T = Thermal gradient [$K \cdot m^{-1}$]



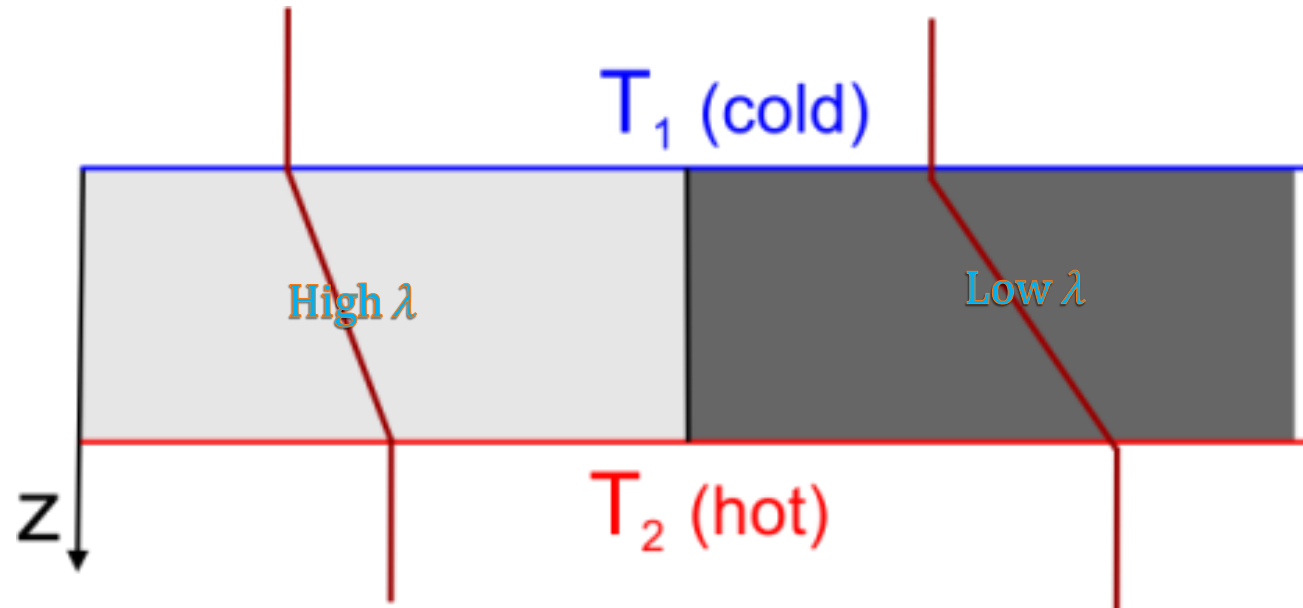
Heat flow and thermal conductivities



- Rate of heat conduction through a solid \propto temperature gradient (∇T)
- High heat flow (q) \propto high temperature gradient (∇T)
- Heat flows from a **hot** body to a **cold** body
- Conductive heat flow is related to a particular property of the material (λ)

Heat flow and thermal conductivities

- High λ → Rapid Heat Transfer → Low thermal Gradient
- Low λ → Slow Heat Transfer → High thermal Gradient



Thermal Conductivity

Thermal conductivity or the thermal conductivity coefficient (λ) of a material defines its ability to transfer heat

There are three mechanisms which contribute to thermal conductivity: (i) the diffusion of heat by phonon propagation (**lattice conductivity k_l**), (ii) the transfer of heat through emission and absorption of photons (**radiative conductivity k_r**) and (iii) the transport of energy by quasiparticles composed of electrons and positive holes (negligible in the lithosphere).

λ ($\text{m}^{-1} \text{s}^{-1} \text{K}^{-1}$ or $\text{W m}^{-1} \text{K}^{-1}$) of rocks is dependent on T , P , porosity (ϕ), composition, and properties of pore-filling fluids and gases.

Material	$\text{Wm}^{-1} \text{K}^{-1}$	Source
Earth's crust	2.0–2.5	Mean value, Kappelmeyer and Hänel (1974)
Rocks	1.2–5.9	Sass et al. (1971)
Sandstone	2.5	Clark (1966)
Shale	1.1–2.1	Clark (1966), Blackwell and Steele (1989)
Limestone	2.5–3	Clark (1966), Robertson (1979)
Water	0.6 at 20 °C	Birch et al. (1942)
Oil	0.15 at 20 °C	Birch et al. (1942)
Ice	2.1	Gretener (1981)
Air	0.025	CRC (1974) Handbook
Methane	0.033	CRC (1974) Handbook

Rock	From published data ^a		After Sharma (2002)
	No. of samples	Average heat conductivity	Average heat conductivity
Sand	1,149	1.79	1.1–2.1
Siltstone	476	1.58	–
Argillite, clay schist	783	1.67	2.09
Clay	660	1.43	0.8–1.5
Marl	217	1.78	–
Limestone	781	2.37	3.44
Chock	21	1.63	–
Granite	383	2.68	3.07
Granodiorite	83	2.79	2.63
Porphyrite	137	1.74	–
Diorite	78	2.10	2.5
Andesites, andesite-basalt	81	1.87	2.26
Basalt	98	2.11	1.69
Diabase	67	2.50	2.2
Gabbro	116	2.47	2.57
Schist	181	2.55	–
Gneiss	88	2.41	2.7–3.1
Amphibolite	47	2.39	3.33
Gneiss-granite	35	2.04	–
Quartzite	–	5.00	5.03
Anhydrite	–	–	5.43
Harzburgite	106	2.69	–
Dunites	23	2.77	–
Olivine gabbro	55	2.65	–
Gabbro-norite	36	2.22	–

Thermal Conductivity of Rocks (sedimentary rocks)

Thermal conductivity k (water-saturated), porosity and density of isotropic sedimentary rocks (Pasquale et al. 2011)

Rock	Lithotype	n	k ($\text{W m}^{-1} \text{K}^{-1}$)		Porosity (%)		Density (kg m^{-3})		
			Range	Mean	Range	Mean	Range	Mean	
Clastic	Marl	19	2.15–3.08	2.77 (0.23)	6.0–37.0	15.1 (8.4)	1787–2530	2278 (240)	
	Silty marl	18	2.85–3.66	3.16 (0.26)	2.0–20.0	12.8 (5.5)	2150–2670	2359 (156)	
	Calcareous marl	6	1.99–2.37	2.17 (0.13)	22.0–35.0	30.8 (5.0)	1693–2008	1801 (123)	
	Argillaceous limestone	3	3.58–3.63	3.60 (0.03)	7.5–12.0	9.3 (2.4)	2477–2588	2520 (80)	
	Argillaceous sandstone	6	2.60–3.40	3.00 (0.29)	8.0–25.0	15.1 (6.2)	1990–2560	2330 (222)	
	Calcareenite	3	2.18–2.50	2.34 (0.16)	25.0–32.0	29.0 (3.6)	1834–1997	1917 (82)	
Chemical- biochemical	Carbonate	Mudstone	5	3.04–3.48	3.30 (0.16)	0.5–6.0	2.7 (2.1)	2550–2695	2630 (59)
		Wackestone	5	3.10–3.20	3.16 (0.04)	3.0–10.0	6.0 (3.0)	2500–2670	2590 (75)
		Packstone	4	3.00–3.45	3.23 (0.18)	3.0–6.0	4.3 (1.3)	2550–2655	2620 (59)
		Grainstone	5	2.95–3.36	3.12 (0.16)	6.5–12.0	8.8 (2.5)	2400–2540	2480 (73)
		Dolostone	5	4.25–5.45	4.60 (0.49)	1.5–7.5	3.8 (2.4)	2630–2800	2735 (73)
	Siliceous	Radiolarite	4	3.16–3.46	3.37 (0.14)	0.5–5.5	2.4 (2.2)	2550–2650	2600 (48)
	Evaporitic	Anhydrite	5	3.15–3.65	3.39 (0.22)	0.5–5.0	2.7 (1.8)	2680–2780	2730 (52)
		Gypsum	5	1.40–1.64	1.54 (0.09)	0.5–7.0	2.4 (2.6)	2260–2400	2350 (61)

The mean thermal conductivity (k) ranges from **1.5** to **4.6 $\text{W m}^{-1} \text{K}^{-1}$** (gypsum and dolostone)

High conductivity: anhydrites, low conductivity: calcareous marls.

Porosity varies from about 3 % (radiolarite, gypsum, mudstone and anhydrite) to 30 % (calcareenite and calcareous marl) and influences k .

Thermal Conductivity of Rocks (Igneous and Metamorphic rocks)

K of homogeneous and macroscopically isotropic rocks ranges between 1.8 to 4.1 W m⁻¹ K⁻¹.

Thermal conductivity k and density of igneous and metamorphic rocks (Pasquale et al. 1988)

Lithotype	n	k (W m ⁻¹ K ⁻¹)		Density (kg m ⁻³)	
		Range	Mean	Range	Mean
Granite	22	2.44–3.49	2.88 (0.26)	2590–2760	2620 (20)
Granodiorite	16	2.24–3.03	2.52 (0.24)	2640–2820	2690 (40)
Tonalite	10	2.06–2.25	2.16 (0.07)	2700–2760	2720 (20)
Syenite	3	2.19–2.34	2.25 (0.08)	2680–2750	2720 (40)
Diorite	14	1.73–2.07	1.89 (0.11)	2740–2940	2840 (60)
Gabbro	12	1.65–2.29	1.94 (0.19)	2800–3060	2940 (80)
Dacite	4	3.56–3.91	3.73 (0.18)	2500–2690	2610 (102)
Anorthosite	4	1.67–1.83	1.76 (0.07)	2660–2810	2730 (60)
Hornblendite	5	2.57–2.79	2.71 (0.08)	3020–3180	3130 (70)
Lherzolite	11	3.31–4.00	3.70 (0.25)	3010–3210	3110 (50)
Harzburgite	3	3.52–3.66	3.60 (0.07)	3070–3110	3090 (20)
Dunite	3	4.04–4.16	4.11 (0.06)	3320–3360	3340 (20)

Rocks' thermal conductivities

Thermal conductivity λ [$\text{W}(\text{m} \cdot \text{K})^{-1}$]
heat [W] transported over a distance [m] with a drop in Temperature [$^{\circ}\text{C}$ or K]

Bulk thermal conductivity

- Porosity and fluid content (commonly water)
- Function of Temperature
- Function of depth (porosity loss with burial - compaction)
- Mineralogy of the framework grains
- Type and amount of material in the matrix (clay minerals)

Thermal Conductivity (Lattice Conductivity)

Phonon or lattice conduction is visualized as vibrations propagating along interatomic bonds

From elementary kinematic theory:

$$\lambda_{ph} = (v c l) / 3$$

v is the mean phonon velocity, c is the specific heat, and l is the mean free path in the lattice

$$\lambda_{ph} = (D \times a \times \theta^3) / (T \times \gamma^2)$$

(Abeles, 1963)

D = a numerical constant

a = the lattice spacing (m)

θ = the Debye temperature (K)

T = temperature (K)

$\gamma = \alpha / (\rho c \beta) =$ the Gruneisen parameter

(α = thermal expansivity, ρ = density, c = specific heat, β = compressibility)

For an isotropic crystal and at temperatures above the Debye temperature ϑ_D (for silicates > 600 K):

$$k_l = \frac{a_i K^{3/2}}{3 \gamma^2 T \rho^{1/2}}$$

Lawson, 1957

a_i is the interatomic distance, K is the bulk modulus, T is the absolute temperature, ρ is the density and γ is the Grüneisen parameter (dimensionless)

Debye Temperature and Grüneisen parameter

Debye temperature ϑ_D is directly related to the maximum frequency of vibration of the solid ν_m :

$$\vartheta_D = \frac{h \nu_m}{k_B}$$

$$\vartheta_D = 61.2 k_l + 385$$

For silicate minerals (Horai and Simmons, 1970)

h = Planck constant (6.626×10^{-34} J s) and k_B = Boltzmann constant (1.381×10^{-23} J K⁻¹)

Grüneisen parameter γ describes the effect that changing the volume of a crystal lattice has on its vibrational properties, and, as a consequence, the effect that changing temperature has on the size or dynamics of the lattice.

$$\gamma = \frac{\alpha K_S}{\rho c_p} = \frac{\alpha K_T}{\rho c_V}$$

$$\frac{1}{K_T} = \frac{1}{\rho} \left(\frac{\partial \rho}{\partial P} \right)_T$$

$$\frac{1}{K_S} = \frac{1}{\rho} \left(\frac{\partial \rho}{\partial P} \right)_S$$

c_p and c_V are the specific heat at constant pressure P and volume V , K_S and K_T are bulk moduli at constant entropy S and temperature T , and α is the thermal expansion coefficient.

Thermal Conductivity (Radiative Conductivity)

The governing function of the radiative conductivity derives from Stefan's law: in a black body the total energy radiated per unit time, E_R , is expressed as: $E_R = ST^4$ $S = \sigma A$ $A = \text{surface}$ $\sigma = \text{Stefan constant } (5.6705 \times 10^{-8} \text{ W m}^{-2} \text{ K}^{-4})$

At the depth of the lower crust and upper mantle the contribution of radiative conductivity (k_r) must be considered.

k_r depends on the mineral opacity ε :
$$\varepsilon = \frac{\ln(I_0/I)}{x}$$

where I_0 is the intensity of the incident radiation and I the intensity of the radiation transmitted by a medium of thickness x .
If opacity is independent from wavelength, the radiative conductivity k_r is:

(Grey body law)
$$k_r = \frac{16 n^2 \sigma T^3}{3 \varepsilon} \quad n = \text{refractive index}$$

with $n = 1.74$ (a typical value of ferromagnesian silicates):
$$k_r = 9.2 \times 10^{-7} \frac{T^3}{\varepsilon}$$

- Since ε is not negligible, k_r remains dominant to at least 800 K

In the lithospheric mantle:
$$k_r = 0.56 \left[1 + \operatorname{erf} \left(\frac{T - 1150}{370} \right) \right]$$

At temperature 1600 K, k_r is 1.1 W m⁻¹ K⁻¹

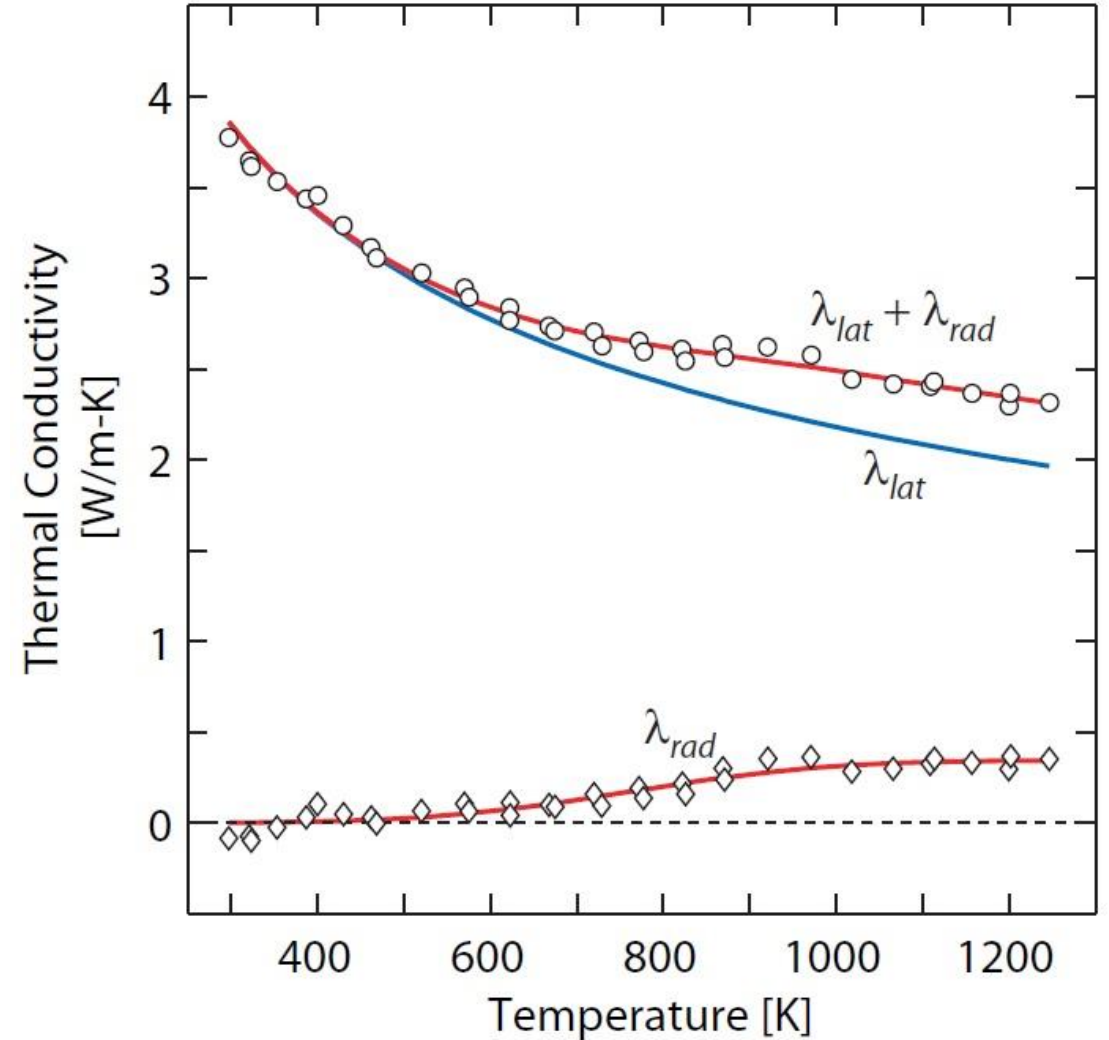
Thermal Conductivity (Lattice+Radiative Conductivity)

$$\lambda_L(P, T) = \lambda_0 \left(\frac{298}{T} \right)^n \left(1 + \frac{K'_T}{K_T} P \right)$$

λ_0 = conductivity at 0 GPa and 298 K
 K_T and K'_T = isothermal bulk modulus and its first pressure derivative
 n = an empirically derived fitting constant.

$$\lambda_R(T) = \frac{1}{2} \lambda_{R_{max}} \left[1 + \operatorname{erf} \left(\frac{T - T_R}{\omega} \right) \right]$$

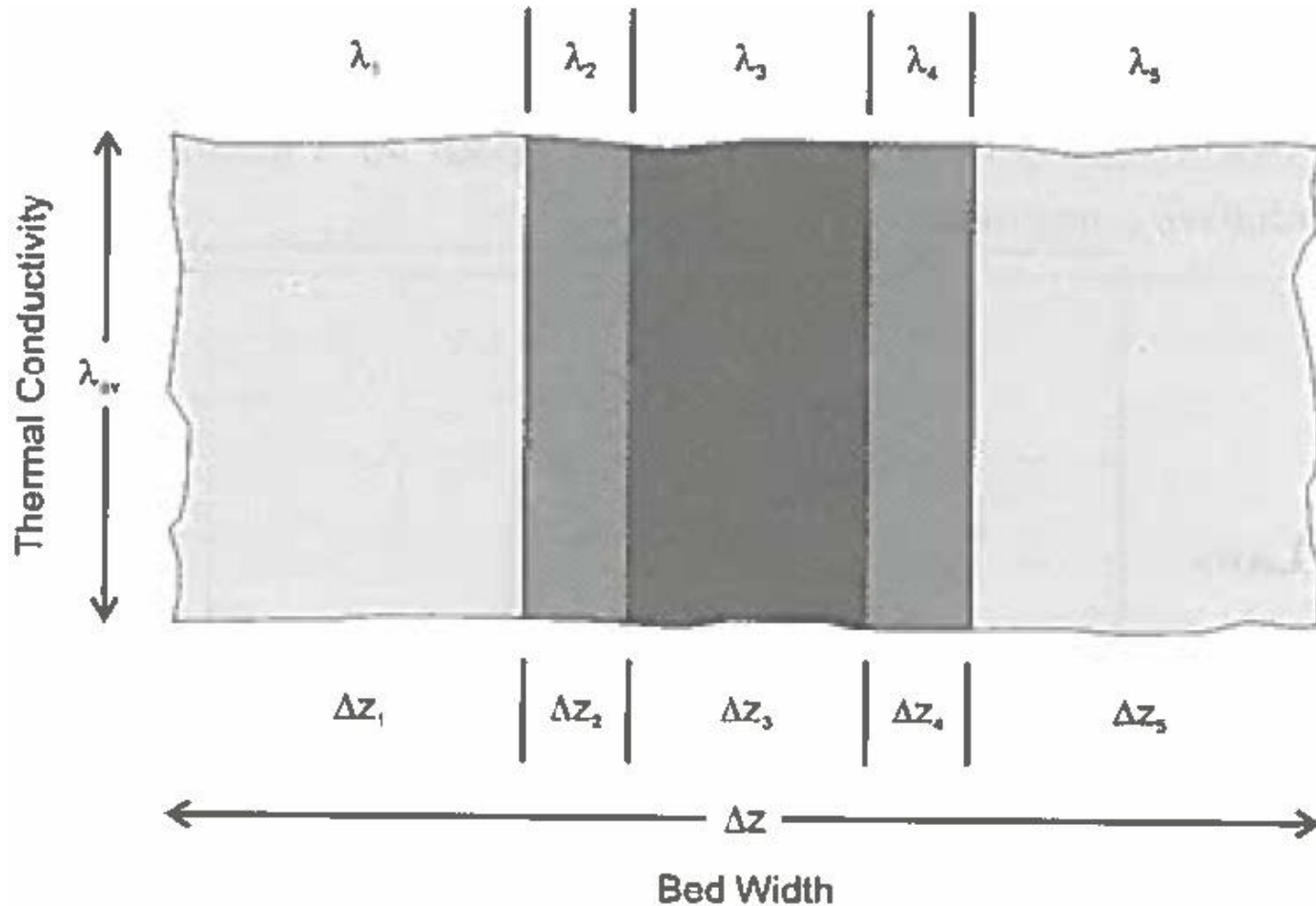
$\lambda_{R_{max}}$ = maximum radiative conductivity,
 ω = scaling factor
 T_R = temperature at $0.5\lambda_{R_{max}}$



Mean thermal conductivity of rocks (mixing models)

Arithmetic Mean: Beds are parallel to the direction of heat flow

$$\lambda_B = \sum_{i=1}^n \phi_i \lambda_i$$



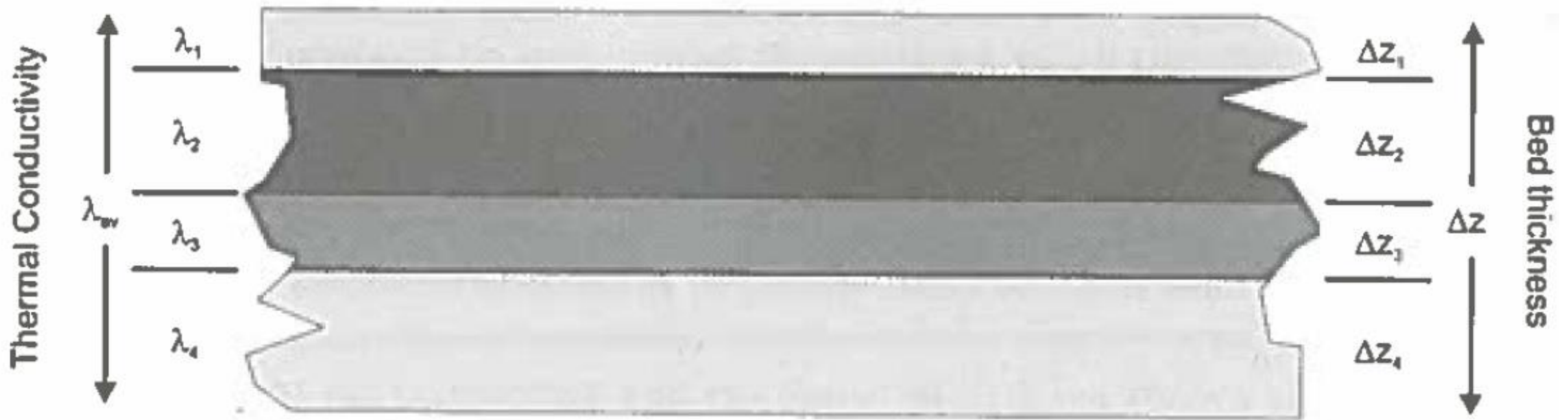
λ_i = thermal conductivity of i th bed
 z_i = thickness of the i th bed

It is applicable in presence of faults, igneous intrusions, and salt domes.

$$\lambda_{av} = [\Delta z_1 \times \lambda_1 + \Delta z_2 \times \lambda_2 + \Delta z_3 \times \lambda_3 + \Delta z_4 \times \lambda_4 + \Delta z_5 \times \lambda_5] / \Delta z$$

Mean thermal conductivity of rocks (mixing models)

Harmonic Mean: Beds are perpendicular to the direction of heat flow



$$\lambda_{av} = \Delta z / [\Delta z_1/\lambda_1 + \Delta z_2/\lambda_2 + \Delta z_3/\lambda_3 + \Delta z_4/\lambda_4]$$

$$\frac{1}{\lambda_B} = \sum_{i=1}^n \frac{\phi_i}{\lambda_i}$$

or

$$\frac{1}{\lambda_B} = \frac{1}{Z} \sum_{i=1}^n \frac{z_i}{\lambda_i}$$

λ_i = thermal conductivity of i th bed

ϕ_i = fractional proportion

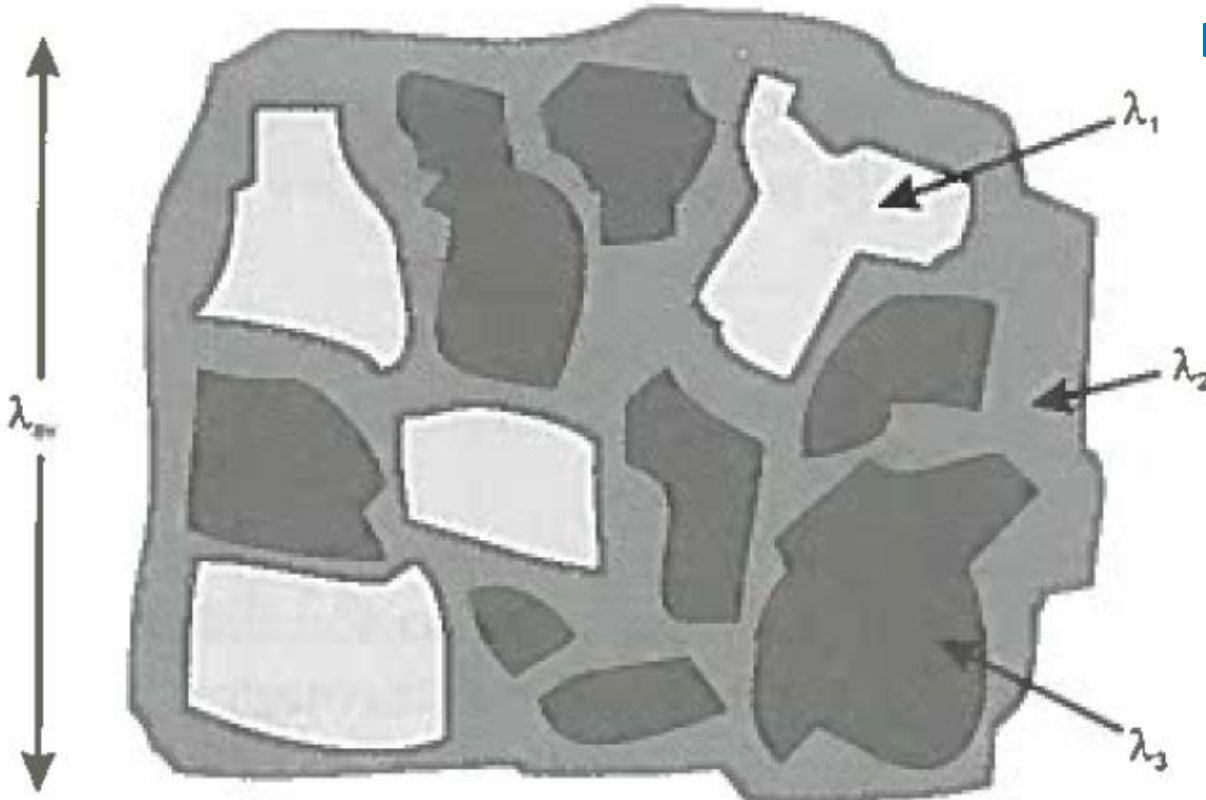
z_i = thickness of the i th bed

Z = total thickness of sequence

Mean thermal conductivity of rocks (mixing models)

Geometric or Square-Root Mean: several components of known conductivity are randomly oriented and distributed within a mixture

It is applicable to a rock composed of a mixture of minerals



Fractional content of:



= ϕ_1



= ϕ_2



= ϕ_3

λ_i = thermal conductivity of i th bed
 ϕ_i = fractional proportion

Geometric Mean

$$\lambda_B = \prod_{i=1}^n \lambda_i^{\phi_i}$$

Square-Root Mean

$$\sqrt{\lambda_B} = \sum_{i=1}^n \phi_i \sqrt{\lambda_i}$$

$$\lambda_{av} = \lambda_1^{\phi_1} \times \lambda_2^{\phi_2} \times \lambda_3^{\phi_3} \text{ OR } \lambda_{av} = [\phi_1 \times \sqrt{\lambda_1} + \phi_2 \times \sqrt{\lambda_2} + \phi_3 \times \sqrt{\lambda_3}]^2$$

Difference between computed and estimated value of λ is $\pm 5-10\%$

Thermal Conductivity and Porosity

$$\lambda(z) = \lambda_m^{1-\phi(z)} \lambda_f^{\phi(z)}$$

Geometric Mean

$$\lambda(z) = [(1 - \phi(z)) \times \lambda_m^{1/2} + \phi(z) \times \lambda_f^{1/2}]^2$$

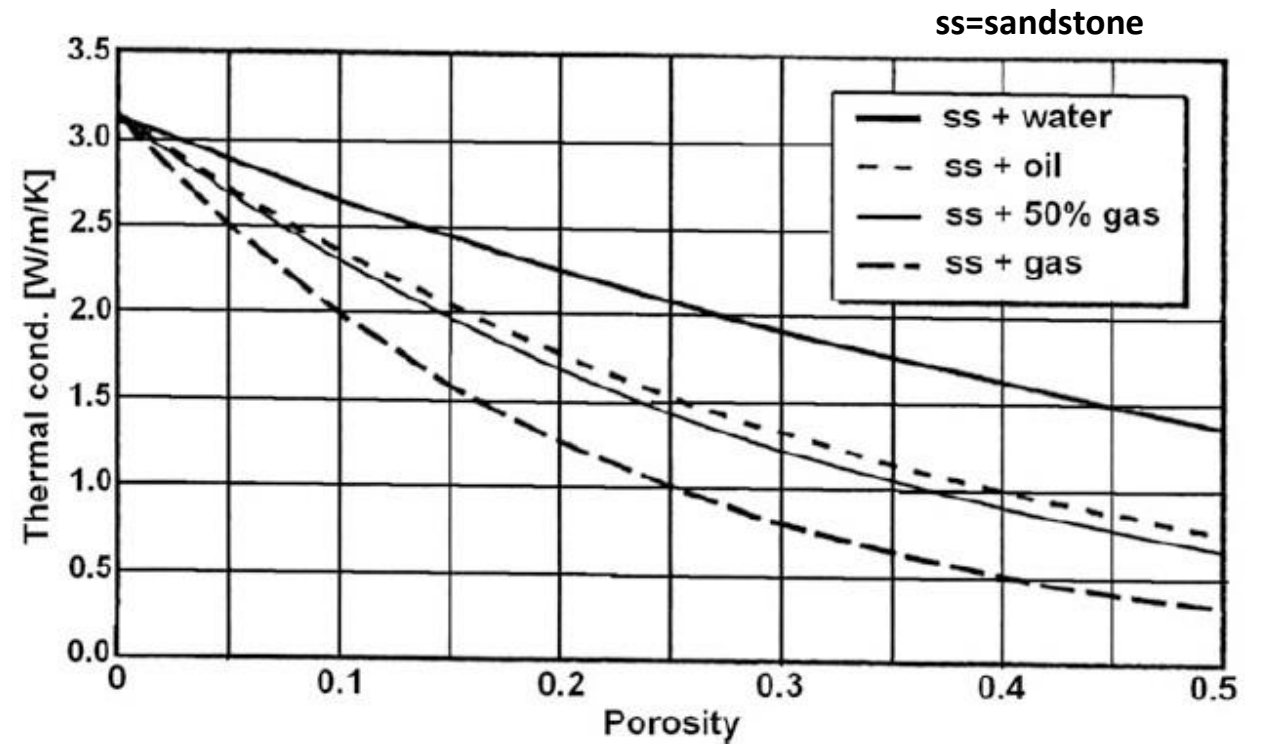
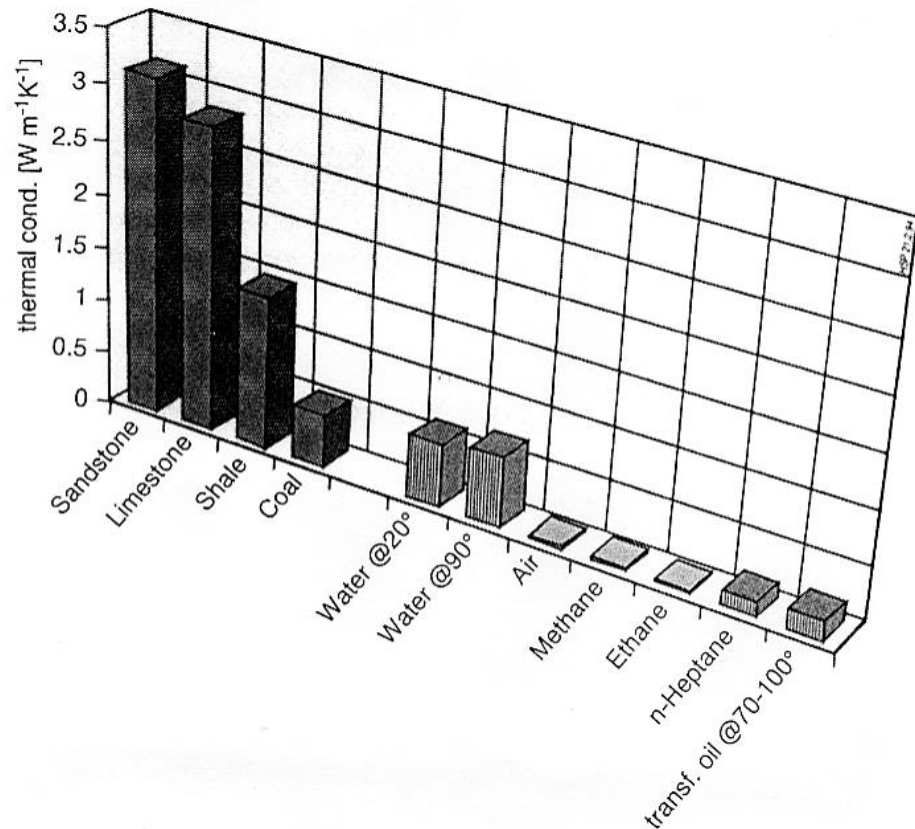
Square-Root Mean

$$\phi = \phi_0 e^{-bz}$$

$$\ln(\phi) = \ln(\phi_0) - bz$$

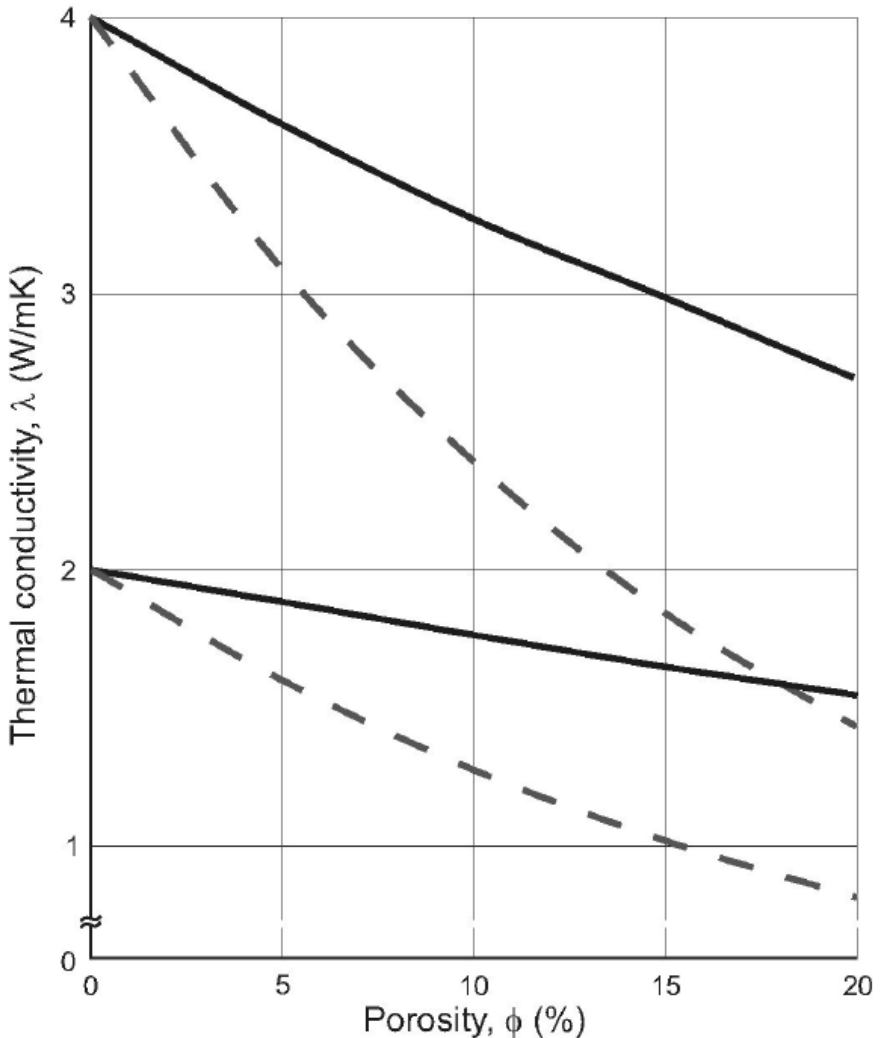
where λ_m and λ_w are the matrix and water thermal conductivity, ϕ is the porosity, b is the compaction factor and ϕ_0 is the surface porosity.

For z in km, b is 0.180 and 0.396 km⁻¹ in carbonate rocks, 0.298 and 0.461 km⁻¹ in marls and silty marls, 0.284 and 0.216 km⁻¹ in sandstones and calcarenites, and 0.293 and 0.379 km⁻¹ in shales and siltstones.



(Poelchau et al., 1997)

Thermal Conductivity and Porosity (Compaction Model)



Water filled
 Air filled

For sandstone

$$\phi = \phi_0 e^{-bz} \qquad \ln(\phi) = \ln(\phi_0) - bz \qquad (\text{Sclater and Christie, 1980})$$

b = compaction constant and ϕ_0 = porosity at the surface

$$1/\phi = 1/\phi_0 + Bz \qquad (\text{Falvey and Middleton, 1981})$$

B = compaction constant

For shale and limestone

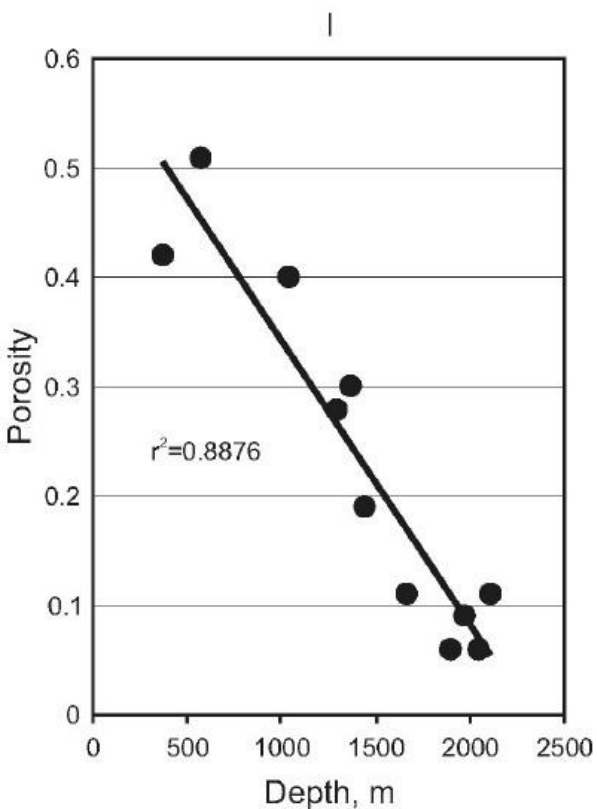
$$z = z_{\max}(1 - \phi)^C \qquad \ln(1 - \phi) = -\ln(z_{\max})/C + \ln(z)/C$$

(Baldwin and Butler, 1985)

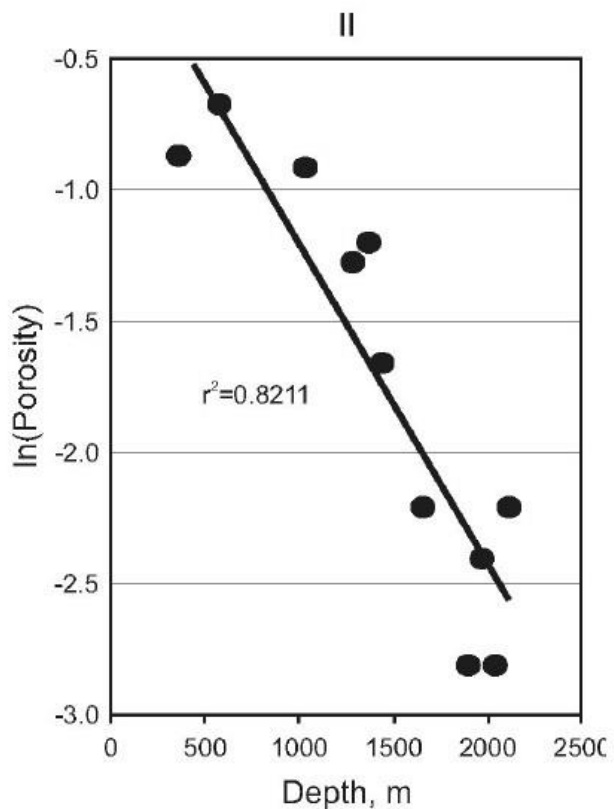
Z_{\max} = depth at which all fluid is expelled
 C = compaction constant

Thermal Conductivity and Porosity (Compaction Model)

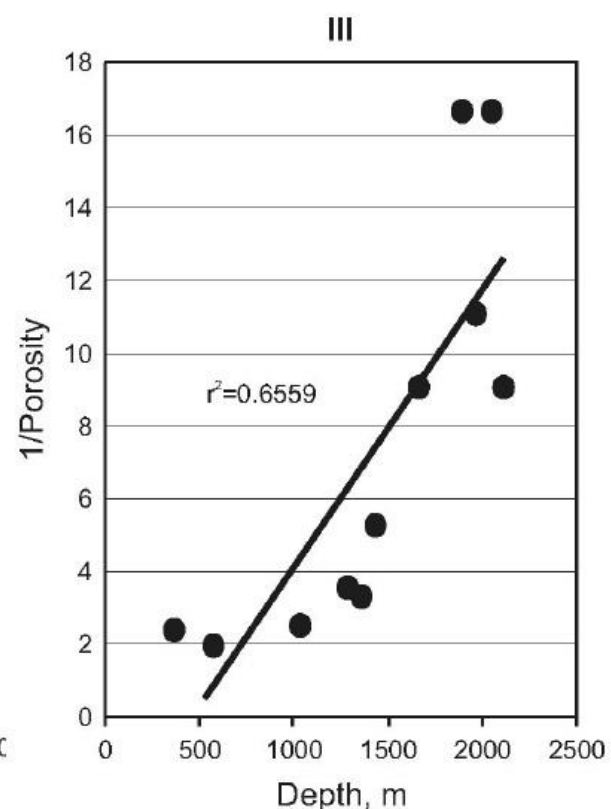
Different lithologies compact at different rates, then the graph producing the most linear plot is the most realistic



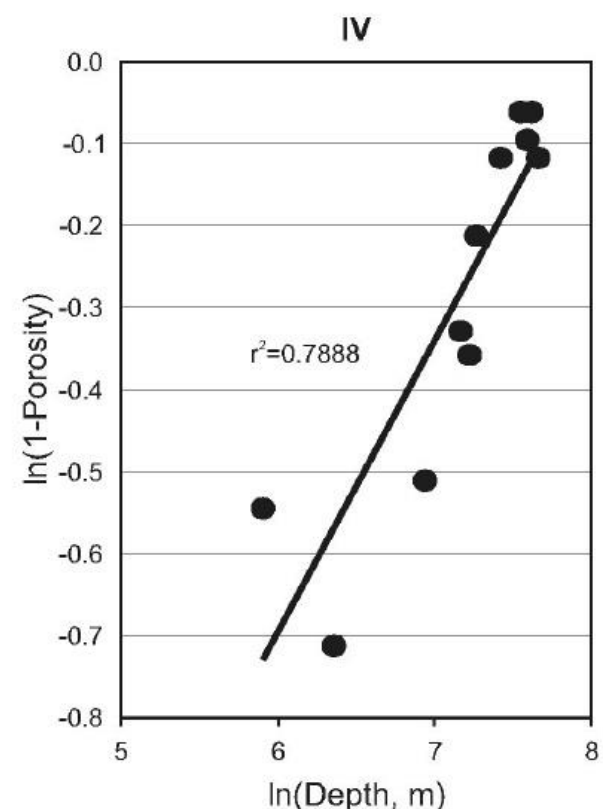
Linear decrease of porosity with depth



Compaction Model II
(Sclater and Christie, 1980)

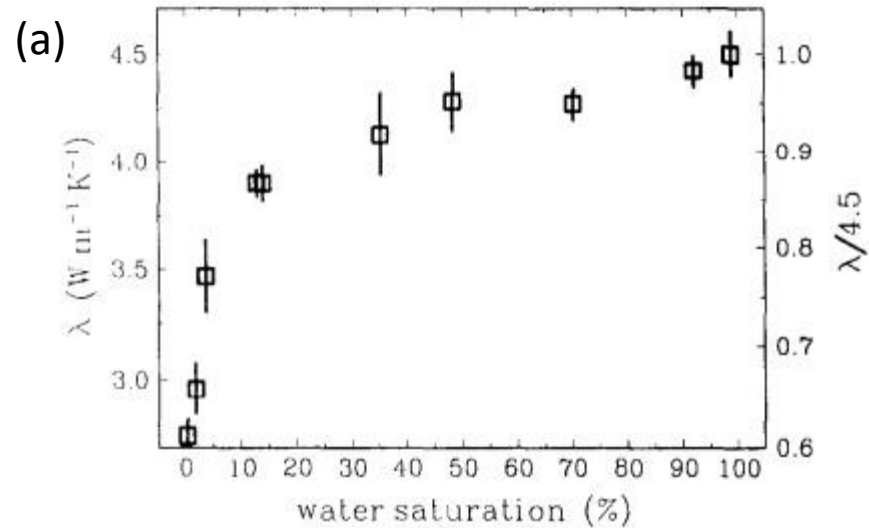


Compaction Model III
(Falvey and Middleton, 1981)

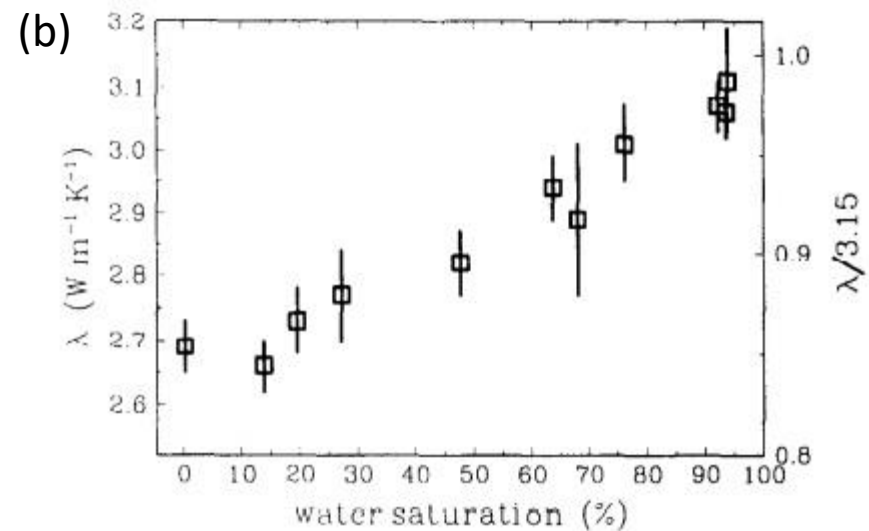


Compaction Model IV
(Baldwin and Butler, 1985)

Thermal Conductivity and Porosity (Partial Saturation)



- **(a) There is a rapid increase of thermal conductivity with saturation:** Starting from completely unsaturated conductivity of about 60% of the saturated value, 80% is reached at a saturation level of only about 10%. The remaining 20% deficit in conductivity is made up for during the remaining 90% of saturation.
- This occurs because the water filling of intergranular spaces, which account for only about 10%-20% of the total porosity, significantly reduces contact resistance between individual grains.



- **(b) Starting from completely unsaturated conditions, with only about 80% of the saturated conductivity, there is a linear increase until 100% is reached for complete saturation.**
- This occurs in the case only fractures contribute to the total porosity

Estimates of Thermal Conductivity (Hashin and Shtrikman)

Matrix thermal conductivity

$$k_{mo} = \frac{(k_U + k_L)}{2} \quad k_U = k_{max} + \frac{A_{max}}{1 - a_{max} A_{max}}$$

$$A_{max} = \sum_{j=1}^n \frac{v_j}{\frac{1}{(k_j - k_{max})} + a_{max}} \quad \text{for } k_j \neq k_{max}$$

k_{mo} = Thermal conductivity matrix
 k_U = Thermal conductivity upper bound
 k_L = Thermal conductivity Lower bound
 k_{max} = maximum k of the mineral phases
 $a_{max} = (3k_{max})^{-1}$
 v_j = volume fraction

Bulk thermal conductivity (considering porosity)

$$k_{HZ} = k_{mo} \frac{[(1 - \phi)(1 - r) + r\beta\phi]}{[(1 - \phi)(1 - r) + \beta\phi]}$$

$$\beta = \frac{(1 - r)}{3} \left[\frac{4}{2 + M(r - 1)} + \frac{1}{1 + (r - 1)(1 - M)} \right]$$

where for $a < 1$ $M = \frac{2\theta - \sin 2\theta}{2 \tan \theta \sin^2 \theta}$

and for $a > 1$ $M = \frac{1}{\sin^2 \theta} - \frac{\cos^2 \theta}{2 \sin^3 \theta} \ln \left(\frac{1 + \sin \theta}{1 - \sin \theta} \right)$

with $\theta = \cos^{-1}(1/a)$. For $a = 1$, $M = 3(1 - r)/(2 + r)$

K_{HZ} = computed thermal conductivity

r = ratio of thermal conductivity of the pore-filling water (k_w) and the matrix thermal conductivity (k_m)

a = aspect ratio (the ratio of the length of the unequal axis to the length of one of the equal axes): pores have spherical, oblate, and prolate shape for $a = 1$, $a > 1$ and $a < 1$.

Bulk Thermal Conductivity

$$k_{in} = k_m^{(1-\phi)} k_w^\phi \quad \phi = \phi_0 e^{-bz}$$

k_m and k_w are the matrix and water thermal conductivity, ϕ is the porosity, b is the compaction factor and ϕ_0 is the surface porosity.

$$k_m = 1.8418 + (k_o - 1.8418) \left(\frac{1}{0.002732 T + 0.7463} - 0.2485 \right) \quad k_o = k_m \text{ at } 20^\circ\text{C} \quad (\text{Sekiguchi, 1984})$$

$$k_w = 0.5648 + 1.878 \times 10^{-3} T - 7.231 \times 10^{-6} T^2 \quad \text{for } T \leq 137^\circ\text{C}$$

$$k_w = 0.602 - 1.31 \times 10^{-3} T - 5.14 \times 10^{-6} T^2 \quad \text{for } T > 137^\circ\text{C}$$

(Deming and Chapman, 1988)

Thermal Conductivity of Common Pore Fluids

Fluid	Conductivity ($\text{W m}^{-1} \text{K}^{-1}$)	Source
Water		
Fresh	$-7.42 \times 10^{-6} \times T^2 + 5.99 \times 10^{-3} \times T - 0.522$	1
Saline	$-7.42 \times 10^{-6} \times T^2 + 5.99 \times 10^{-3} \times T - 0.5$	
Hydrocarbon		
Oil	0.1	1
Gas	$0.000143 \times T - 0.0159$	1
Air	0.023	2

Note: T = absolute temperature in the range 295–450 K.

Source: 1 = Touloukian et al. (1970a), 2 = Giancoli (1984).

Thermal Conductivity and Temperature

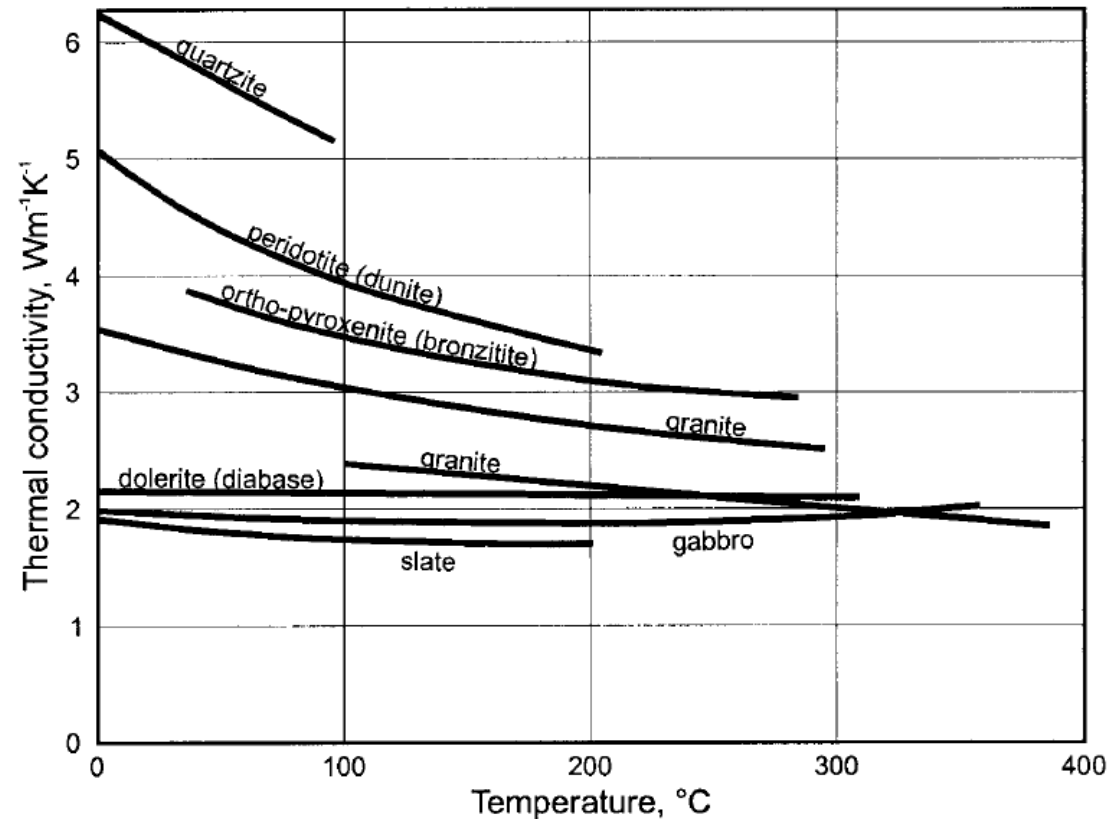
$$k_l = \frac{1}{a + bT}$$

Up to $T \leq 700 \text{ }^\circ\text{C}$

$a = 0.33 \text{ m K W}^{-1}$ and $b = 0.33 \times 10^{-3} \text{ m W}^{-1}$ for the upper crust

$a = 0.42 \text{ m K W}^{-1}$ and $b = 0.29 \times 10^{-3} \text{ m W}^{-1}$ for the lower crust

k_l is between 1 and $7 \text{ W m}^{-1} \text{ K}^{-1}$ (in most of rocks). It decreases from $3.0 \text{ W m}^{-1} \text{ K}^{-1}$ at the surface to about $2.0 \text{ W m}^{-1} \text{ K}^{-1}$ at $400 \text{ }^\circ\text{C}$, and then decreases only very slightly at higher temperatures. In the lithospheric mantle, k_l is $2.0\text{--}2.5 \text{ W m}^{-1} \text{ K}^{-1}$.



Thermal Conductivity and Temperature

$$\lambda = \frac{\lambda_0}{1 + cT^{\circ}\text{C}} \quad \lambda(T) = A + \frac{B}{350 + T^{\circ}\text{C}}$$

(Cermak and Rybach, 1982)

(Zoth and Hanel, 1988)

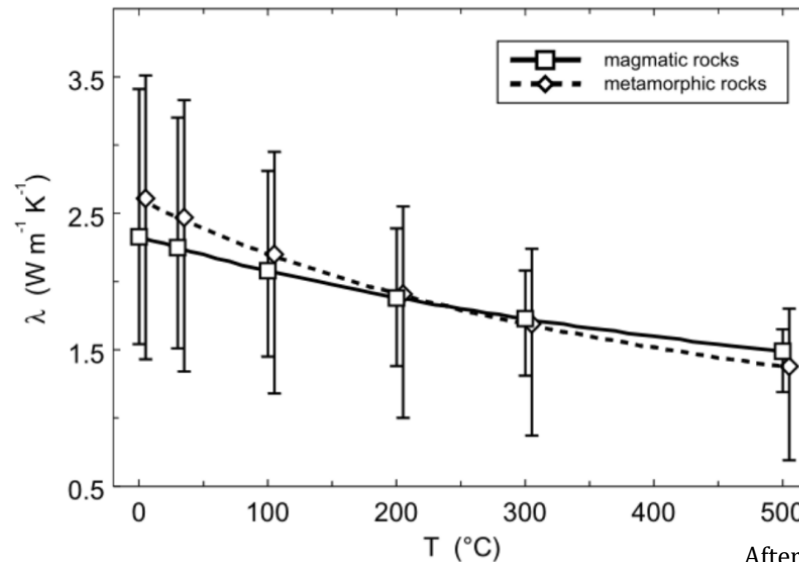
where λ_0 is the thermal conductivity at 0°C and near-surface pressure conditions, and c is a material constant (in the range of 0–0.003°C⁻¹). Empirical constants A and B are determined from a least-squares plot of measured data for different rock types.

$$k(T) = \frac{k_0}{0.99 + T(a - b/k_0)}$$

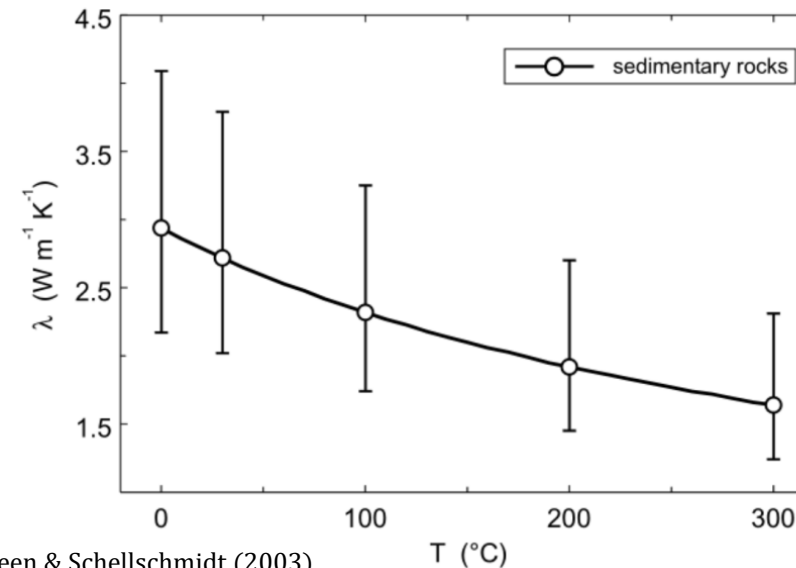
$k(0)$ = thermal conductivity at 0°C

$a = 0.0030 \pm 0.0015$, $b = 0.0042 \pm 0.0006$ for crystalline rocks, and
 $a = 0.0034 \pm 0.0006$, $b = 0.0039 \pm 0.0014$ for sedimentary rocks.

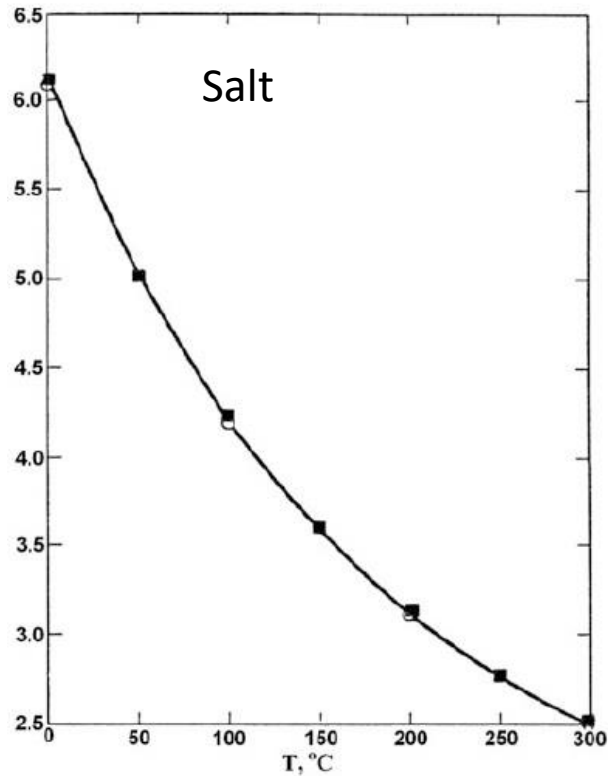
- For sedimentary rocks at T of up to 573 K, there is a reduction of λ of a factor of 2
- For volcanic rocks λ decreases to ~1173 K, at which point is ~50% of its value at ambient T (above this T the radiative component of λ starts to rise)



After Vosteen & Schellschmidt (2003)



Thermal Conductivity and Temperature



Temperature effect on thermal conductivity in $10^{-3} \text{ cal s}^{-1} \text{ cm}^{-1} \text{ }^\circ\text{C}$

Formation	ρ (g/cm ³)	0 °C	50 °C	100 °C	200 °C	300 °C	400 °C	500 °C
Dolomite	2.83	11.9	10.30	9.30	7.95			
Limestone	2.60	7.20	6.14	5.53	4.77			
Limestone, parallel	2.60	8.24	7.55	7.04	6.54			
Limestone, perpend.	2.69	6.09	5.68	5.41				
Quartz-sandstone, parallel	2.64	13.6	11.80	10.60	9.00			
Quartz-sandstone, perpend.	2.65	13.1	11.40	10.30	8.65			
Shale			2.17	2.25	2.38	2.54	2.68	2.83
Slate, parallel	2.70	6.35	6.05	5.85	5.50	5.20	4.95	4.80
Slate, perpend.	2.76	4.83	4.40	4.23	4.08			
Calcite, parallel		27.3	22.40	19.00	15.1	12.30	10.30	
Calcite, perpend.		16.3	13.50	11.80	9.70	8.40	7.40	
Halite	2.16	14.6	12.00	10.05	7.45	5.95	4.98	

The reciprocal of thermal conductivity is a linear function of T :

$$\lambda^{-1} = a_0 + a_1 T \quad \text{For } T \leq 300 \text{ }^\circ\text{C}$$

Rock	a_0 (m °C/W)	$a_1 \times 10^4$ (m/W)
Salt	0.1605	7.955
Granite	0.3514	3.795
Basalt	0.8684	-6.146
Shale _{vert}	0.5297	2.215
Shale _{hor}	0.7167	2.949

$$\lambda_T = \lambda_{20} - (\lambda_{20} - 3.3) \left[\exp\left(0.725 \frac{T - 20}{T + 130}\right) - 1 \right]$$

where λ_{20} is λ at 20 °C in $10^{-3} \text{ cal s}^{-1} \text{ cm}^{-1} \text{ }^\circ\text{C}$

Thermal Conductivity and Temperature

$$\lambda = (T_0 T_m / (T_m - T_0)) (\lambda_0 - \lambda_m) ((1/T) - (1/T_m)) + \lambda_m$$

(Sekiguchi et al., 1984)

$\lambda_m = 1.05 \text{ Wm}^{-1}\text{K}^{-1}$ (calibration coefficient)

λ_0 = thermal conductivity at T_0

T_0 = lab temperature (K)

$T_m = 1473 \text{ K}$ (calibration coefficient)

Correction applicable for a T range 0-300°C, independent on mineralogy, porosity and pore fluid

For individual lithology a different correction can be applied: $\ln(\lambda) = \ln(\lambda_0) + \ln(T/T_0)M$ with $M = \text{constant}(\text{lithology})$

Correction applicable for a T range 300-500 K (depths 6-8 km)

Coefficient, M , for Equation (4.60) for Different Lithologies

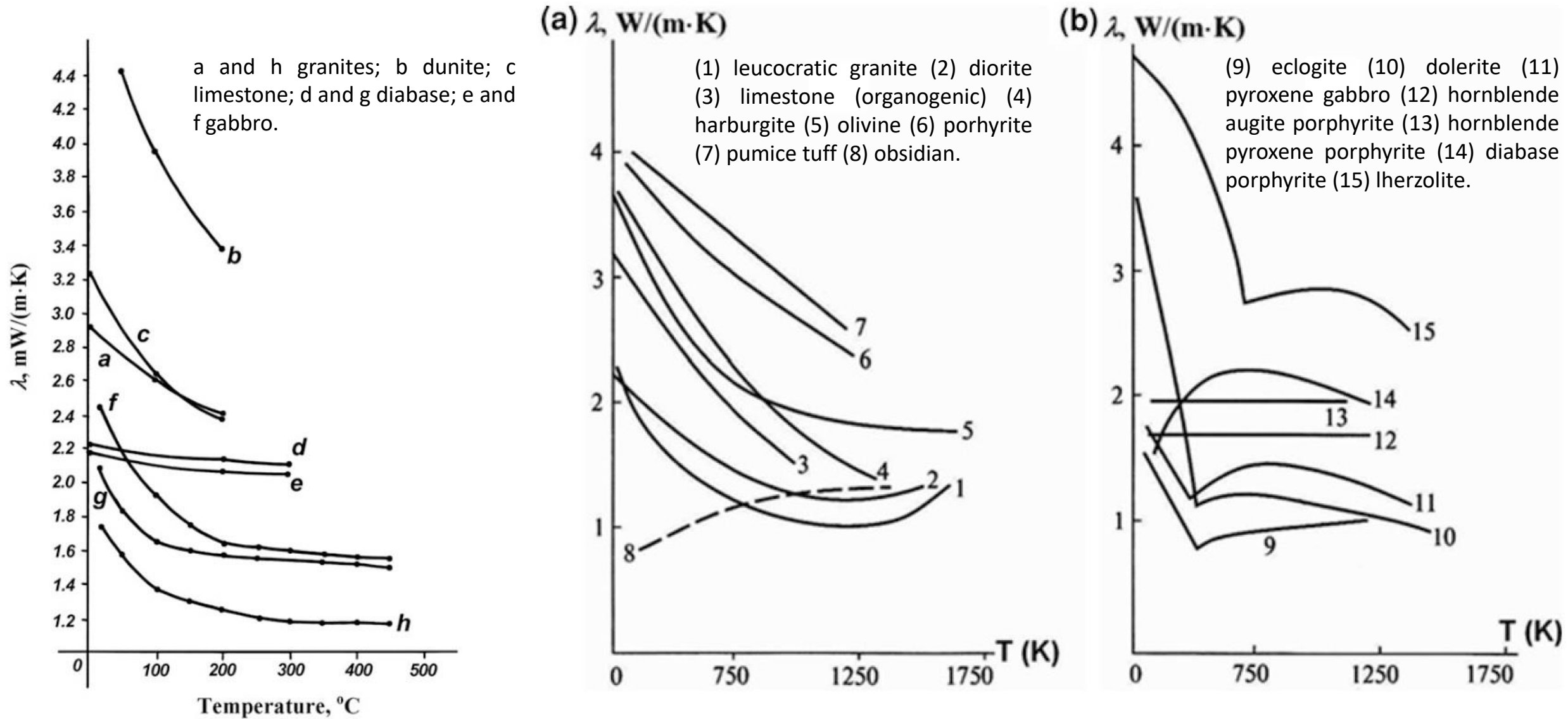
Lithology	M	Lithology	M
Sandstone	Variable	Coal	0.714
Limestone	-0.185	Dolomite	0.0
Clay	0.0	Halite	-1.37
Granite	0.0	Loose sand	0.0
Basalt	0.5	Tuff	0.25

Source: Touloukian et al. (1970b).

For some lithologies (basalts, coal, and tuff) λ increases

Thermal Conductivity of Rocks

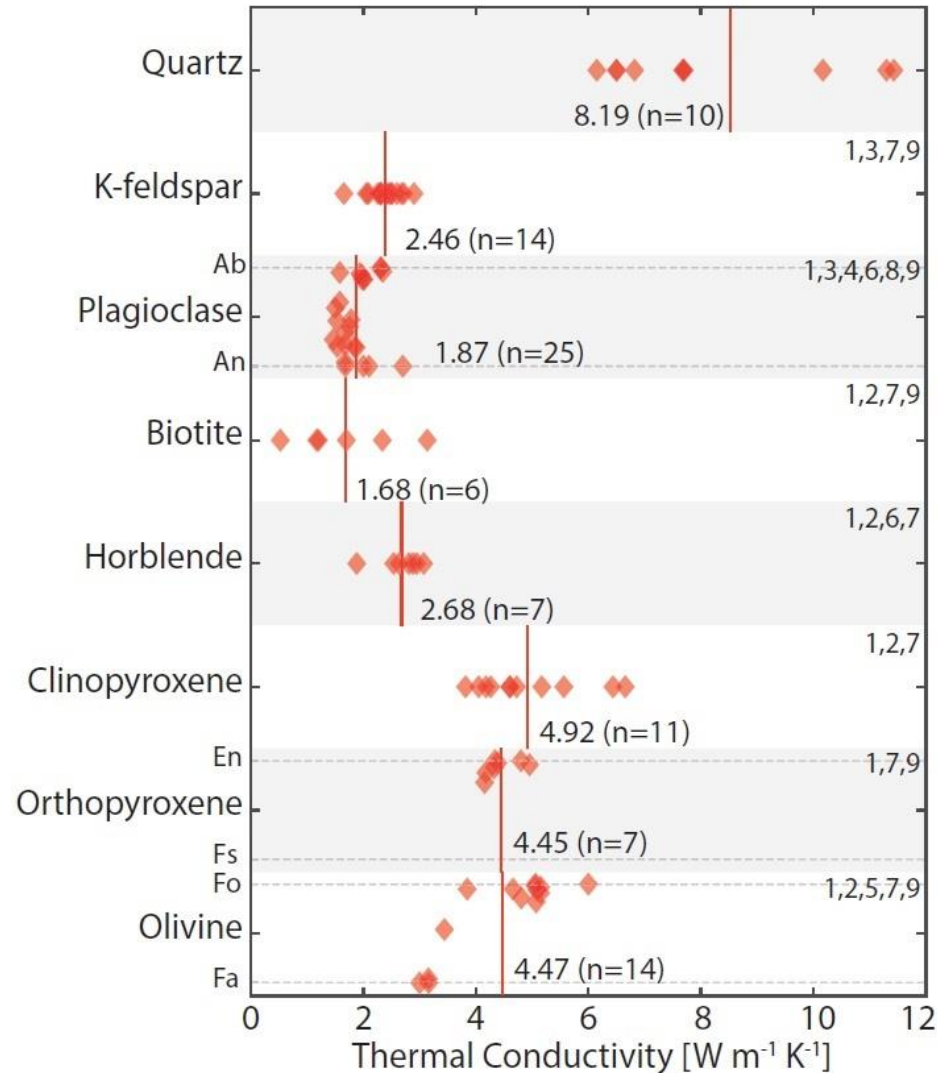
There is not always a clear correlation between thermal conductivity and temperature



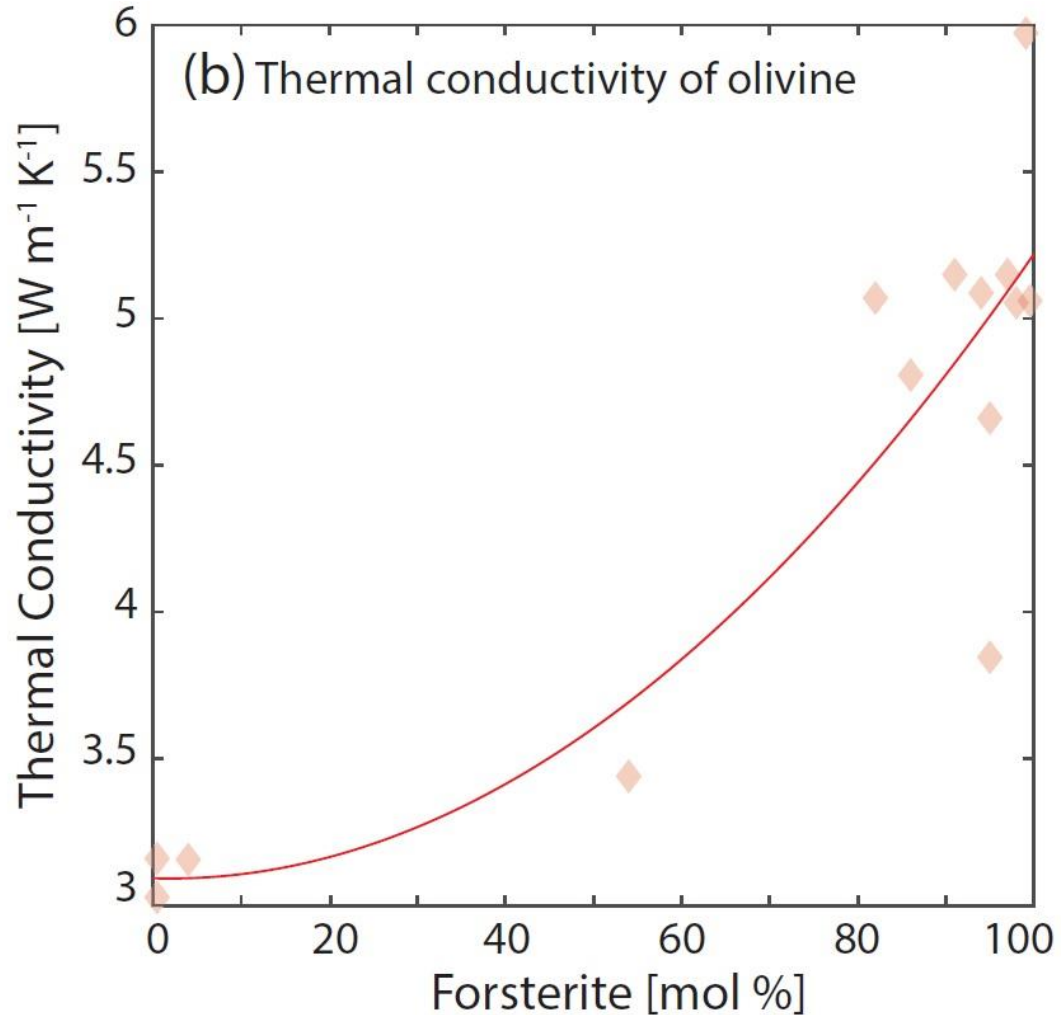
(after Dortman, 1976 and Yerofeyev et al., 2009).

Thermal Conductivity of Rocks

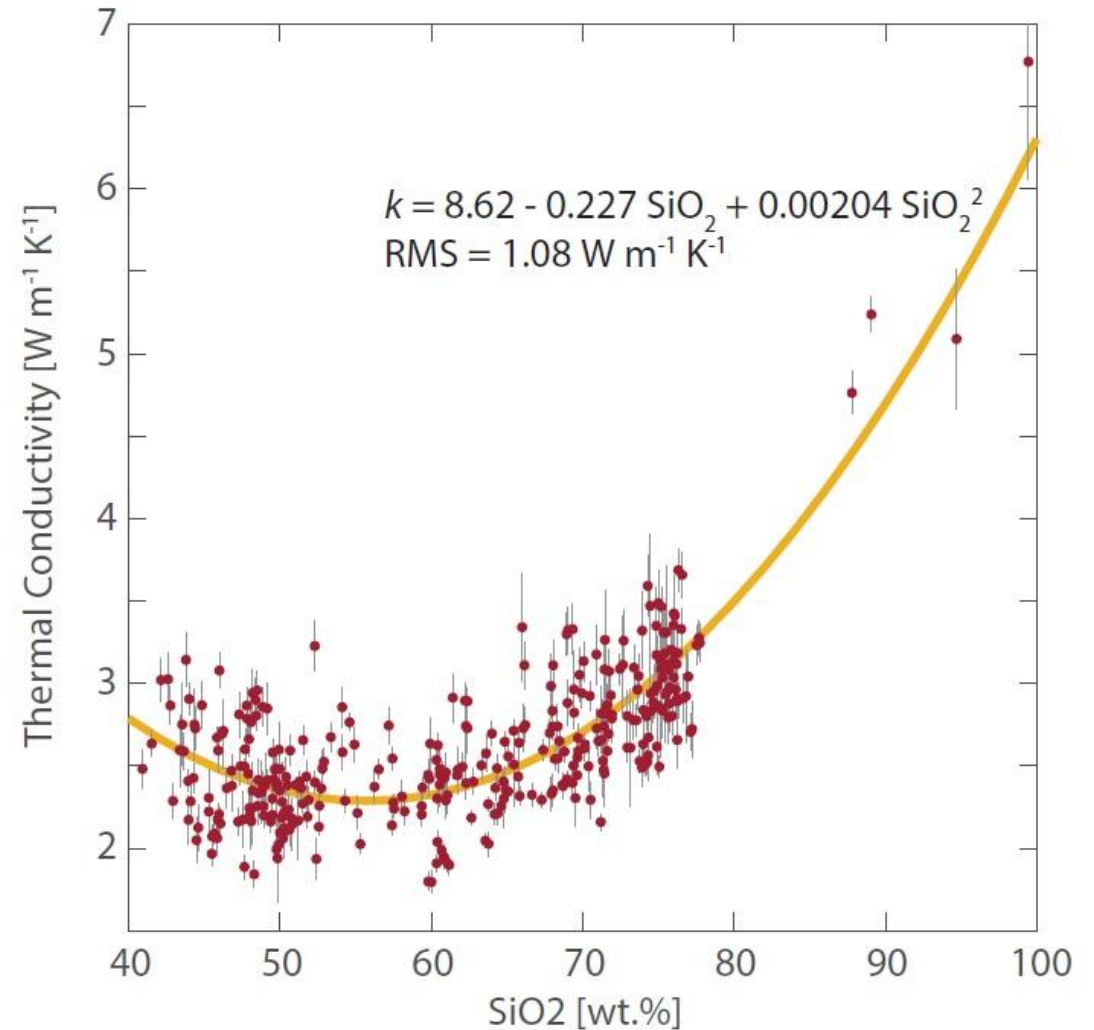
- Quartz has a conductivity value three to four times higher than the feldspar minerals, while pyroxenes and olivine have significantly higher conductivities than that of the feldspars.
- Conductivity decreases with increasing maficity, as a direct result of decreasing quartz content.
- Higher conductivity values observed in peridotites and high-magnesium rocks are due to the abundance of olivine and pyroxene.



Thermal Conductivity vs Composition



Jennings et al., 2019, GJI, 219



Goes et al., 2020, PEPI, 306

- The dominant compositional control on thermal conductivity is SiO_2 , both to its relatively high abundance in comparison to the other oxides and also its presence throughout the entire compositional range. At high SiO_2 values (>60 per cent), a rapid increase in thermal conductivity is the result of increased SiO_2 uptake into quartz.

Thermal Conductivity vs Pressure

$$\lambda = \lambda_0(1 + \delta p)$$

λ_0 = thermal conductivity coefficient at normal pressure and δ = pressure coefficient of the thermal conductivity

- From experiments at pressures up to 10,000–12,000 kg cm⁻² the calculated values of δ are small: for **rocksalt** 3.6×10^{-5} kg⁻¹ cm²; for **dry and wet limestone** with a density of 2.31 g/cm³, 9.5×10^{-5} and 1.35×10^{-5} kg⁻¹ cm², and for **dry and wet sandstone** with a density of 2.64 g/cm³, 2.5×10^{-4} and 5.7×10^{-5} kg⁻¹ cm².
- The correction on λ for igneous and metamorphic rocks at a pressure up to 100 MPa is positive (on average about 10 %). Under a higher pressure, there is a slight increase of λ , on average by 0.002 W m⁻¹K⁻¹per 100 MPa, due to the crystal lattice deformation up to the elastic limit.
- For granite and metamorphic rocks, there is about a 10 % increase in λ over the entire range of P from 0 to 500 MPa, but the increase is the greatest over the first 50 MPa.

Sample	λ at 0.4 kg/cm ² (10 ⁻³ cal/cm s °C)	Pressure (kg/cm ²)	δ (10 ⁻³ kg/cm ²)
<i>Sandstone</i>			
No. 172	6.84	0.4–164	0.434
No. 224	5.51	0.4–164	0.612
No. 234	6.69	0.4–164	0.626
No. 286	7.50	0.4–164	0.931
No. 313	9.44	0.4–164	0.905
No. 343	8.51	0.4–41	3.43
<i>Limestone</i>			
No. 19	5.06	0.4–164	0.599
No. 34	4.22	0.4–164	0.185
No. 102	7.67	0.4–164	0.406
No. 260	4.33	0.4–123	0.808
No. 270	3.53	0.4–164	0.579
<i>Dolomite</i>			
No. 103	7.62	0.4–123	1.71
No. 365	6.18	0.4–123	0.928

Mineral	P_{\max} (MPa)	$\lambda^{-1} \partial \lambda / \partial P$ (10 ⁻⁴ MPa ⁻¹)
Mg ₂ SiO ₄	500	16.0
Mg _{1.8} Fe _{0.2} SiO ₄	200	12.0
Mg _{1.8} Fe _{0.2} SiO ₄	1,000	9.0–12.0
Mg _{1.8} Fe _{0.2} SiO ₄	4,800	~ 4.8
Mg _{1.8} Fe _{0.2} SiO ₄	5,600	6.0–7.0
Mg _{1.8} Fe _{0.2} SiO ₄	5,600	5.0–6.0
Mg _{1.8} Fe _{0.2} SiO ₄	8,300	3.2–3.8
Mg _{1.8} Fe _{0.2} SiO ₄	9,000	5.5
Mg _{1.8} Fe _{0.2} SiO ₄	10,000	4.4
Mg _{0.85} Fe _{0.15} O ₃	5,600	7.0
MgO	5,000	2.0–4.0
MgO	1,200	5.0
Coesite	4,000	3.9
Coesite	5,600	1.4–4.4
Py ₂₅ Al ₇₄ Gr ₁ (garnet)	8,300	4.6
NaAlSi ₂ O ₆	3,000	4.6

Thermal Conductivity vs Temperature, Pressure, and Density

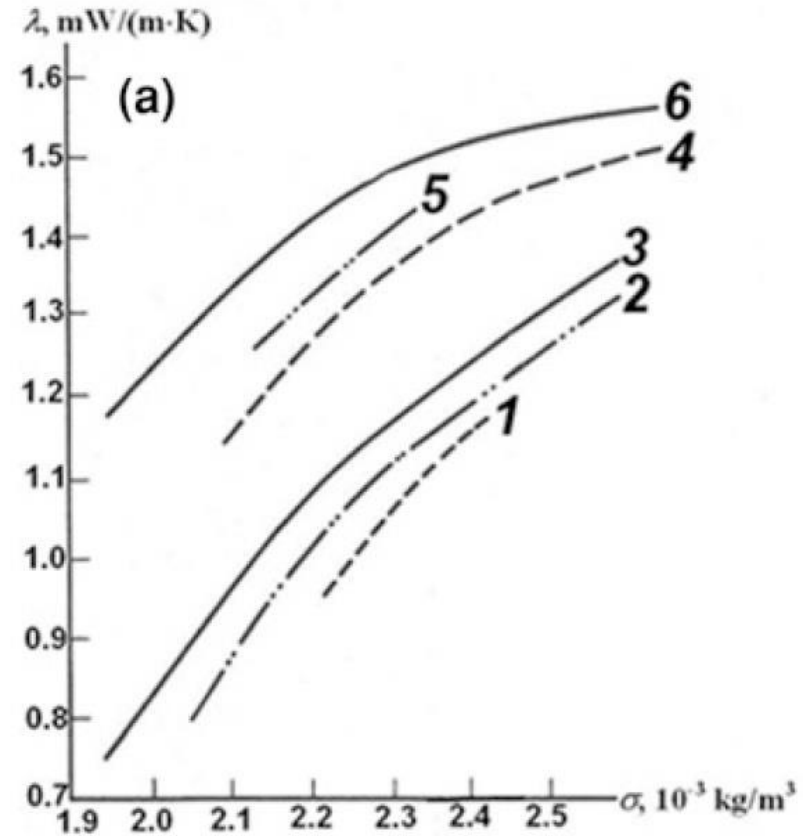
- Thermal conductivity of most rocks at crustal conditions varies inversely with temperature and directly with pressure (or depth) according to the relation.

$$k(T,z) = k_0 (1 + c z)/(1 + bT)$$

$b = 1.5 \times 10^{-3} \text{ K}^{-1}$ for the upper crust and $b = 1.0 \times 10^{-4}$ for the lower crust.

c (pressure coefficient) = $1.5 \times 10^{-3} \text{ km}^{-1}$ for the entire crust

$k_0 = 3.0$ and $2.6 \text{ W m}^{-1} \text{ K}^{-1}$ for the upper and lower crust, respectively.



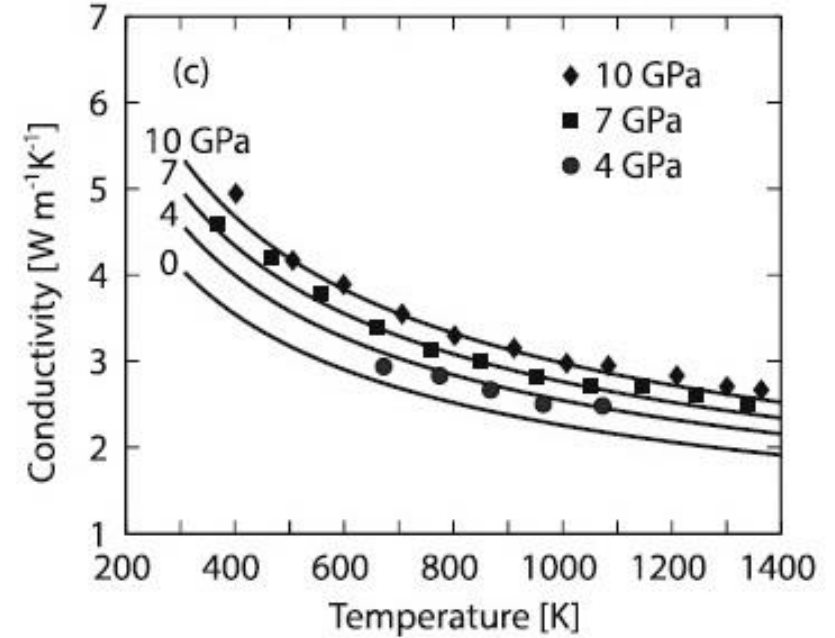
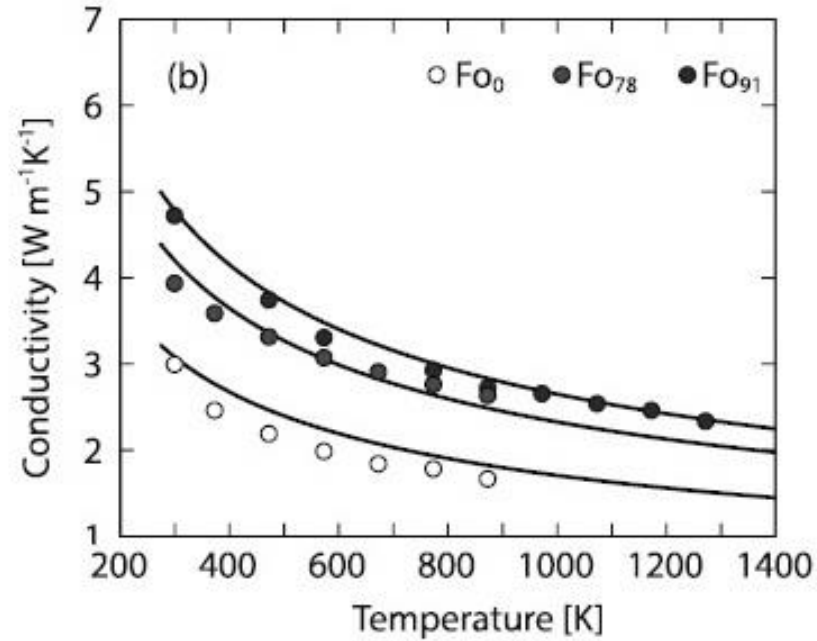
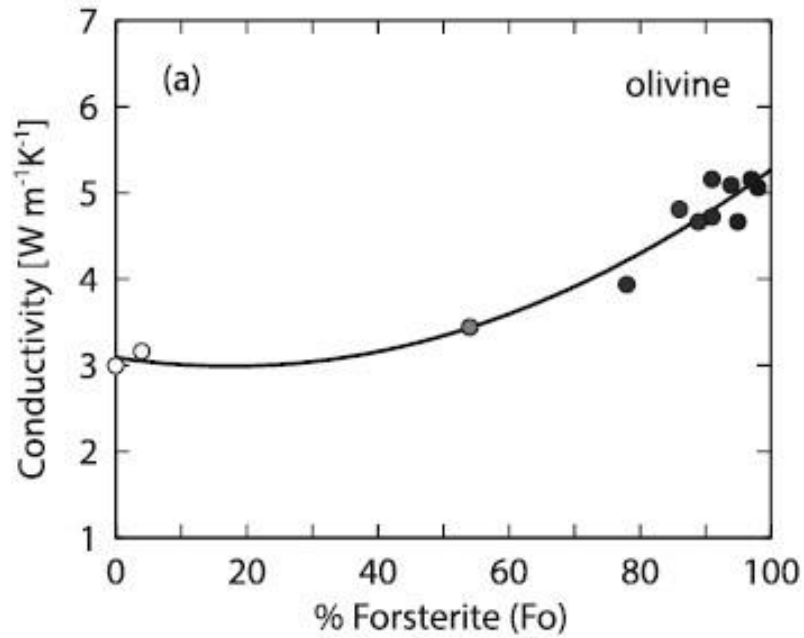
(1) dry siltstone (2) dry argillite (3) dry sandstone (4) water-saturated siltstone (5) water-saturated argillite (6) water-saturated sandstone.

$$\ln \lambda_{(T=293\text{K})} = 0.36\sigma - 0.20$$

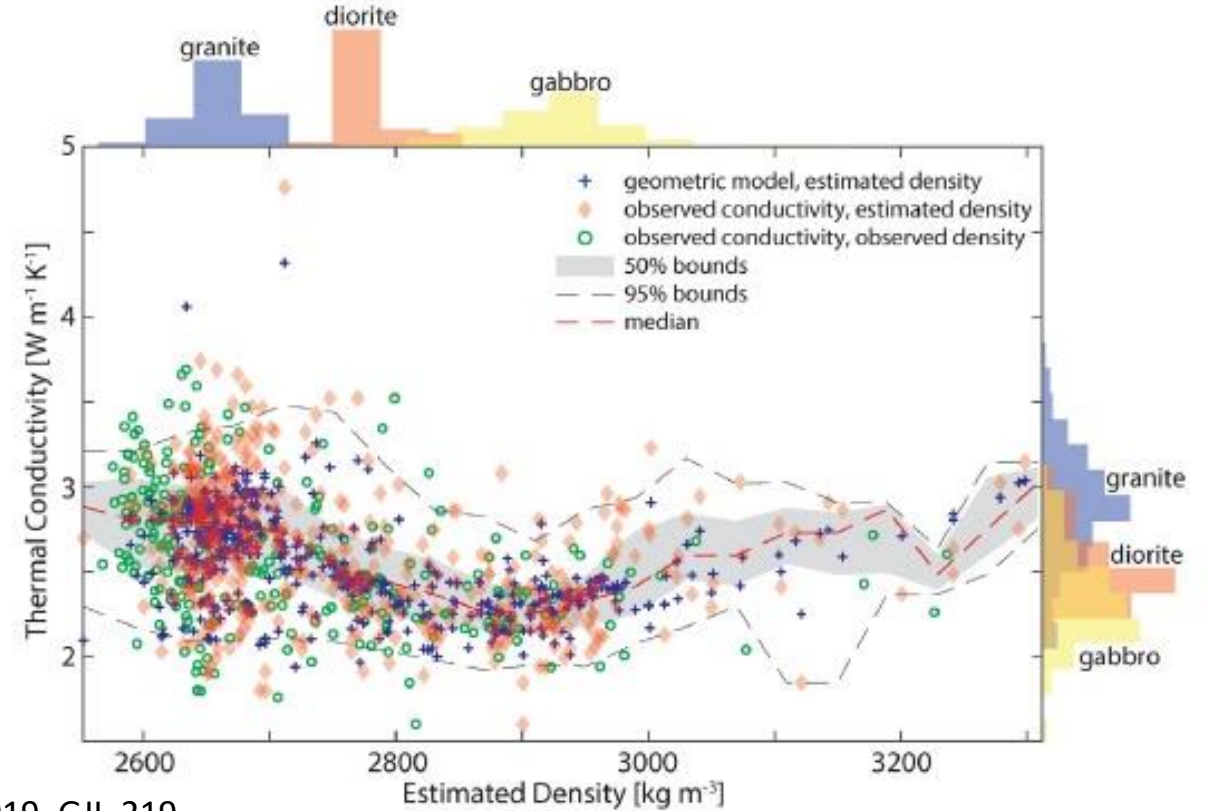
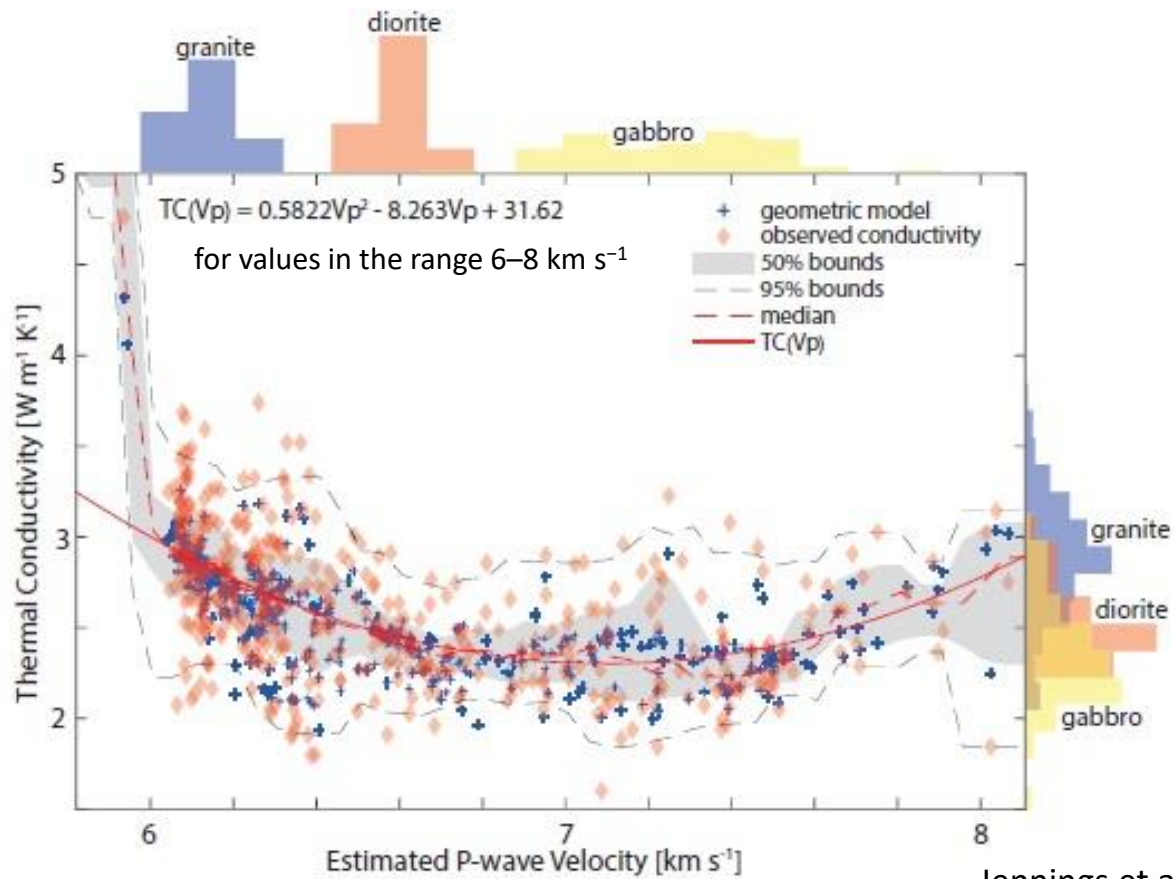
σ =density with a correlation coefficient of 0.74

Thermal Conductivity vs Temperature, Pressure, and Composition

$$k(P,T) = (3.09 - 1.17 Fo + 3.35 Fo^2) (298 T^{-1})^{0.49} (1 + P K_T' K_T^{-1})$$



Thermal Conductivity vs Velocity and Density

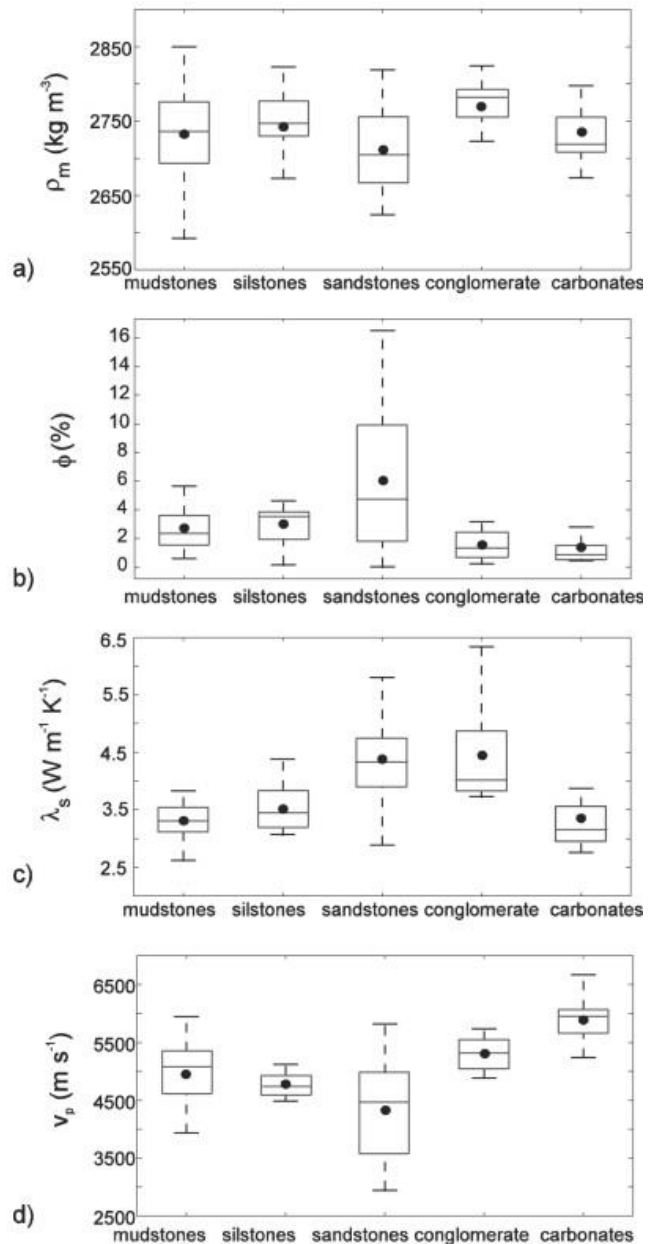


Jennings et al., 2019, GJI, 219

- *P*-wave velocity increases while thermal conductivity rapidly decreases from ~ 5.8 to 6.3 km s^{-1} and tends to $\sim 2.4 \text{ W m}^{-1} \text{K}^{-1}$ for velocities $> 6.5 \text{ km s}^{-1}$. This trend occurs through the entire distribution of granite and through the compositional distribution of both diorite and gabbroic samples (decrease in the amount of quartz present and consequent increase in feldspars and mafics).
- As *P*-wave velocity increases above 7.5 km s^{-1} , conductivity begins to increase slightly due to the increasing maficity and a transition from gabbroic to ultramafic compositions (increase of pyroxenes and olivine with respect of feldspars).
- The scatter of the conductivity-density values is due because occurring felsic minerals such as quartz, albite, and orthoclase all share similar densities between 2650 and 2570 kg m^{-3} and quartz has a much larger conductivity value than feldspar minerals.

Thermophysical Properties

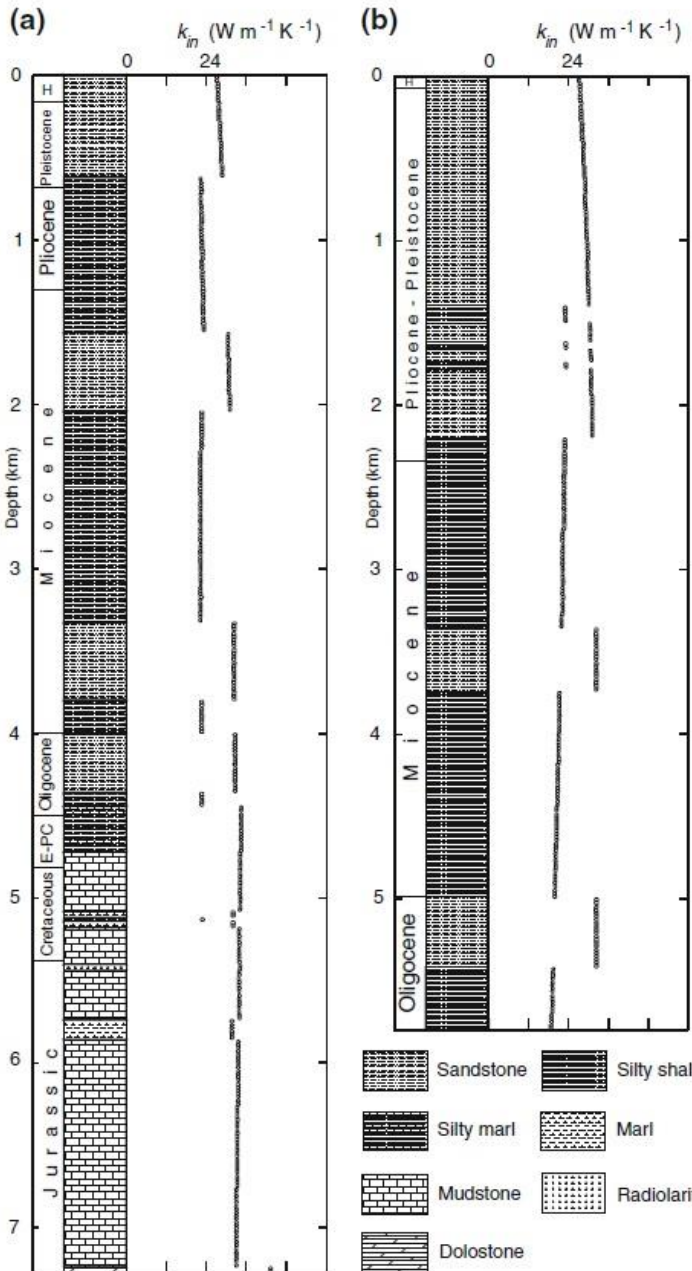
- Thermal conductivity of rocks is a petrophysical property which depends on the rock's porosity, mineralogy, and size and distribution of mineral grains.
- The high variation of saturated thermal conductivity in the sandstones and conglomerates of Paleozoic formations is linked to heterogeneous distribution of quartz grains of varying size and variation in porosity within the cores.
- Due to the high clay content, the sandstones have sometimes very low quartz content.



Jorand et al., 2015, Geothermics, 53

Statistical variations of rock properties for the different lithologies of Paleozoic formations: (a) matrix density, (b) porosity, (c) saturated thermal conductivity, (d) P-wave velocity . Full circle – mean, box – quartile; line – median.

Thermal Conductivity of Rocks (empirical relationships)



Thermal conductivity can be derived for crystalline rocks from other well-log parameters: Density (RHOB, g/cm³), photoelectric capture cross section (PEF, barns/electron, b/e), full-waveform sonic (v_p and v_s , m/s) and temperature (T, K).

$$\lambda = 0.7531 + 0.1005 \times (a v_m \mu^2 / 3 K_S T) \quad \text{Williams and Anderson, 1990}$$

$$a = \text{mean interatomic distance} \approx 10^{-9} \times ((5.32 \times \text{PEF}^{0.2778} + 13.8) / (1000 \times \text{RHOB}))^{1/3} \text{ m}$$

$$v_m = \text{mean phonon velocity} = 3^{1/3} (1/v_p^3 + 2/v_s^3)^{-1/3} \text{ m s}^{-1}$$

$$\mu = \text{shear modulus} = 1000 \times \text{RHOB} \times v_s^2$$

$$K_S = \text{bulk modulus} = 1000 \times \text{RHOB} (v_p^2 - \frac{4}{3} v_s^2)$$

For siliclastic rocks with water-filled pores

$$\lambda = 77 \times V / (a \times (c + T)) \text{ W m}^{-1} \text{ K}^{-1} \quad a = 1.039, c = 80.031.$$

V=acoustic velocity (km/s) T=temperature (°C)

Houbolt and Wells, 1980

Thermal Conductivity of Anisotropic Rocks

Thermal conductivity parallel to the mineral sheets >> Thermal conductivity perpendicular to the sheets

Average Thermal Conductivity for a Number of Sheet Silicates, Parallel and Perpendicular to Main Cleavage Plane, and for a Mixed Aggregate

Mineral	Average Conductivity (W m ⁻¹ K ⁻¹)		
	Parallel	Perpendicular	Aggregate
Muscovite	3.89	0.52	2.35
Phlogopite	4.01	0.48	
Biotite	3.14	0.52	2.02
Lepidolite		0.48	2.30
Phyrophyllite	6.17	1.15	4.50
Talc	11.5		2.97
Chlorite			2.52
Clinochlore	10.3	1.97	

Sources: Diment and Pratt (1988) and Williams and Anderson (1990).

Thermal conductivity remains constant or decreases with depth in anisotropic rocks, since during compaction there is:

- Water expulsion (e.g., porosity decreases from 75% to 60% in 50 m), then $\lambda >>$
- Progressive rotation of clay sheets to a preferred horizontal orientation, then matrix thermal conductivity, $\lambda_m <<$

Verical matrix thermal conductivity of the clay and mica during burial is: $\lambda_m = 2.899 - 0.251z$

For a shale (anisotropic rock):

$$\lambda_{av} = \lambda_{max}^{2/3} \times \lambda_{min}^{1/3}$$

Since anisotropy decreases with increasing conductivity:

$$\lambda_z = \exp[(\ln(\lambda_{ag}) - 0.6267/0.5480)]$$

λ_z = Thermal conductivity perpendicular to the sheet λ_{ag} = Thermal conductivity of the aggregate

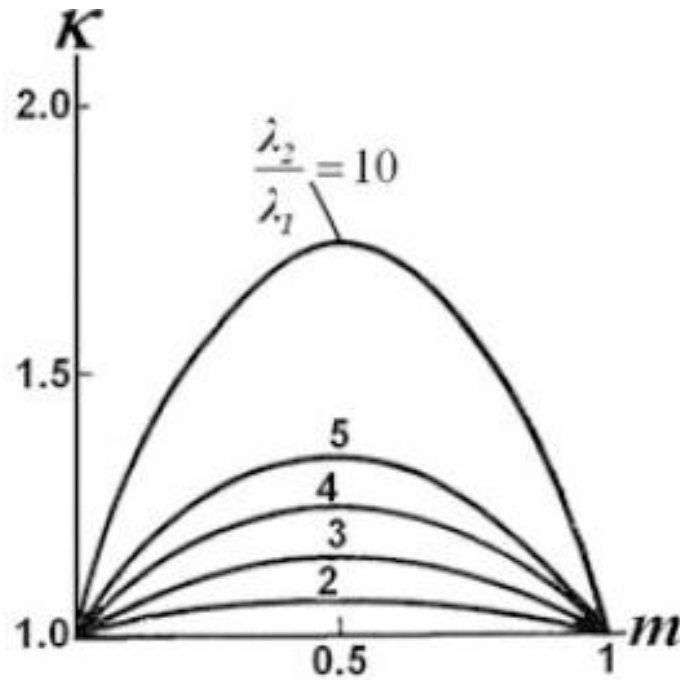
Effect of thermal anisotropy

In case of two-component medium consisting of interbedding of alternation with a thickness h_1 and h_2 and thermal conductivity λ_1 and λ_2 .

λ_τ =longitudinal thermal conductivity

λ_n =trasversal thermal conductivity

κ (coefficient of thermal anisotropy) = κ_{max} when $m=0.5$



$$\kappa = \sqrt{\frac{\lambda_\tau}{\lambda_n}} = \sqrt{1 + \frac{m(1-m)(\lambda_1 - \lambda_2)^2}{\lambda_1\lambda_2}}, \quad m = \frac{h_1}{h_1 + h_2}$$

Specific Heat Capacity

- The specific heat defines the amount of energy required to raise the temperature of a unit of the mass of a substance by 1°C.
- The thermal (heat) capacity (c) indicates the capability of the formations to store heat (J/K).
- For a reversible transformation the change in internal energy U is the sum of the heat stored in the system Q and of the work done by the system:

$$dU = dQ - PdV \approx TdS - PdV \quad S=\text{entropy}$$

- The specific heat at constant volume C_V relates the internal energy U to changes in T and is:

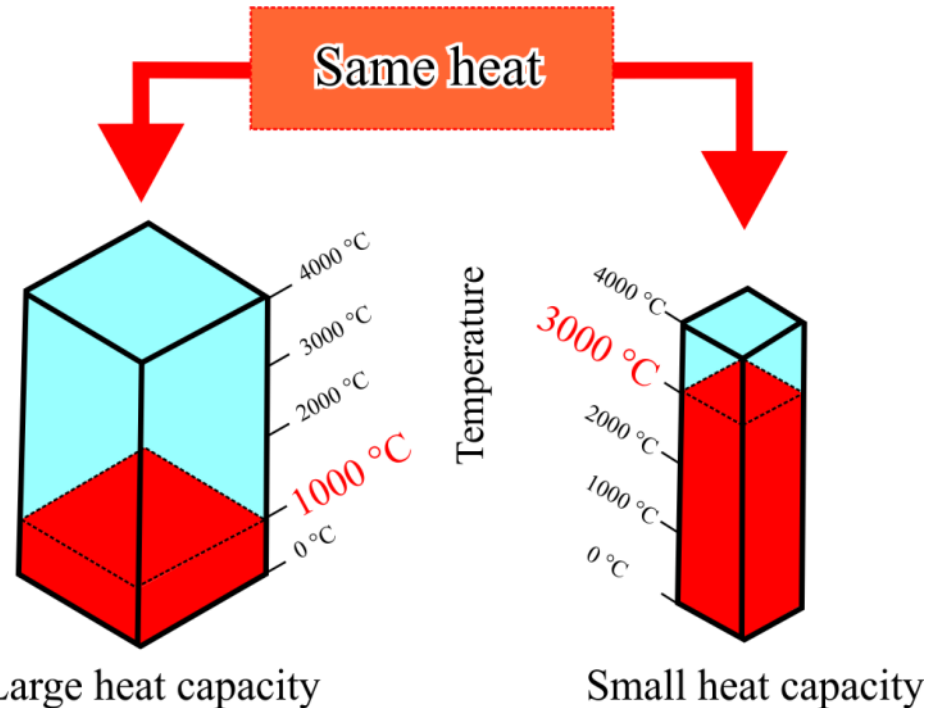
$$C_V = \left(\frac{\partial U}{\partial T} \right)_V = T \left(\frac{\partial S}{\partial T} \right)_V$$

- The specific heat at constant pressure C_P relates the enthalpy ($H=U+PV$) to changes in T and is :

$$C_P = \left(\frac{\partial H}{\partial T} \right)_P = T \left(\frac{\partial S}{\partial T} \right)_P$$

Under high P and T: $C_P/C_V=1+\alpha\gamma T$

SPECIFIC HEAT CAPACITY c_p SI $\left[\frac{J}{kg \cdot K} \right]$



In an object with a large c_p , the temperature rise is smaller than in one with a smaller c_p

Specific Heat Capacity

The average specific heat capacity at constant pressure (C_p) for magmatic, metamorphic, and sedimentary rocks depends on T and increases from $\sim 760, 770,$ and $810 \text{ J kg}^{-1} \text{ K}^{-1}$ at 273 K, to $\sim 970, 970,$ and $1,010 \text{ J kg}^{-1} \text{ K}^{-1}$ at 573 K

$$c_p = 0.75(1 + 6.14 \times 10^{-4} T - 1.928 \times 10^{-4} T^2)$$

$$C_p = c_0 + c_1 T^{-1/2} + c_3 T^{-3}$$

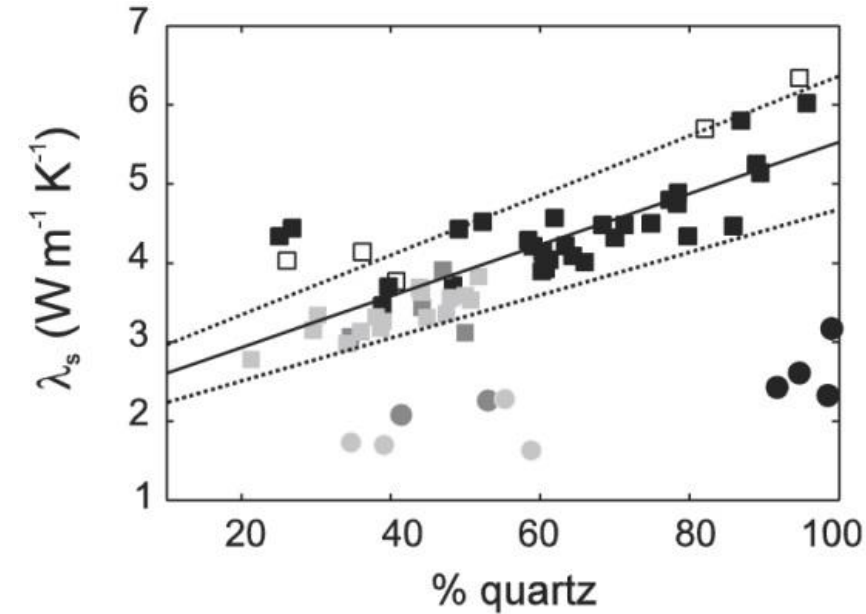
For Fosterite $c_0 = 233.18, c_1 = -1801.6$ and $c_3 = -26.794 \times 10^7$:

For Fayalite $c_0 = 252, c_1 = -2013.7$ and $c_3 = -6.219 \times 10^7$

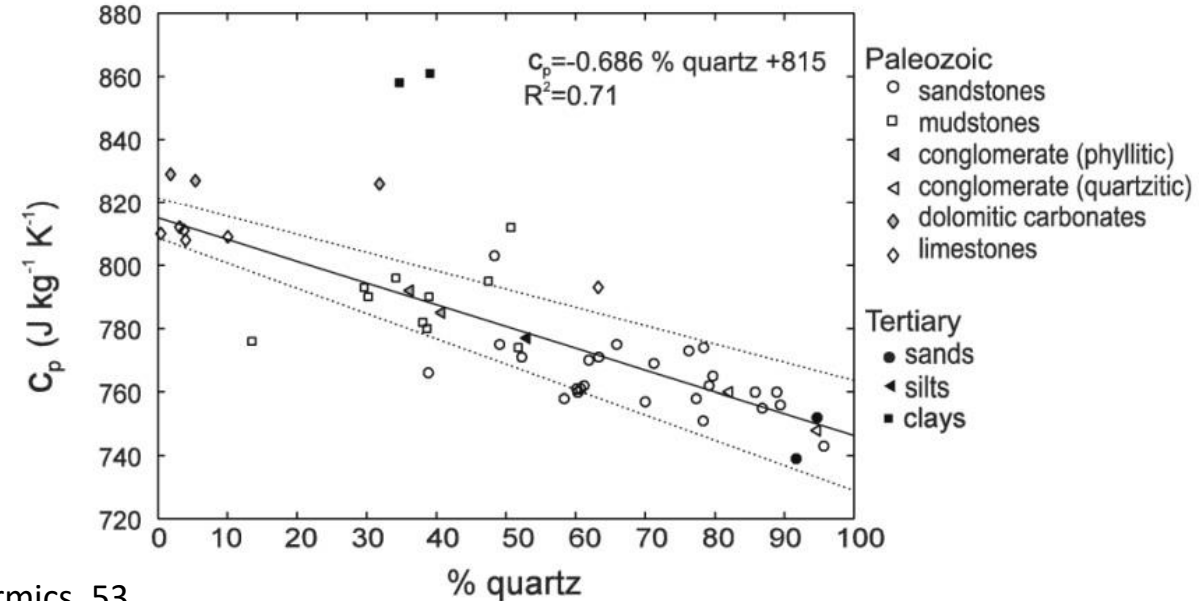
C_p is in KJmol^{-1} and T in Kelvin

Rock	N	c	Rock, mineral	Specific heat capacity [kJ/(kg K)]	Material	Thermal conductivity ($\text{W m}^{-1} \text{K}^{-1}$)	Density (kg m^{-3})	Specific heat ($\text{J kg}^{-1} \text{K}^{-1}$)
Sand	130	0.96	Augite	0.8	Quartz- α	7.69 ^a	2647 ^a	740 ^b
Siltstone	42	0.87	Basalt rock	0.84	Quartz microcrystalline	3.71 ^a	2618 ^a	735 ^b
Argillite, clay schist	18	0.86	Dolomite rock	0.92	Plagioclase	1.97 ^a	2642 ^a	837 ^b
Clay	116	1.10	Garnet	0.75	K-feldspar	2.40 ^a	2562 ^a	700 ^b
Marl	19	1.55	Granite	0.79	Calcite	3.59 ^a	2721 ^a	815 ^b
Limestone	108	0.89	Hornblende	0.84	Dolomite	5.51 ^a	2857 ^a	870 ^b
Chock	13	1.86	Hypersthene	0.8	Sheet silicates	1.88 ^c	2630 ^c	832 ^d
Granite	87	0.95	Labradorite	0.8	Anhydrite	4.76 ^a	2978 ^a	585 ^b
Granodiorite	11	1.02	Lava	0.84	Gypsum	1.30 ^e	2320 ^b	1070 ^b
Porphyrite	11	0.91	Limestone	0.84	Air	0.026	1.225	1005
Diorite	4	1.00	Sand	0.8	Water	0.60	1000	4186
Basalt	12	1.23	Sandstone	0.92				
Diabas	12	0.87	Serpentine	1.09				
Gabbro	13	0.98						
Schist	95	1.10						
Gneiss	14	1.02						
Amphibolite	7	1.13						
	15	1.11						

Thermal Conductivity and Specific Heat Capacity



Jorand et al., 2015, Geothermics, 53



- Thermal conductivity and specific heat capacity are linearly correlated with quartz content (but with opposite trend).
- The Tertiary samples are more porous (e.g. sand = 40(3)%) than the Paleozoic samples and only partially saturated (then the thermal conductivity is even lower).

Volumetric heat capacity

Volumetric heat capacity (ρc)= product between density and specific heat

Volumetric heat capacity of a dry rock $(\rho c)_r$ can be computed as the weighted average of the volumetric heat capacity of the matrix $(\rho c)_m$ and of the air $(\rho c)_a$ in the voids.

$$(\rho c)_r = (1 - \phi)(\rho c)_m + \phi (\rho c)_a \quad (\rho c)_m = \sum_{j=1}^n v_j \rho_j c_j \quad \sum_{j=1}^n v_j = 1$$

Where ϕ is porosity, v_j , ρ_j and c_j are the volume fraction, density and specific heat of the j th mineral and n is the number of mineral components.

Specific Heat of matrix and water depends on temperature:
$$c_w = \frac{(4245 - 1.841 T) \times 10^3}{\rho_w} \quad \rho_w = \frac{\rho_{w20}}{1 + (T - 20) \alpha_w}$$

where $(\rho_w)_{20}$ the water density at 20 ° C, and α_w thermal expansion coefficient of water.

$$\alpha_w = 0.0002115 + 1.32 \times 10^{-6} T + 1.09 \times 10^{-8} T^2$$

$$(\rho c)_m = (\rho c)_{m20} (0.953 + 2.29 \times 10^{-3} T - 2.835 \times 10^{-6} T^2 + 1.191 \times 10^{-9} T^3)$$

where $(\rho c)_{m20}$ is the volumetric heat capacity of the rock matrix at 20 °C

Thermal Diffusivity

Thermal diffusivity (α or κ) is a physical property that controls the rate at which heat dissipates through a material

Thermal Diffusivity (α or κ): how fast the temperature field of a solid changes with time
$$a = \frac{\lambda}{\rho c} \quad \text{or} \quad \kappa = \frac{k}{\rho c}$$

Material	n	ρ, ρ_{aver} (g/cm ³)	$\lambda, \lambda_{\text{aver}}$ (10 ⁻³ cal/cm s °C)	n	c, c_{aver} (cal/g °C)	a, a_{aver} (10 ⁻³ cm ² /s)
Anhydrite	7	2.65–2.91 2.80	9.80–14.50 12.61	7	–	17.00–25.7 22.41
Clay	3	2.49–2.54 2.52	5.20–5.40 5.30	3	0.213–0.240 0.223	8.53–10.18 9.50
Clay marl	7	2.43–2.64 2.54	4.14–6.15 4.87	7	0.186–0.234 0.205	8.01–11.66 9.34
Claystone	15	2.36–2.83 2.60	4.17–8.18 5.68	9	0.197–0.223 0.211	8.24–15.80 12.18
Dolomite	6	2.53–2.72 2.63	6.01–9.06 7.98	6	0.220–0.239 0.228	10.75–14.97 11.17
Schistose clay	3	2.42–2.57 2.49	4.60–5.50 5.13	3	0.218–0.222 0.220	8.10–10.24 9.37
Limestone	11	2.41–2.67 2.55	4.05–6.40 5.28		0.197–0.227 0.204	8.24–12.15 10.54
Limestone	6	2.58–2.66 2.62	5.58–8.38 6.75	6	0.197–0.220 0.210	10.78–15.21 12.18
Lime marl	2	2.43–2.62 2.53	4.40–5.74 5.07	2	0.200–0.227 0.214	9.04–9.64 9.34
Marl	3	2.59–2.67 2.63	5.55–7.71 6.44	3	0.217–0.221 0.219	9.89–13.82 11.18
Marly clay	2	2.46–2.49 2.47	4.21–4.82 4.52	3	0.183–0.236 0.210	7.17–10.72 8.94
Clay slate		2.62–2.83	3.45–8.79	5	0.205–0.205	6.42–15.15
	5	2.68	5.13		0.205	9.26
Salt		2.08–2.28	10.7–13.7	14	–	25.20–33.80
	14	2.16	13.19		–	30.60
Salt slate		2.13–2.57	3.00–10.00	7	–	6.38–21.70
	7	2.37	6.59		–	13.90
Sandstone		2.35–2.97	5.20–12.18	31	0.182–0.256	10.94–23.62
	54	2.65	7.75		0.197	16.45

For many rocks a ranges between 0.8 and 2.5 $\sim 10^{-6}$ m²/s

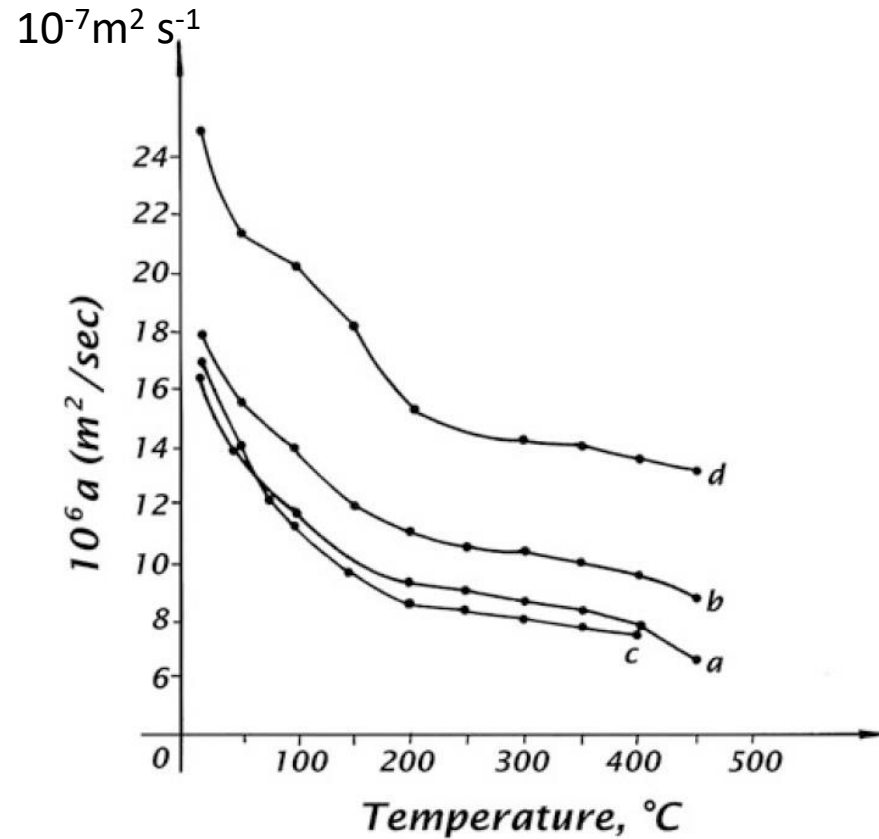
Rock	N	a cm ² /s
Sand	154	9.57
Siltstone	45	10.28
Argillite, clay schist	23	9.76
Clay	126	7.30
Marl	26	7.53
Limestone	115	10.92
Chock	13	4.77
Granite	92	9.13
Granodiorite	16	5.15
Porpyrite	23	9.54
Diorite	10	6.38
Basalt	13	5.34
Diabas	13	9.93
Gabbro	21	9.70
Schist	106	9.60
Gneiss	15	7.98
Amphibolite	9	6.84
Gneiss–granite	18	7.24

Thermal Diffusivity

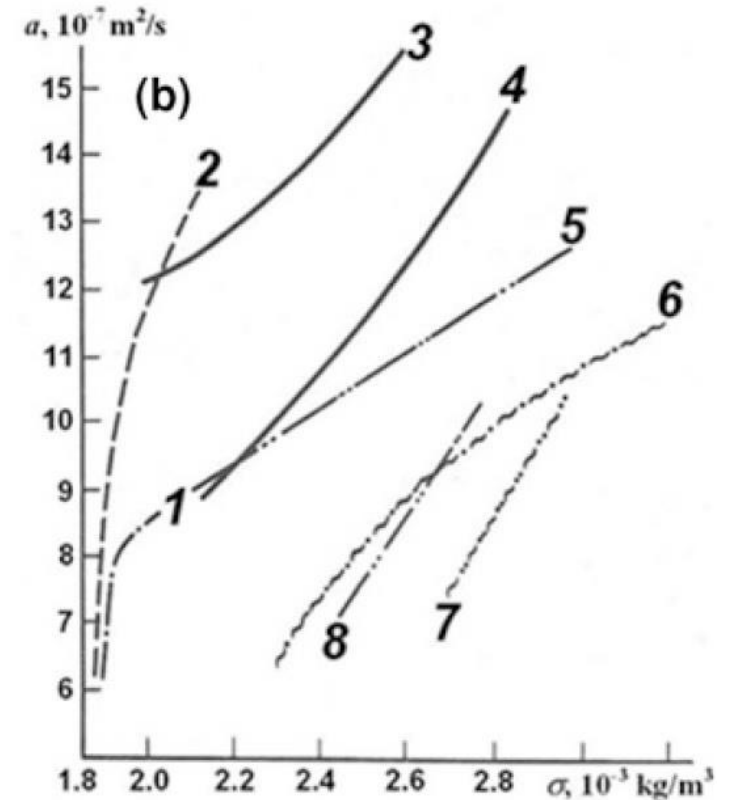
Physical properties

Table D.7. Thermal diffusivity of water, ice and some rock types

Rock	κ ($\times 10^{-6} \text{ m}^2 \text{ s}^{-1}$)
Basalt	0.9
Gabbro	1.2
Granite	1.6
Peridotite	1.7
Sandstone	1.3
Quartzite	2.6
Limestone	1.2
Dolomite	2.6
Marble	1.0
Shale	0.8
Water	0.15
Ice	1.2



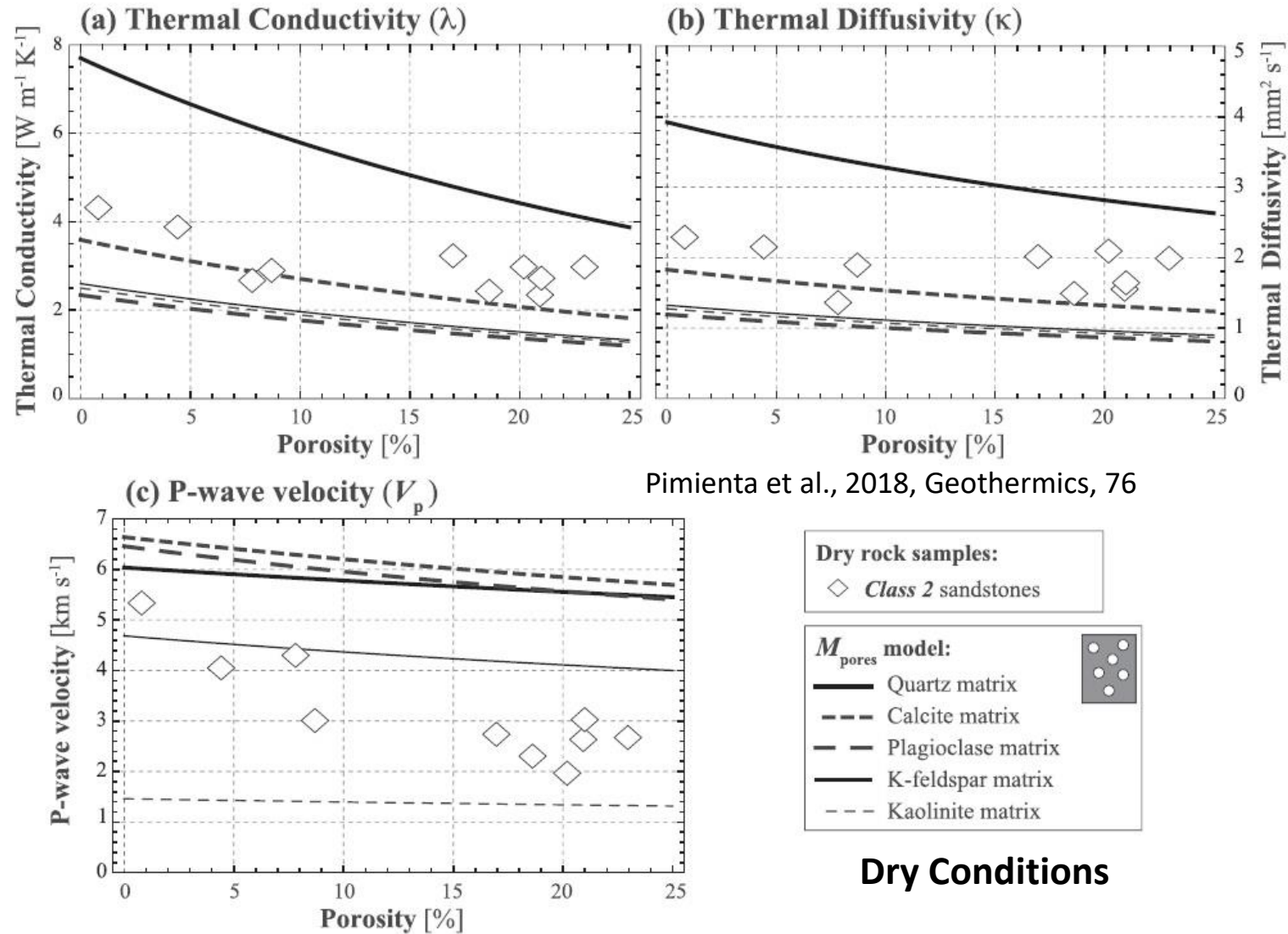
a gabbro; b diabase; c granite; d granite-gneiss



(1) (3) and (4) sandstone (2) water-saturated sandstone (5) and (8) limestone (6) siltstone (7) dolomite.

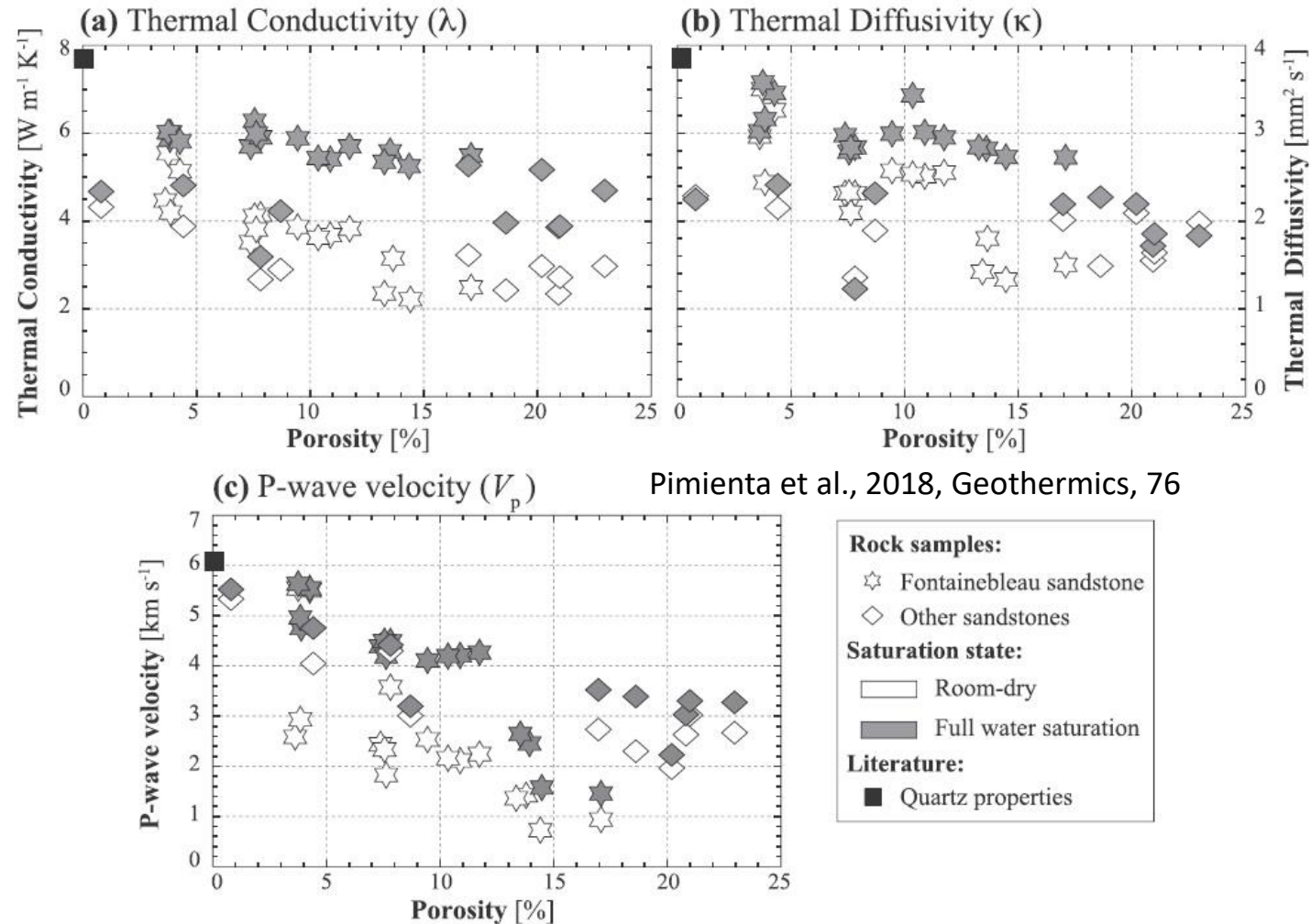
- For magmatic, metamorphic, and sedimentary rocks within a T interval of 273–573 K, the thermal conductivity, λ , decreases by 25–44 % and thermal diffusivity, a , decreases by 42–54 %.
- Thermal diffusivity for all the rocks drops from 1.8–2.2 mm^2/s at 298 K to 0.3–0.5 mm^2/s at 1,200–1,250 K and from 1.5–2.5 mm^2/s at ambient conditions to about 0.5 mm^2/s at mid-crustal temperatures (middle-lower crust is a very effective thermal insulator).
- Results showing that the substitution of $\sim 10\%$ Fe for Mg in forsterite lowers the thermal diffusivity by $\sim 50\%$.
- At ambient temperature rocks saturated with water have their thermal diffusivity increased by as much as 24 %.

Thermal Conductivity, Thermal Diffusivity, and P-wave velocity



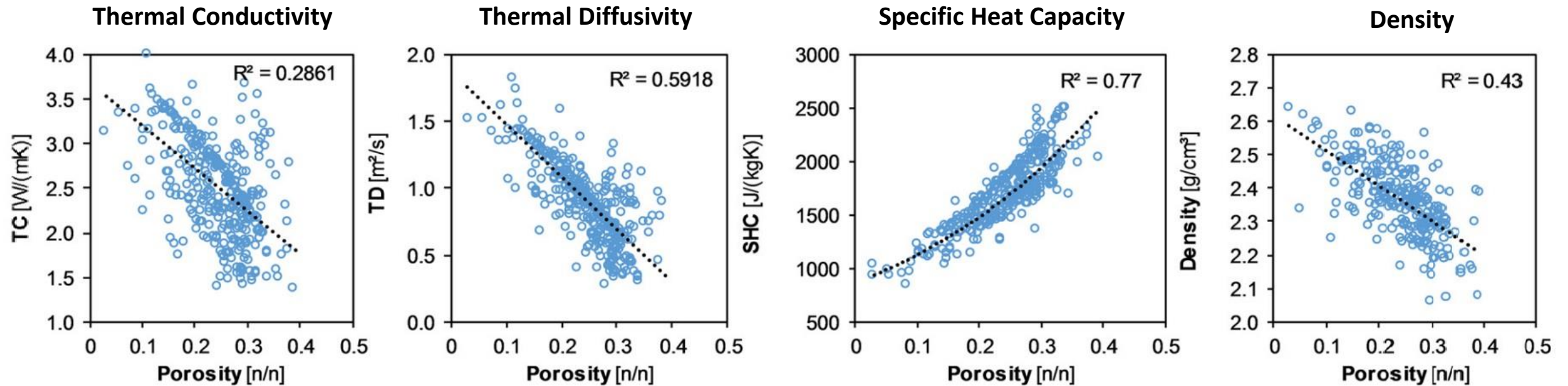
- While rocks with quartz, plagioclase or calcite matrices differ negligibly in their elastic properties, their thermal properties allow to distinguish between quartz and other typical rock minerals. These differences are greatest for a mono-mineral rocks, and the effect of “mineral inclusions” is much smaller.

Thermal Conductivity, Thermal Diffusivity, and P-wave velocity



- Looking at the porosity dependence, the velocity change occurs at a porosity of about 13%, i.e., at the transition from low- to high-porosity sandstones. In case of low porosity, λ and V_p depends in the same way on water saturation, while it changes in case of high porosity.
- For loosely cemented rocks, the stiffness of the grain contact controls the effective elastic properties: a strong elastic weakening at full water saturation is expected (adsorption of water molecules at grain contact, occurring in loosely cemented granular rocks).

Thermal Parameters variations with Porosity

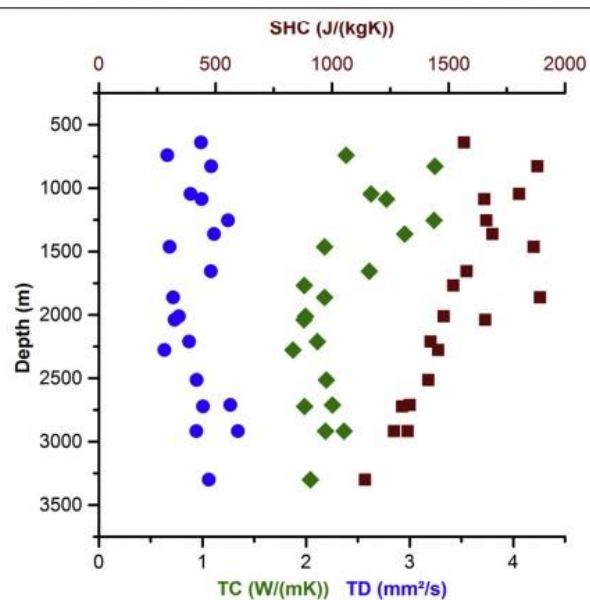
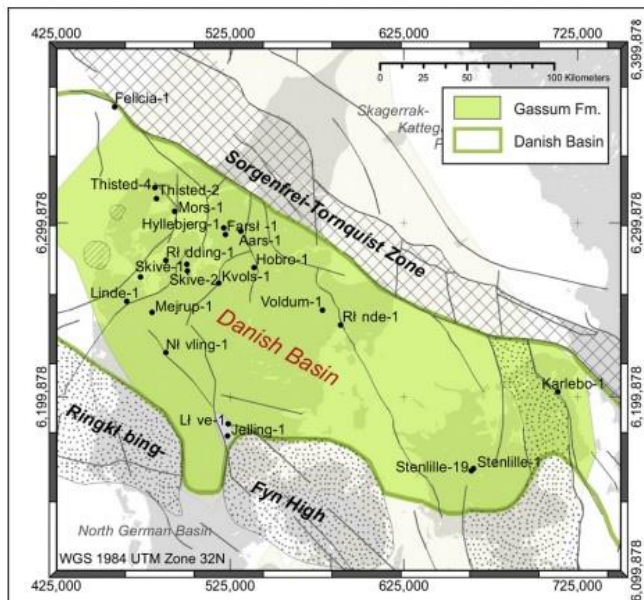


Fuchs, 2018, Geothermics, 76

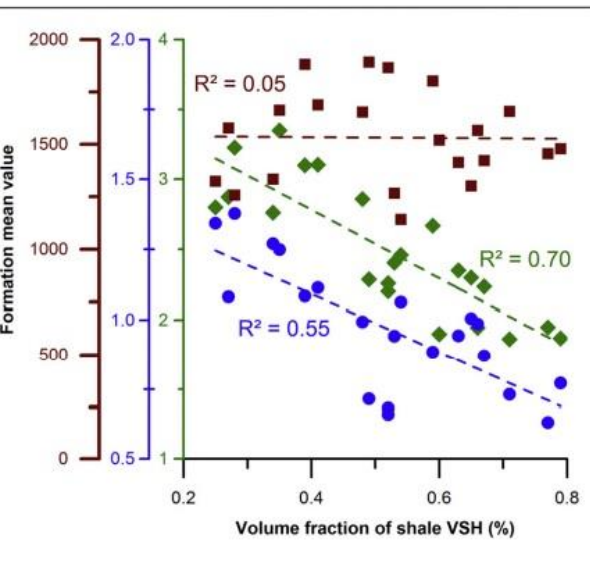
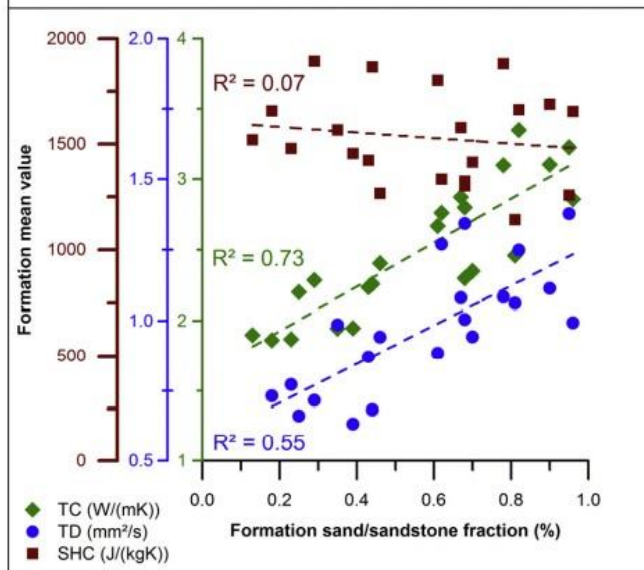
The degree of correlation between rock thermal properties and porosity varies greatly:

- A strong positive linear correlation can be obtained for SHC and porosity ($R^2=0.77$).
- TD and porosity show a moderate to strong negative correlation ($R^2=0.60$).
- Thermal conductivity and porosity show some scatter and a weak negative correlation ($R^2=0.29$).
- The formation bulk density (range: 2.1–2.7 g/cm³) shows a moderate negative correlation with the mean porosity ($R^2=0.43$).

Thermal Parameters variations with Depth & Composition



- The strong correlations between TD and SHC with porosity, are reflected by the correlation between TD and SHC with increasing depth (decreasing porosity).
- The moderate negative correlation between TC and porosity results in a less determined pattern of TC with depth.
- For the formation sandstone fraction, strong positive correlations are observed for both TC and TD. In contrast, a non-correlation is obtained for SHC.
- A similar but inverse pattern is observed for the volume fraction of shale.



Melting Point

- The melting point of a substance is the T at which the solid and liquid phases exist in equilibrium and the substance can be transformed from solidus to liquidus and viceversa.
- The amount of energy absorbed (released) by a substance during a change of state from a solid (liquid) to a liquid (solid) is named ***latent heat of fusion (crystallization)***.
- The melting point of rocks and minerals drops significantly with increases in H_2O , CO_2 , and Fe content.

Mineral	Melting point (K)	References
Fayalite	1,490	Hewins et al. (1996)
Fayalite	1,478	Yoder (1976)
Forsterite	2,163	Hewins et al. (1996)
Forsterite	2,163	Yoder (1976)
Forsterite	2,171	Speight (2005)
Enstatite	1,830	Speight (2005)
Clinoenstatite	1,830	Hewins et al. (1996)
Ferrosilite	1,413	Speight (2005)
Albite	1,391	Hewins et al. (1996)
Albite	1,393	Hall (1995)
Anorthite	1,830	Hewins et al. (1996)
Christobalite	1,996	Hewins et al. (1996)
Diopside	1,664	Hewins et al. (1996)
Diopside	1,665	Wenk and Bulakh (2004)
Fe metal	1,889	Hewins et al. (1996)
Wollastonite	1,813	Nikonova et al. (2003)
Augite	1,440–1,455	Thy et al. (1999)
Low-Ca pyroxene	1,386–1,426	Thy et al. (1999)
Olivine (Fo82)	1,955	Del Gaudio et al. (2009)
Olivine (Fo85)	1,993	Del Gaudio et al. (2009)
Pyrope	1,575–1,609	Van Westrenen et al. (2001)
Pyrope	1,570	Téqui et al. (1991)
K-feldspar	1,423	Best (2002)
Pure leucite	1,958	Best (2002)

Rock	Melting point (K)	References
Basalts	~ 1,473	Adylov and Mansurova (1999)
Basic rocks with Fe# = 0.35	~ 1723	Yoder (1976)
Basic rocks with Fe# = 0.50	~ 1,503	Yoder (1976)
Basic rocks with Fe# = 1.00	1,273	Yoder (1976)
Basalt (beginning of melting at 0.1 MPa)	1,273	Yoder (1976)
Basalt	1,343	Hall (1995)
Basalt	1,413	Hall (1995)
Basalts	1,473	Faure (2000)
Basalt, gabbro	1,473	Bayly (1968)
Rhyolite, granite	1,073	Bayly (1968)
Granites	973–1,123	Attrill and Gibb (2003)
Granite	1,173	Hall (1995)
Granite	1,223	Hall (1995)
Komatiites	2,063	Grove and Parman (2004)
Andesite	1,373	Tamura et al. (2003)
Andesite	1,343	Hall (1995)
Eclogite	1,573	Anderson (2007)
Tonalite	1,173	Hall (1995)
Tholeiitic basalt ^a	1,423–1,498	Hall (1995)
Basaltic andesite ^a	1,293–1,383	Hall (1995)
Leucite basalt ^a	1,368	Hall (1995)
Rhyolite ^a	1,008–1,163	Hall (1995)
Rhyodacite ^a	1,173–1,198	Hall (1995)
Andesite pumice ^a	1,213–1,263	Hall (1995)
Dacite ^a	1,198	Hall (1995)
Peridotite	1,363	Faure and Mensing (2007)
MORB ^a	1,516–1,624	Falloon et al. (2007)
OIB ^a	1,559–1,645	Falloon et al. (2007)

^a Extrusion temperatures of lavas

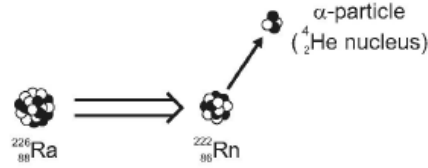
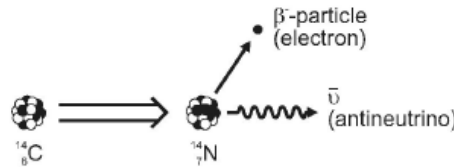
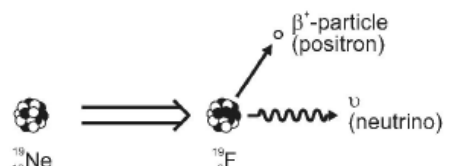
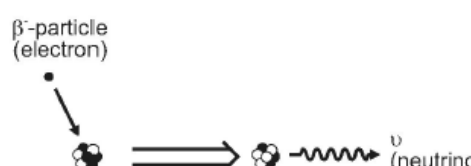
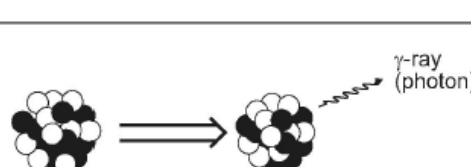
Melting Point and Pressure

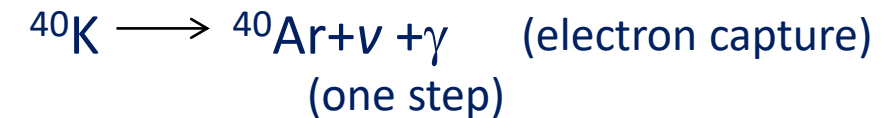
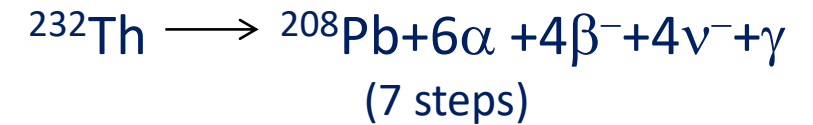
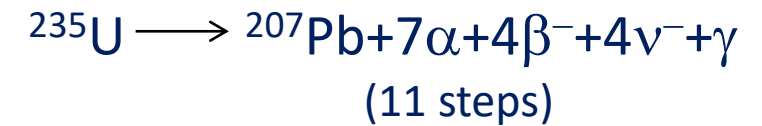
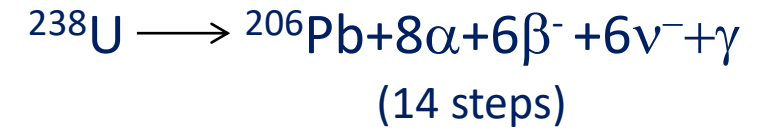
- At a standard pressure, peridotites melt at temperatures of $\sim 1,400$ K in the absence of water and other volatiles, and their solidus increases with pressure to around 1,700 K at ~ 3 GPa.
- Concentrations of H_2O of only 0.1 % reduce the standard pressure melting point to $\sim 1,340$ K and decreases with pressure, reaching a minimum near 1,270 K at ~ 3 GPa.
- At higher pressures and greater water content, the melting point of peridotite can drop by about 300–400 K.
- In the presence of CO_2 , the peridotite solidus T decreases by ~ 200 K at a depth of about 70 km, while at larger depths the CO_2 can reduce the initial melting temperatures of a carbonated peridotite ~ 450 –600 K.

Peridotite	Pressure (GPa)	Melting point (K)	References
	0	1,363	Faure and Mensing (2007)
Dry peridotite	~ 3	1,613	Faure and Mensing (2007)
	~ 13.2	1,973	Faure and Mensing (2007)
	1	1,483	Lee et al. (2009)
Dry lherzolite solidus	~ 3	1,713	Lee et al. (2009)
	~ 6	1,973	Lee et al. (2009)
Dry peridotite	0	1,400	Schubert et al. (2001)
	~ 3	1,700	Schubert et al. (2001)

Radioactive Decay

- Radioactive decay generally results in releasing of energy through the emission of alpha (α), beta (β) particles from the nucleus, and by the emission of gamma (γ) rays.
- On a geological time scale, more than 98 % of the heat now being produced in rocks is yielded by the radioactive decay of unstable isotopes ^{238}U , ^{235}U , ^{232}Th , and ^{40}K

<p>α-decay</p> <p>Nucleus emits an α-particle (Helium nucleus). Atomic number of parent is reduced by 2, and atomic mass by 4. Mass difference carried as kinetic energy by α-particle.</p>	
<p>β-decay</p> <p>In β-decay, a neutron becomes a proton, ejecting an antineutrino and electron from the nucleus and raising the atomic number of the atom by 1.</p>	
<p>In β^+-decay, it is a positron and a neutrino that are ejected, a proton becomes a neutron and atomic number is lowered by 1.</p>	
<p>Electron capture occurs when an orbiting electron is captured by the nucleus, which emits a neutrino and reduces its atomic number by 1.</p>	
<p>γ-decay</p> <p>A nucleus in a state of excitement jumps down to ground-state, releasing a high energy photon.</p>	



Radiogenic Heat Generation (Heat Producing Elements)

- Heat generation by radioactive decay may significantly affect the heat flow in sedimentary basins (up to 60% of surface heat flow).
- The energy radiated during the decay process is converted into heat by absorption. The radiogenic heat, A , can be calculated from the concentration of uranium, thorium and potassium.

Major Heat-Generating Elements in Rocks

Element	Heat Generation, A' ($\mu\text{W}/\text{kg}$ element)	Average Crustal Abundance, n (weight/weight)	$A' \times n$ ($\mu\text{W}/\text{kg}$ rock)
Uranium	96.7	2.3 ppm	2.22×10^{-4}
Thorium	26.3	8.1 ppm	2.13×10^{-4}
Potassium	0.0035	1.84%	6.44×10^{-5}

Sources: Emsley (1989) and Jessop (1990).

Heat production constants

Element	Isotope	Half life (Ga)	Power ($\mu\text{W}/\text{kg}$ of element)	Isotope / element	Natural abundance (%)	Half-life (y)	Energy per atom ($\times 10^{-12}$ J)	Heat production per unit mass of isotope/element (W kg^{-1})
Uranium	^{238}U	4.468	94.35	^{238}U	99.27	4.46×10^9	7.41	9.17×10^{-5}
	^{235}U	0.7038	4.05	U	0.72	7.04×10^8	7.24	5.75×10^{-4}
Thorium	^{232}Th	14.01	26.6	^{232}Th	100	1.40×10^{10}	6.24	2.56×10^{-5}
Potassium	^{40}K	1.250	0.0035	Th				2.56×10^{-5}
				^{40}K	0.0117	1.26×10^9	0.114	2.97×10^{-5}
				K				3.48×10^{-9}

From Rybach (1988).

Radiogenic Heat Generation

Radiogenic heat production A [μWm^{-3}] is the product of:

- Isotopic abundance in a rock of HPEs [ppm or %]
- Energy release per unit mass of HPEs [$\mu\text{W}/\text{kg}$]
- Density of the rock [kg/m^3]

$$A = \rho \sum P A_s c$$

ρ is the rock density, P the abundance and A_s the rate of heat generation per kg of isotope and c the concentration.

Originally, A was measured in HGU: $1\text{HGU} = 10^{-13}\text{cal}/\text{cm}^3\text{s} = 0.4184 \mu\text{Wm}^{-3}$

A is in $\mu\text{W m}^{-3}$, ρ in kg m^{-3} , the U and Th concentrations (c_U and c_{Th}) in ppm (or mg kg^{-1}) and K (c_K) in %

Radiogenic Heat Generation

$$A = \rho \sum P A_s c$$

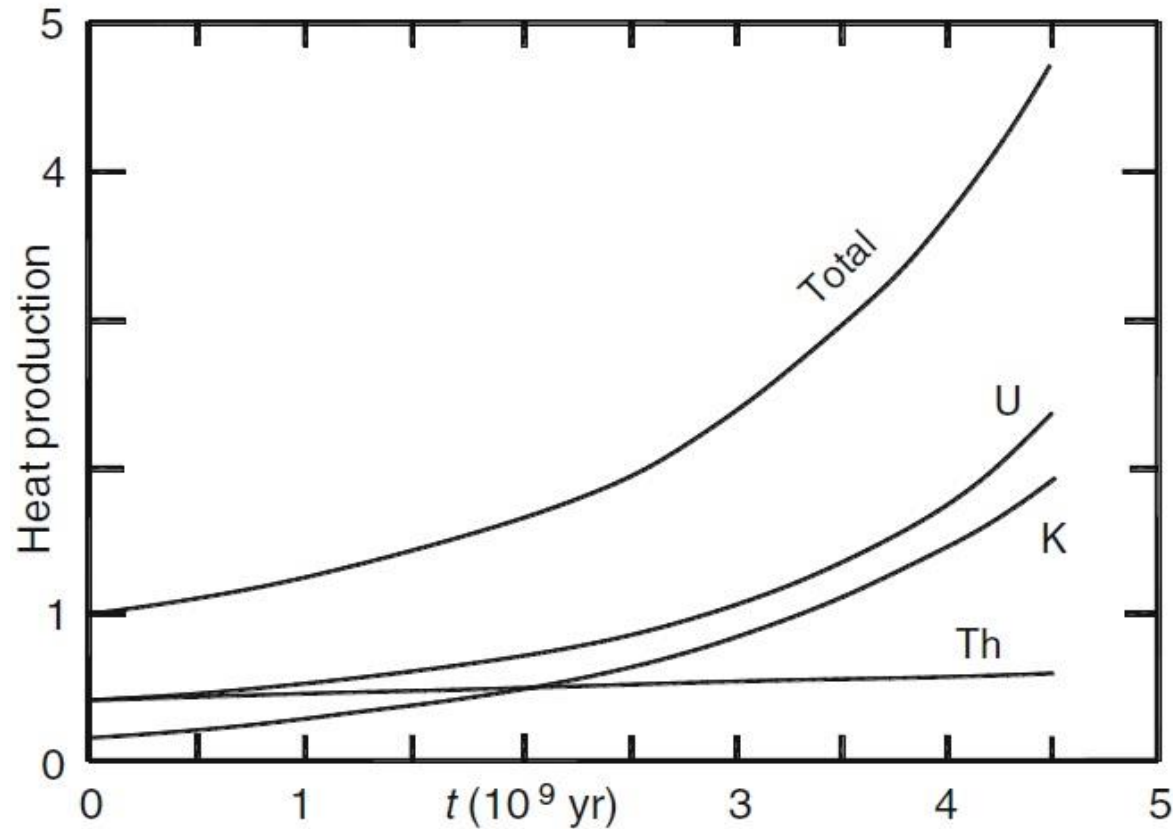
$$c_t = c \exp(t \ln 2 / \tau)$$

$$A = \rho \left[0.993 c_U A_{U^{238}} \exp(t \ln 2 / \tau_{U^{238}}) + 0.0071 c_U A_{U^{235}} \exp(t \ln 2 / \tau_{U^{235}}) \right. \\ \left. + c_{Th} A_{Th^{232}} \exp(t \ln 2 / \tau_{Th^{232}}) + 0.00012 c_K A_{K^{40}} \exp(t \ln 2 / \tau_{K^{40}}) \right]$$

c_t = concentration of an isotope at time t
 $\tau = \ln 2 / \lambda$ = half life with λ decay constant

$$A_0 = 3.2 \exp(-0.3t)$$

t is in 10^9 years



Radiogenic Heat Generation of rocks

U, Th and K average concentrations, Th/U ratio and radiogenic heat A in rocks of the Ligurian Alps
(after Chiozzi et al. 2001; Verdoya et al. 2001)

Tectonic/ sedimentary environment	Age	Rock type	n	U ppm	Th ppm	K %	Th/U	A $\mu\text{W m}^{-3}$
Ophiolitic complex	Middle-late Jurassic	Metagabbro	31	0.3	0.3	0.29	1.00	0.14
		Metabasalt	23	0.4	0.3	0.52	0.75	0.19
		Serpentinite schist	41	0.5	<0.3	0.08	0.60	0.16
	Jurassic	Lherzolite	10	<0.2	<0.3	<0.03	1.50	0.08
		Prasinite	12	0.4	<0.3	0.51	0.75	0.18
	Middle Jurassic	Ophicalcite	10	0.4	<0.3	0.24	0.75	0.15
Metaophiolite		12	0.6	1.3	0.37	2.17	0.27	
Pelagic siliceous sediments	Late Jurassic	Chert	10	3.2	15.2	5.14	4.75	2.20
	Jurassic	Quartz-schist	16	1.2	6.5	1.79	5.42	0.93
Shelf sediments	Middle-late Triassic	Dolomite	15	5.6	0.5	0.17	0.09	1.49
Pelagic sediments	Early Cretaceous	Limestone	14	2.2	5.2	1.25	2.36	1.04
	Lias	Limestone	13	2.6	3.8	1.11	1.42	1.04
Pelitic-pelagic sediments	Early-middle Cretaceous	Phyllitic schist	10	3.0	13.3	3.07	4.43	2.00
		Phyllite	20	2.9	10.6	2.52	3.36	1.73
	Jurassic	Calc-schist	20	3.0	13.3	3.18	4.43	2.01
	Pliocene	Marl	10	2.7	5.5	1.37	2.04	1.21
	Dogger	Calcareous shale	10	2.8	10.1	2.41	3.61	1.66
	Flysch	Late Cretaceous	Shale	15	4.1	16.7	3.60	4.07
Early Eocene		Marly limestone	10	1.8	4.2	1.15	2.33	0.87
Molassic deposit	Middle Cretaceous Oligocene	Shale	15	2.6	8.5	1.61	3.27	1.42
		Arenaceous marl	10	2.4	8.8	2.19	3.65	1.45
Metamorphic	Eocene	Conglomerate	10	1.1	1.6	0.43	1.45	0.42
		Breccia	10	0.4	0.3	0.14	0.75	0.14
	Pre-Carboniferous	Orthogneiss	94	4.1	17.6	4.23	4.29	2.65
		Paragneiss	38	3.1	16.8	3.47	5.42	2.30
		Migmatite	6	6.1	16.8	3.83	2.75	3.13
Amphibolite	Amphibolite	31	0.5	1.2	0.69	2.40	0.30	
	Micaschist	30	4.1	17.5	3.92	4.27	2.66	

n is the number of measurements

Rock type	U [ppm]	Th [ppm]	K [%]
Granite	4.7	20	4.2
Shale	3.7	12	2.7
Average continental crust	1.42	3.6	1.43
Reference mantle	0.031	0.124	0.031

Heat generation (A) in rocks of the crust and upper mantle

Rock types	Heat generation A ($\mu\text{W m}^{-3}$)		
	After Vinogradov (1962)	After Tilton and Reed (1963)	After Pollack (1982)
Granites	2.5100	2.3900	2.500
Intermediate magmatic rocks	1.2600	1.2600	1.100–1.500
Basalts	0.5000	0.5400	0.300
Peridotites	–	0.0040	0.010
Dunites	0.0050	0.0008	0.002
Sedimentary	1.7000	–	–
Chondrites	0.0190	0.0170	–

Layer	Heat generation A ($\mu\text{W m}^{-3}$)
Sedimentary	1.39
Granite-metamorphic	2.57
Diorite-trachandesite	1.31
Basalt	0.47
Upper mantle	0.13

Basalts and andesites have typically low radiogenic heat values ($0.6\text{--}1.3 \mu\text{W m}^{-3}$)
 Trachytic and Rhyolitic rocks have larger values ($6.6\text{--}7.1 \mu\text{W m}^{-3}$)
 Basaltic trachandesites are characterized by an intermediate value ($4.2 \mu\text{W m}^{-3}$)

Radiogenic Heat Generation of rocks

Radiogenic heat A of volcanic rocks of the Aeolian arc (Tyrrhenian Sea) and the contribution supplied by each radioelement (after Verdoya et al. 1998a; Chiozzi et al. 2002)

Rock type	A_U %	A_{Th} %	A_K %	A $\mu\text{W m}^{-3}$
Basalt	43.7 (4.4)	38.4 (7.5)	17.9 (3.0)	0.6 (0.1)
Basaltic andesite	44.9 (4.2)	39.0 (5.7)	16.1 (2.7)	1.1 (0.6)
Andesite	45.7 (4.8)	39.4 (6.6)	14.9 (2.7)	1.3 (0.8)
Basaltic trachyandesite	48.1 (0.3)	43.2 (1.5)	8.6 (1.9)	4.3 (0.8)
Trachyte	52.0 (2.1)	43.0 (3.4)	5.0 (3.5)	7.1 (0.7)
Rhyolite	50.2 (0.7)	44.3 (1.2)	5.4 (0.6)	6.6 (0.9)

Standard deviation in parentheses

Element concentration and heat production for some common rocks in ppm.

Rock type	U	Th	K	K/U	pW kg ⁻¹	$\mu\text{W m}^{-3}$
Granite	4.6	18	33,000	7,000	1,050	3
Alkali basalt	0.75	2.5	12,000	16,000	180	0.5
Tholeiitic basalt	0.11	0.4	1,500	13,600	27	0.08
Peridotite	0.006	0.02	100	17,000	1.5	0.005

Radiogenic Heat Generation (correlation with age)

Values of the relative concentration of the radioisotopes are normalized to the abundance of total U: U:Th:K = 1:4:(1.27 x 10⁴), where ²³⁸U/U = 0.9927, ²³⁵U/U = 0.0072, and ⁴⁰K/K = 1.28 x 10⁻⁴, and ²³²Th/Th=1.

Relative abundance of long-lived radioisotopes and their radiogenic heat production throughout the Earth's evolution

Isotope	Half-life, Ga	Heat production (μW/kg)	Relative abundances of radioisotopes in:					
			0 Ga	1 Ga	2 Ga	3 Ga	4 Ga	4.6 Ga
²³⁸ U	4.47	94	0.9927	1.159	1.354	1.581	1.846	2.026
²³⁵ U	0.704	570	0.0072	0.019	0.052	0.138	0.370	0.667
²³² Th	14.00	26.6	4.0	4.203	4.416	4.641	4.876	5.023
⁴⁰ K	1.25	27.9	1.6256	2.830	4.928	8.580	14.939	20.836

- Relative content of long-lived radioactive isotopes was ~4 times > at the time of accretion than it is currently and the energy released by them was ~5 times > than it is now.

Relative heat production by different long-lived radioisotopes

Age (Ga)	Relative content of radioisotopes	Relative heat produced per unit of radioisotope (relative concentration · heat production)				Relative total heat produced per unit	No. of times present value of heat was produced
		²³⁸ U	²³⁵ U	²³² Th	⁴⁰ K		
0	6.6255	93.314	4.104	106.400	45.354	249.172	1.00
1	8.204	108.946	10.830	111.780	78.957	310.509	1.25
2	10.750	127.276	29.640	117.466	137.491	411.873	1.65
3	14.940	148.614	78.660	123.451	239.382	590.106	2.37
4	22.031	173.524	210.900	129.702	416.798	930.924	3.74
4.6	28.552	190.444	380.190	133.612	581.324	1,285.570	5.16

Radiogenic Heat Generation (correlation with age)

Geothermal flow versus geological age (after Pasquale 2012)

Oceanic area	Age (10^6 yr)	160–120	120–80	80–40	40–20	20–10	10–0
	mW m ⁻²	50–55	55–60	60–75	75–120	120–150	>150
Continental area	Age (10^6 yr)	>1700	1700–800	800–250	250–50	50–0	
	mW m ⁻²	30–40	40–50	50–60	60–65	65–100	

Estimates of the bulk continental crust heat production from heat flux data (after Jaupart and Mareschal 2003, 2007; Jaupart et al. 2007)

Geological age	Heat generation (A) ($\mu\text{W m}^{-3}$)
Archaean	0.56–0.73
Proterozoic	0.73–0.90
Phanerozoic	0.95–1.21

Why do the Archean rocks have a lower heat generation than Proterozoic and Paleozoic rocks?

- (1) The depth of the magma is increased with time and the magma passing through several lithospheric layers would be more highly enriched in radioactive elements, and could deliver them to the surface.
- (2) The heat generation age-trend is related to differences not in the heat generation within the crust of these areas, but to mantle heat flow which is greater in younger regions.
- (3) An unusual heat generation age-trend may be related to the formation of sediments (the second highest source of heat generation after granitic rocks).

Radiogenic Heat Generation in Depth

$$A(z) = A_0 \exp\left(-\frac{z}{D}\right) \quad q_0 = q_a + A_0 D \quad \text{The linear relationship supposes an exponential variation of } A$$

A_0 (in $\mu\text{W m}^{-3}$) = radiogenic heat at the surface and D (km) = rate of heat decrease (5-15 km), q_0 = heat flowing out from the Earth's surface, and q_a is a constant component of heat flow from the mantle (the HF if there are no radiogenic heat sources)

If the thickness of D -layer is much smaller than the scale of horizontal fluctuation in radioactivity, the effect of lateral heat production variation on Q is negligible.

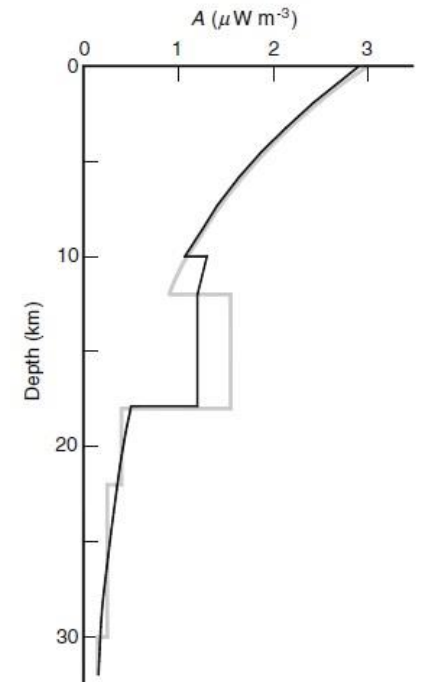
$A = 2.5 \mu\text{W/m}^3$ through a depth of 10 km produce a surface heat flux of 25 mWm^{-2} (about half of typical continental heat fluxes)

For magmatic and metamorphic rocks $A=2.5\text{--}3.5 \mu\text{W m}^{-3}$

Measurements in boreholes have shown that A does not systematically decrease with depth, since tectonics can modify the distribution

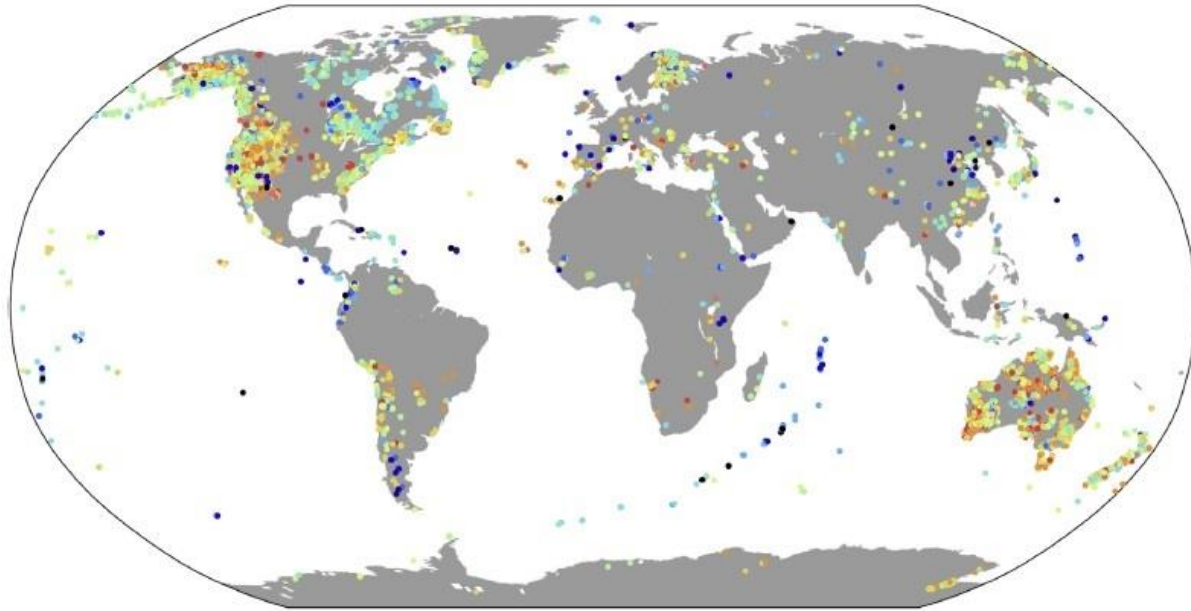
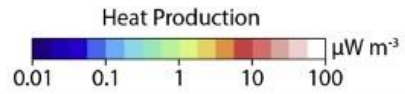
Compositional model of the Variscan crust as inferred from the $v_p(z)$ structure and the corresponding radiogenic heat A deduced from petrographical data (after Verdoya et al. 1998b)

Depth range (km)	Lithotype	Percentage of rock type	A ($\mu\text{W m}^{-3}$)
<i>Upper crust</i>			
0–12	Granite-granodiorite	100	3.0
12–18	Granitic gneiss	55	1.6
	Granite-granodiorite	20	
	Tonalitic gneiss	25	
<i>Lower crust</i>			
18–22	Amphibolite	60	0.4
	Mafic granulite	40	
22–30	Mafic garnet granulite	65	0.3
	Amphibolite	35	
30–32	Mafic garnet granulite	100	0.2

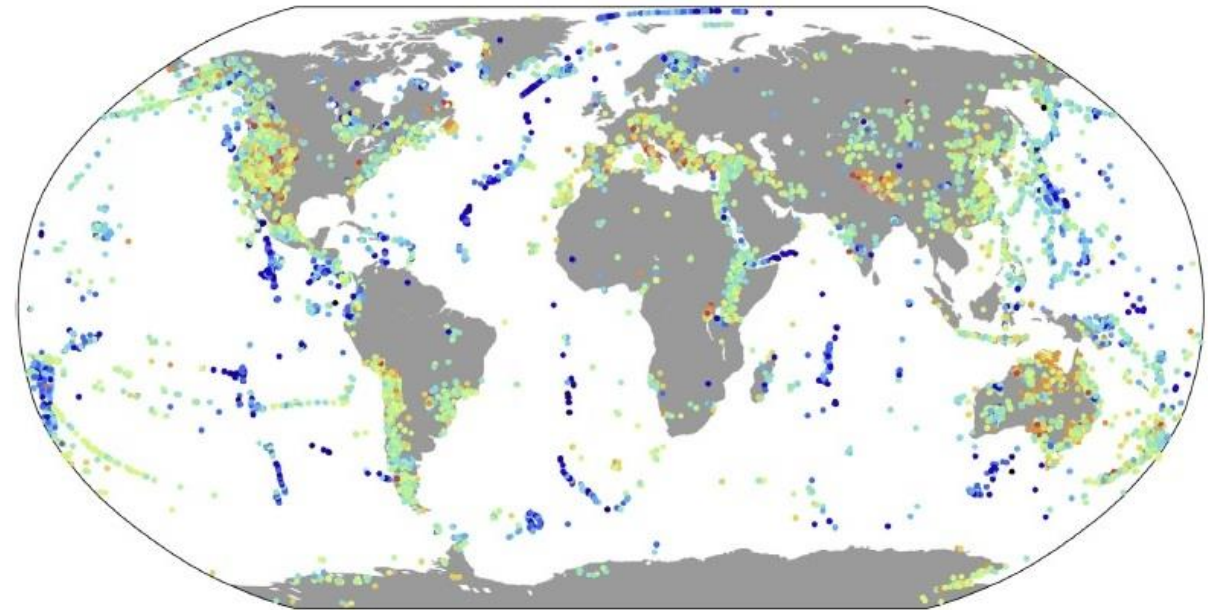


For the lower crust, xenolith lead to a global average of 0.28 mWm^{-3}

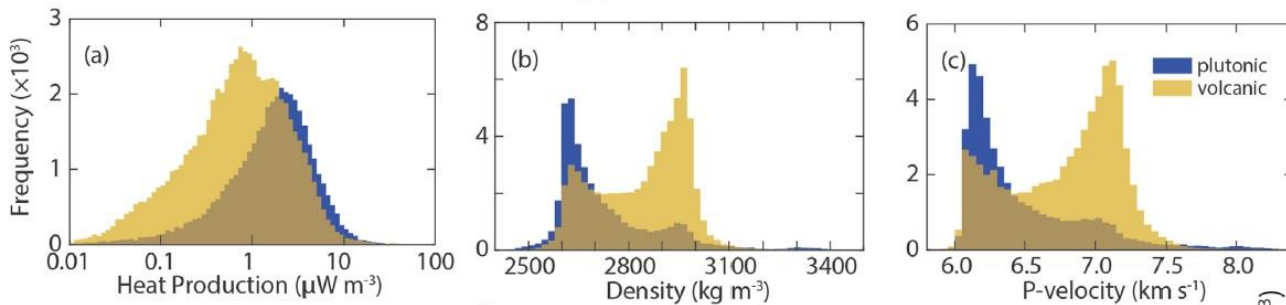
Radiogenic Heat Generation of igneous rocks



(a) plutonic

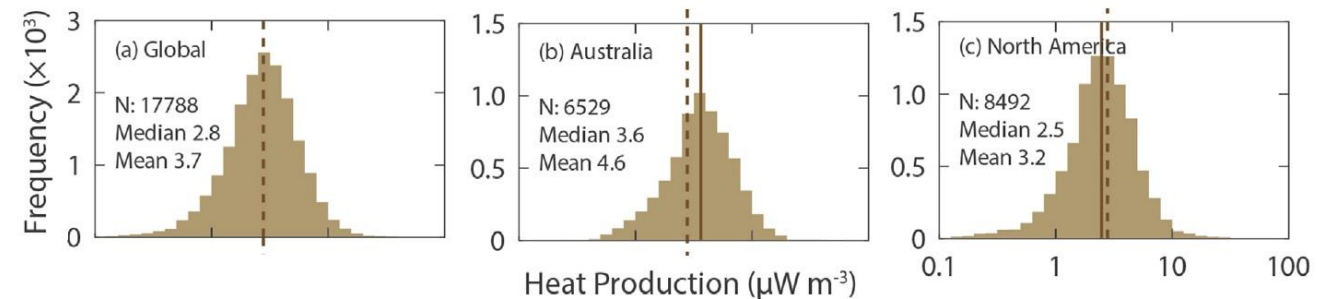


(b) volcanic

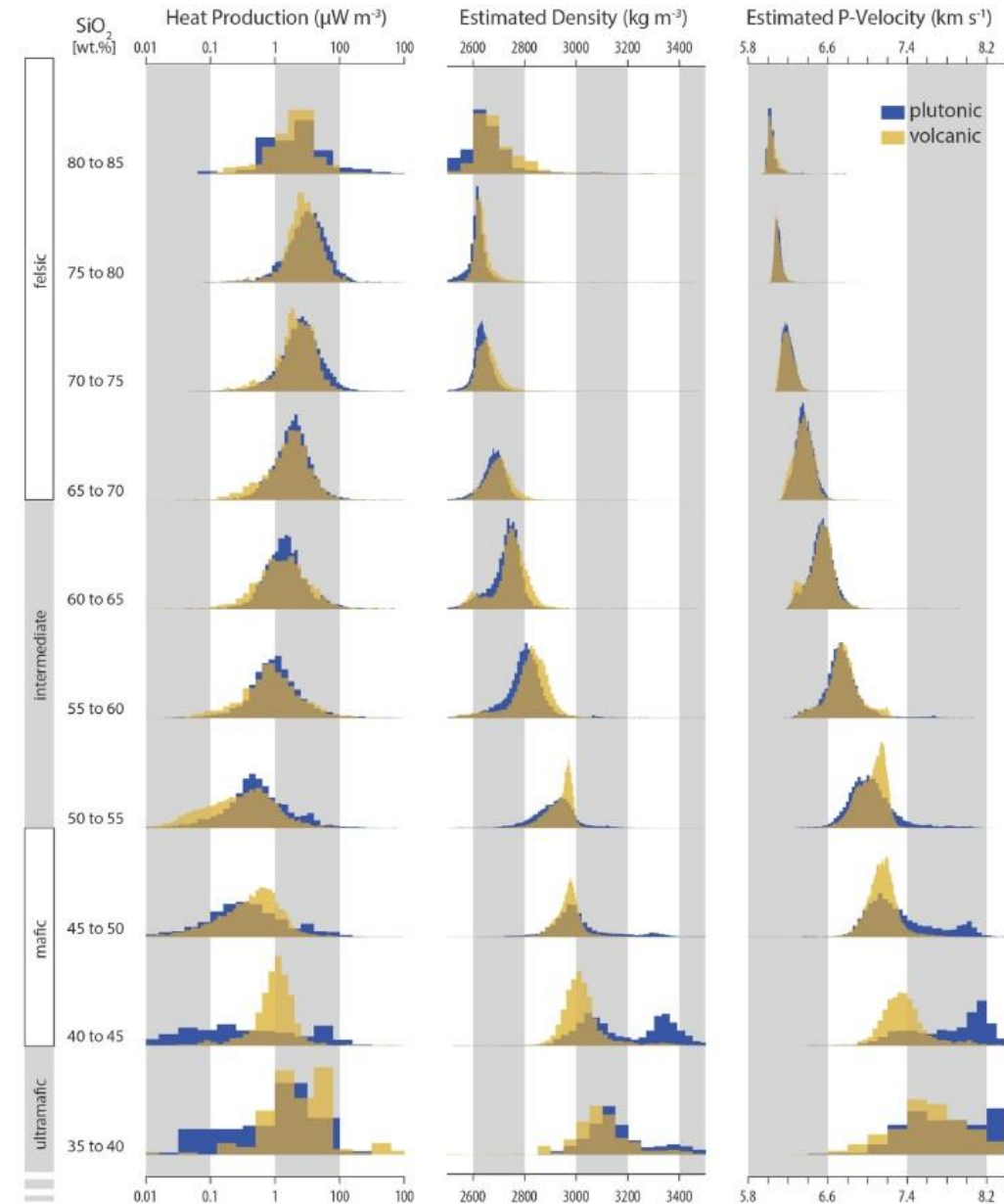


Hasterok and Webb, 2017, *Geoscience Frontiers*, 8

Heat production estimates range from a maximum of $14,000 \mu\text{W m}^{-3}$ to a minimum of $0.001 \mu\text{W m}^{-3}$, but the vast majority of the data fall between 0.01 and $30 \mu\text{W m}^{-3}$.



Radiogenic Heat Generation, density, and P -wave velocity: dependency on SiO_2 (first order compositional variations)



- Density and seismic velocity generally increase as composition ranges from felsic to mafic, while heat production decreases from felsic to mafic compositions.
- Density and seismic velocity distributions show a more complex behaviour for $\text{SiO}_2 < 65$ wt.%, while heat production distribution for $\text{SiO}_2 < 55$ wt.%, due to the presence of other oxides in the rocks.

Thermal Inertia and Thermal Resistance

Thermal Inertia

It is a measure of the rock responsiveness to temperature variations: $\frac{k}{\sqrt{\kappa}} = \sqrt{k \rho c}$

If $k = 2.3 \text{ W m}^{-1} \text{ K}^{-1}$ and $\kappa = 0.8 \times 10^{-6} \text{ m}^2 \text{ s}^{-1}$, the thermal inertia is: $\sim 2.6 \text{ kJ m}^{-2} \text{ K}^{-1} \text{ s}^{-1/2}$

Thermal Resistance (R)

R = it measures how effectively it retards the flow of heat (mKW^{-1})

$$R = \int (1/\lambda) \partial z \quad \mathbf{Q}_d = \lambda_d \times (\partial T / \partial z)_d \quad \mathbf{Q}_0 = \mathbf{Q}_d + \int A(z) \partial z = \lambda_d \left[\frac{\partial T}{\partial z} \right]_d + \int A(z) \partial z$$

$$\mathbf{Q}_d = (\lambda / \partial z)_d \partial T = (1 / \partial R)_d \partial T = (\partial T / \partial R)_d \quad \mathbf{Q}_0 = \mathbf{Q}_d + \int A(z) \partial z \quad (\partial T / \partial R)_d = \mathbf{Q}_0 - \int_0^d A(z) \partial z$$

At any depth d heat flow is equal to the gradient of temperature with respect to the thermal resistance

For individual formation of layers:

$$R = \sum_i \left(\frac{\Delta z_i}{\lambda_i} \right) \quad R = \Delta z \cdot \sum_i \left(\frac{1}{\lambda_i} \right)$$

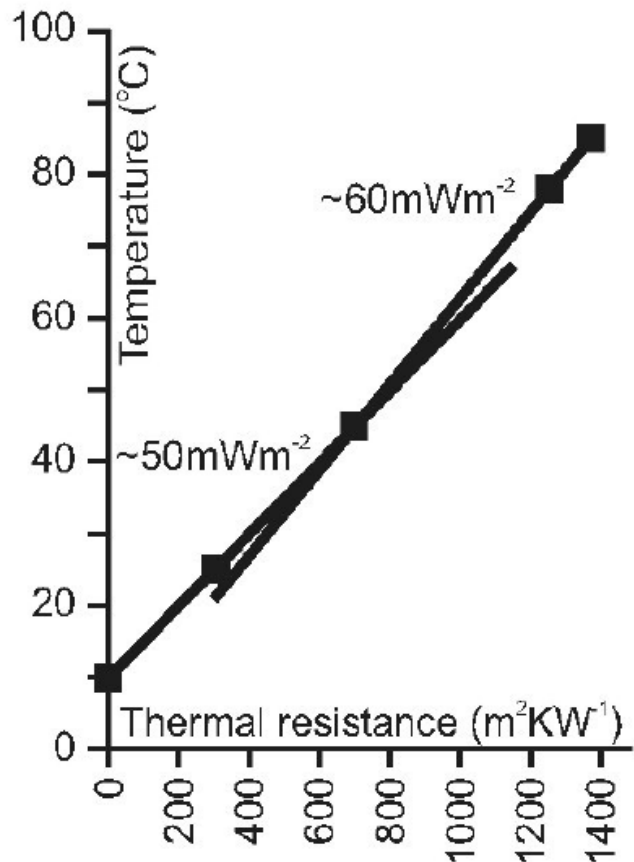
If thermal conductivity is derived from well logs Δz is constant

Bullard Plot

- Points on a Bullard plot should lie on a straight line for a section supporting a constant heat flow.
- Errors in thermal conductivity and temperature data cause points on a Bullard plot to be scattered (linear regression required).

Bullard plot

: linear relationship between temperature and thermal resistance with depth



Non-linear Bullard plots are related to:

- Systematic errors in estimating thermal conductivity (e.g., sediment compaction is under/overestimated) produce convex-up or converse shape of the curve.
- High heat generation results in a decrease in heat flow with depth.
- Introduction/removal of heat from the system cause variation of heat flow from the depth (e.g., fluid migration, diagenetic/metamorphic processes).

References

Main Readings:

- Eppelbaum, Kutasov, and Pilchin, 2014: Applied Geothermics, Chapter 2: Thermal Properties of Rocks and Density of Fluids, 99-104.
- Pasquale, Verdoja, Chiozzi, 2014, Geothermics Heat Flow in the Lithosphere Chapter 2: Heat Conduction and Thermal Parameters, 15-49.
- Beardsmore and Cull, 2001: Crustal Heat Flow, Chapter 2, Heat Generation, 23-43.
- Beardsmore and Cull, 2001, Crustal Heat Flow, Chapter 4, Thermal Conductivity, 90-144.

Further Readings:

- Clauser and Huenges, 1995. Rocks Physics and Phase Relations. A Handbook of Physical Constants.
- Fuchs, 2018. The variability of rock thermal properties in sedimentary basins and the impact on temperature modelling – A Danish example. Geothermics, 76, 1-14.
- Goes et al., 2020. Continental lithospheric temperatures: A review. Physics of the Earth and Planetary Interiors 306, 106509.
- Hasterock and Chapman 2011. Heat production and geotherms for the continental lithosphere, EPSL, 307, 59-70.
- Hasterok and Webb 2017. On the radiogenic heat production of igneous rocks, GeoscienceFrontiers, 8, 919-940.
- Jaupart et al., 2016. Radiogenic heat production in the continental crust. Lithos 262, 398–427.
- Jennings et al., 2019. A new compositionally based thermal conductivity model for plutonic rocks. Geophys. J. Int., 219, 1377–1394
- Jorand et al., 2015. Statistically reliable petrophysical properties of potential reservoir rocks for geothermal energy use and their relation to lithostratigraphy and rock composition: The NE Rhenish Massif and the Lower Rhine Embayment (Germany). Geothermics, 53, 413-428.
- Pimienta et al., 2018. Comparison of thermal and elastic properties of sandstones: Experiments and theoretical insights. Geothermics, 76, 60-73.